Polyelectrolyte Multilayer Thin Films with Antimicrobial, Antifouling and Drug Releasing Properties

by

Sze Yinn (Jessie) Wong

M.S. Chemical Engineering Practice
Massachusetts Institute of Technology (2008)
B.S. Bioengineering (Biotechnology)
University of California, San Diego (2006)

SUBMITTED TO THE DEPARTMENT OF CHEMICAL ENGINEERING IN PARTIAL FULFILLMENT OF THE REQUIREMENTS FOR THE DEGREE OF

DOCTOR OF PHILOSOPHY IN CHEMICAL ENGINEERING
AT THE
MASSACHUSETTS INSTITUTE OF TECHNOLOGY

MAY 9 2011
[June 2011]

Signature of Author: _____

Sze Yinn Wong
Department of Chemical Engineering
May 9, 2011

Certified by: _____

Paula T. Hammond
Bayer Professor of Chemical Engineering
Thesis Supervisor

Accepted by: _____

William M. Deen
Carbon P. Dubbs Professor of Chemical Engineering
Graduate Officer

Polyelectrolyte Multilayer Thin Films with Antimicrobial, Antifouling and Drug Releasing Properties

by

Sze Yinn (Jessie) Wong

Submitted to the Department of Chemical Engineering on May 9 2010 in Partial Fulfillment of the Requirements for the Degree of Doctor of Philosophy in Chemical Engineering

Abstract

This thesis work focuses on designing thin polyelectrolyte multilayer (PEM) films via layer-by-layer (LbL) deposition technique with the ability to kill pathogenic bacteria and inactivate human viruses, especially the influenza (flu) virus on contact. This work builds on four years of research at the Institute for Soldier Nanotechnologies (ISN) focusing on creating new, non-leaching microbicidal material; this film is envisioned to be used as permanent surface coatings for weapons, equipments, uniforms, personal items, etc. because a small reduction in the rate of infection will greatly enhance the readiness and performance of soldiers and other military personnel. Extending this application to everyday life, commonly handled objects such as doorknobs, computer keyboards, and touch screens can also be made sterile by coating them with these highly effective microbicidal PEM films. These films can also be used to prevent infections and long-term bacterial biofilms on implant surfaces. The ultimate aim of this thesis work is to create a broadly applicable multifunctional platform film technology that will satisfy various thin film surface coating applications; this film will impart a surface with long term antimicrobial / antifouling functionality via a permanent microbicidal base, and controlled delivery of a therapeutic agent via a hydrolytically degradable top film as needed. Efforts were focused on maximizing and understanding the factors that influence the microbicidal / antifouling property of the film; thus far, we successfully designed a set of contact-killing ionically cross-linked polymeric thin films; a hydrophobic polycation, linear *N,N*-dodecyl,methyl- poly(ethylenimine) (DMLPEI) with microbicidal activity was layered with a hydrophilic polyanion, such as poly(acrylic acid) (PAA), to create LbL films highly effective against *Escherichia coli* and *Staphylococcus aureus* (Gram negative and positive bacteria, respectively), as well as the influenza A/WSN (H1N1) virus. The microbicidal film was also demonstrated to significantly resist adsorption of protein from blood plasma relative to an uncoated substrate. By generating PEM films assembled with the hydrophobic *N*-alkylated poly(ethylenimine) and the hydrophilic poly(acrylic acid), an ultrathin film that exhibited antifouling and antimicrobial properties was created. Results showed that a fine balance of hydrophobicity and hydrophilicity on the surface of the films was needed to create molecular-level heterogeneities unfavorable to protein adsorption; due to the contrasting nature of the polymer making up the film, nanoscale segregation of the polymer segments into hydrophobic and hydrophilic moieties could occur on the surface. We then moved on to design a dual functional LbL film construct combining the permanent microbicidal / antifouling base film with

a hydrolytically degradable PEM top film offering controlled and localized delivery of therapeutics (e.g. antibiotic, anti-inflammatory drug, etc.). When the degradable top film is completely eroded, the surface will be left with the permanent microbicidal film for long-term prevention of fouling by biomolecules and microorganisms (e.g., proteins and bacteria).

Thesis Supervisor: Paula T. Hammond, Bayer Professor of Chemical Engineering

Thesis Supervisor

Paula T. Hammond, Ph.D

Bayer Professor and Executive Officer of Chemical Engineering

Massachusetts Institute of Technology

Thesis Committee

Jianzhu Chen, Ph.D

Cottrell Professor of Immunology and Biology

Massachusetts Institute of Technology

Alexander M. Klibanov, Ph.D.

Novartis Professor of Chemistry and Biological Engineering

Massachusetts Institute of Technology

Gregory Stephanopoulos, Ph.D.

Bayer Professor of Chemical Engineering

Massachusetts Institute of Technology

Acknowledgments

I have been very fortunate to have extraordinary people around me during my doctoral work at MIT; I would not have been able to complete the thesis presented here without them.

First and foremost, I am very grateful to have Professor Paula T. Hammond as my thesis advisor. I thank her for giving me the support, encouragement, and mentorship in both research and personal development. I am very thankful to her for giving me the scientific freedom to pursue projects that I am passionate about; in return, I became a more independent researcher, being able to plan and execute my plans accordingly.

I also wish to thank my thesis committee members, Professor Alexander M. Klibanov, Professor Jianzhu Chen, and Professor Gregory Stephanopoulos. Special thanks go to Professor Alexander M. Klibanov who has been an invaluable part of my thesis work; regular meetings with him to discuss my project have ensured that I am heading down the right path. I also thank my committee members for giving me helpful feedbacks on my research during my committee meetings.

I would not have been able to accomplish my thesis work without the indispensable help that I have received from the undergraduates that I have been privileged to work with. I thank Qing Li, Jovana Veselinovic, Ksenia Timachova, and Ryan Rosario for working with me on the various projects, and staying motivated all the time.

I cannot imagine being a member of another research group. I thank Professor Byeong-Su Kim for helping me get started in lab when I first joined. I also thank Bryan Hsu for teaching me the synthesis of the polymer that has been a crucial part of my research, as well as handling of the influenza virus. I would also like to thank the LbL drug delivery subgroup in the Hammond lab for insightful discussions all the time. In particular, I am grateful to Joshua S. Moskowitz for working with me on a major project during my doctoral work; he was a crucial part in finishing the project in a very timely and organized manner. I also appreciate his level of enthusiasm in everything he does, which rubs off on people who he works with. Dr. Jinkee Hong has also been a very helpful part of my thesis work, in particular for insightful discussion and hands on help with characterization of the LbL films. Also, Dr. Md Nasim Hyder and Dr. Lin Han have been very helpful with characterization of my LbL films too. I thank my office mates Anita Shukla, Kittipong Saetia, Dr. Raymond Samuel, and Bryan Hsu for being my sounding boards on both research and personal issues. Special thanks to Anita for making me feel welcome at the ISN when I first came. Last but not least, I would like to thank the Hammond lab for being such an awesome group to be part of; everyone is ever ready to help and to bounce ideas with.

I am grateful to the lab and administrative staffs at the ISN and ChemE MIT who make sure that everything keeps running. Christine Preston has been such a great help in making sure that everything gets done in a timely manner, Marlisha McDaniels for help with everything office related especially in getting our mail organized. I thank Dr. Steve Kooi and William Dinatale at the ISN for help with equipments in the ISN.

Finally, I thank my family and friends for their unconditional support and love throughout this journey. Thanks mom and dad for paving the way for me to come all this way; without your support, I would not have ended up where I am today. I thank my brother and sister for their limitless love even though we are far away from one another. I am grateful to my boyfriend and his family for supporting me unconditionally in everything that I choose to venture

in, and being very patient with me. Last but not least, I would like to thank my friends (you know who you are) who have hung out with me through the times, listened to me vent about everything, shared my passion for Apple Inc. products, and ventured out with me for yummy food!

This acknowledgement is by no means comprehensive. So much have gone into making my doctoral work possible that I should finish up by saying a big thank you to everyone who has been a part of my life.

JESSIE (SZE YINN) WONG

Massachusetts Institute of Technology Department of Chemical Engineering,
May 9 2011

Financial support for this work is gratefully acknowledged from U.S. Army through the Institute for Soldier Nanotechnologies (ISN) at the Massachusetts Institute of Technology (MIT) and the National Institutes of Health, National Institute of Aging (5R01AG029601-03). I thank the ISN, Center for Materials Science and Engineering (CMSE), the Biotechnology Process Engineering Center, and the Belcher Lab at MIT for the use of their equipment.

Table of Contents

List of Figures

List of Tables

Chapter 1: Background and Significance

1.1 Introduction

One of the main focuses of this thesis work is to create polyelectrolyte multilayer (PEM) films via the Layer-by-Layer (LbL) deposition technique with the ability to kill pathogenic bacteria and inactivate human viruses, especially the various pathogenic strains of influenza viruses. PEM films are attractive because of their simple and economical fabrication process, and they can be built on most surfaces of various shapes and sizes with nanometer scale control over morphology and surface properties. [1] PEM films are also known to be robust and adhere to surfaces well; hence, PEM films have tremendous potential to be used as coatings on various surfaces and objects to impart them with microbicidal functionality. On top of that, PEM films have also been investigated extensively for use in biomedical applications, [2-5] membranes and electrodes for energy applications, [6-8] and various stimuli-responsive surfaces. [9-11]

The thesis work presented here builds on four years of Institute for Soldier Nanotechnologies (ISN) research focused on creating new, non-leaching bactericidal, virucidal, and fungicidal surfaces, which will dramatically reduce the spread of influenza and possibly other pathogenic microbe infections in the battlefield. These microbicidal films can be used to coat surfaces on weapons, equipments, uniforms, personal items, filters and so on because a small reduction in the chances of influenza infections will greatly enhance the readiness and performance of soldiers and other military personnel. Extending this application to everyday life, imagine if commonly handled objects like doorknobs, computer keyboards, and toys can be made microbicidal (bactericidal and virucidal) by coating them with these PEM films. Bacteria

such as *Escherichia coli (E.coli)* and *Staphylococcus aureus (S.aureus)* are the most common cause of infections in people, and the rise of antibiotic resistant strains of these bacteria (e.g., methicillin-resistant *S.aureus* (MRSA)) has become a serious problem. On the other hand, annually approximately 5% to 20% of the United States population acquires the influenza (flu) virus. Out of this percentage, more than 200,000 people are hospitalized, and about 36,000 people die. [12] The flu virus is one of the most common and dangerous human pathogens; it becomes a very serious problem when a new, most likely an avian strain of the flu virus becomes infective to humans. These viruses spread easily from person to person through droplets formed while coughing and sneezing. In addition, touching respiratory droplets on surfaces of objects can also transmit the flu virus; [13] therefore, if common surfaces can be made microbicidal, bacterial infections and the spread of influenza can be reduced drastically.

Apart from the above mentioned applications, PEM films have also been investigated extensively to deliver therapeutic agents such as antibiotics [2, 14], proteins [15], anti-inflammatory agents [3, 16], and growth factors [5, 17, 18] for medical applications. These films can also be built using degradable polymers, creating the opportunity to design multifunctional combination films consisting of permanent and degradable multilayers within a single film construct. One of the most attractive properties of these PEM films is that the therapeutic agents can be incorporated into them at the exact layer of interest, resulting in high drug loading per volume of the film. Also, since most of the time the LbL technique is carried out in an all-aqueous fabrication condition, incorporation of biologically active materials such as anti-inflammatory agents, proteins, and DNA are possible without denaturing them.

In recent years, there has been great interest in designing drug – device combinations for medical applications, including cardiovascular prostheses, orthopedic implants, stents, etc. [2, 19-22]

with the idea of reducing adverse foreign body response (FBR) and other implant-related complications (e.g., bacterial infections and fouling by biomolecules and microorganisms) via localized delivery of therapeutics. When a foreign material is implanted in a person's body, protein from blood adsorbs onto the surface within seconds (biofouling by protein), [23] which then triggers an inflammation cascade as part of the wound healing response to protect the body from foreign objects; in some cases, this may lead to encapsulation of the implanted material. [24, 25] Localized delivery of anti-inflammatory agents could help in mediating a FBR, or if surfaces of medical implants/devices can be functionalized with a film construct that prevents fouling by protein in the first place, complications arising from FBR can be drastically reduced.

Implant-related infections can occur on any implanted objects ranging from minimally invasive contact lenses and temporary urinary catheters, to permanent cardiac valves and orthopedic implants. [20] More importantly, systemic bacteria circulating the bloodstream can become pathogenic upon attachment to a foreign material surface at any time after implantation; upon attachment, the bacteria colonize the surface ultimately leading to the formation of a biofilm, which is a matrix of sessile bacteria consisting of approximately 15% bacterial cells and 85% hydrophobic exopolysaccharide fibers.[24] Biofilms can damage surrounding tissues and give rise to planktonic bacterial cells capable of spreading infections.[26] This again necessitates the design of drug – device combination that provide long-term prevention of bacteria colonization, and at the same time capable of eliminating pre-existing infection at the implant site.

As mentioned before, biofouling by protein on the surface of medical implants triggers a FBR; in general, biofouling can be described as undesired accumulation of biomolecules and organisms (proteins, bacteria, algae, etc.) on wetted surfaces. This is a major problem not only in medical applications, but also in the food packaging industry, membranes filtration devices,

marine equipments, and so on. [27-29] Biofouling usually results in reduction of sensitivity and efficacy of the devices. Protein adsorption on surfaces has also been shown to create an environment suitable for bacterial colonization, and eventually forming a biofilm. [24]

In this thesis work, I present a set of multifunctional nondegradable contact killing microbicidal and antifouling PEM films, incorporating a family of polymeric hydrophobic quaternary polycations with potent microbicidal activity into LbL films. We then move on to design a single film construct combining the microbicidal / antifouling film with a hydrolytically degradable top film incorporating therapeutic agents for biomedical implants applications.

1.2 Layer-by-Layer (LbL) Deposition of Polyelectrolyte Multilayer (PEM) Films

LbL deposition is a very attractive assembly technique for PEM films. This assembly method was first described in the early 1990s by Decher et al. [30] In this technique, multivalent species (molecules, polymers, nanoparticles, etc.) with complementary functional groups are adsorbed sequentially onto a functionalized substrate; the films can be built up via electrostatic or other non-covalent interactions, including hydrogen bonding. [31,32] For example, a positively charged polyelectrolyte (polycation) is adsorbed onto a negatively charged substrate, followed by the adsorption of a negative polyelectrolyte (polyanion). [30,33] This LbL deposition techniques can also be started with a positively charged substrate. The PEM film is built up by repeating the bilayer assembly process shown in Figure 1-1. A bilayer architecture is denoted: $(\text{polycation/polyanion})_n$, where n is the number of bilayers adsorbed on the substrate. This is carried out by dipping the negatively charged substrate in bath containing a positively charged species, followed by rinsing of the non-specifically bound species. This assembly technique is

possible because with each step, slight charge overcompensation prevents more like-charged polyelectrolyte from adsorbing but allows the next oppositely charged polymer to be adsorbed. [33, 34, 35] This charge overcompensation is possible due to charge screening and is favored because of entropy gain from the release of counter ion when the polyelectrolyte is incorporated into the interface. It has also been shown that the polyelectrolyte layers formed are not well stratified, instead they interdigitate. [36]

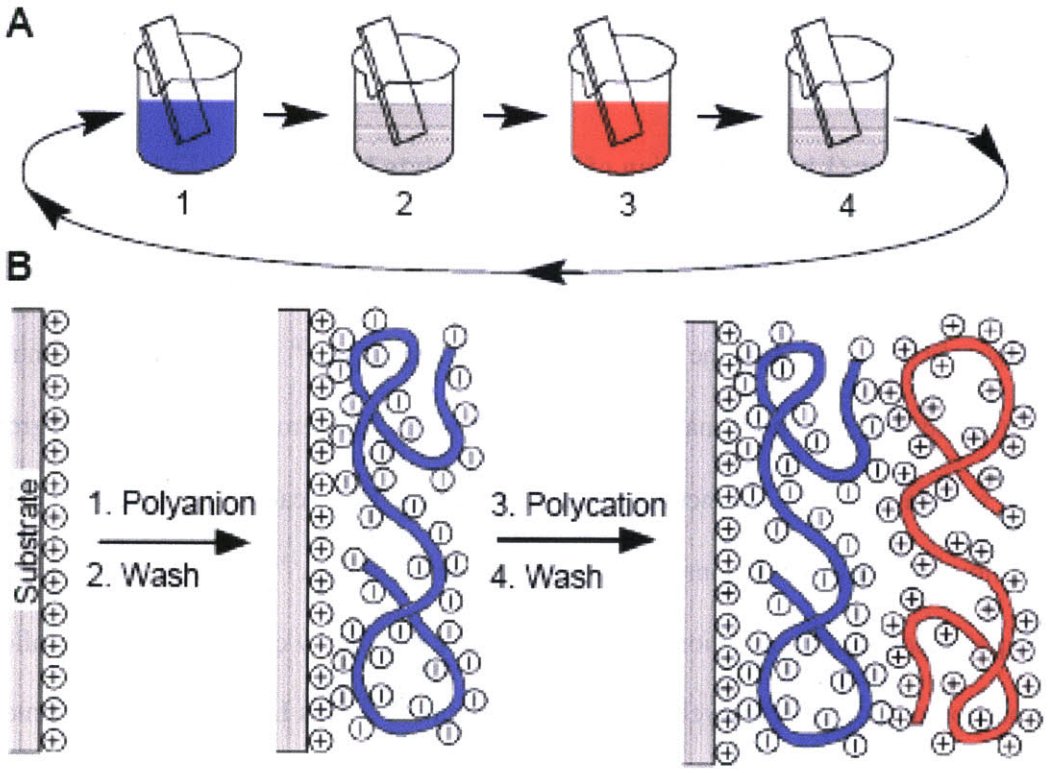

Figure 1-1: Schematic of layer-by-layer assembly. Beaker 1 = polyanion, beaker 2 & 4 = water rinse bath, beaker 3 = polycation. [33]

Some of the factors that control the growth behavior of a PEM film are pH, ionic strength (salt concentration), molecular weight of polymer, solvent used, humidity, temperature, drying between steps, deposition time, and polymer concentration. Schoeler et al. show that film

thickness is a strong function of pH, [37] and that for a weak polyelectrolyte system of poly(acrylic acid) and poly (allylamine hydrochloride) $(PAA/PAH)_n$, the thickness of a single layer of polymer can be adjusted from 0.5 nm to 8 nm by changing the charge density of the weak polyelectrolyte. [38]

The film thickness is highly dependent upon the salt concentration of the polymer solution as well. Dubas and Schlenoff observed that the film thickness of a 10 bilayer poly(styrene sulfonate) (PSS) / poly(diallyldimethylammonium chloride) (PDADMAC) system increased linearly over a NaCl concentration range of 10^{-2} M to 2 M. [39] At low salt concentration, the polymer can displace the salt ions more effectively and bind more tightly to the substrate. At high salt concentration, the polymer will adhere to the substrate more loosely, thus forming a loopier molecular layer. At high enough salt concentration, it is possible for the polymer to completely desorb from the surface. [40] Also, using salt ions with higher valency is functionally similar to having higher salt concentration of a lower charge salt ion.

The effect of molecular weight of polymer on the morphology of PEM films is species dependent because of difference in charge densities, steric hindrance, etc. along the polymer backbone. Four different PEM systems were studied by Houska *et al.* and it was concluded that the thickness of the first deposited layer did not depend on the molecular weight of the polymer. However, the overall thickness of the PEM film does increase with increasing molecular weight. [41] Lower molecular weight polymers have shorter chains thus cannot make as many ion pairs with the substrate surface as compared to higher molecular weight polymer which has longer chains. The insufficiency in ion pairs sometimes allow the shorter chain polymer to detach during subsequent deposition step due to interaction with larger polyelectrolyte of opposite charge. [42] The three-zone model for PEM film: [43] precursor zone (I), core zone (II), and outer

zone (III) was verified by Porcel *et al.* where it was shown that the core zone eventually reaches a constant size at which point the film growth transitions into the linear regime. They also found that the molecular weight of the polymer does not significantly affect the linear growth regime of a hyaluron (HA) / poly(L-lysine) (PLL) and poly(glutamic acid) (PGA) / PAH systems. Both of these systems have been shown to grow exponentially in the initial stages, but transition to linear growth after more than 15 bilayers. [44] PEM film has been shown to exhibit two type of film growth behavior: linear and exponential.

Drying between deposition steps has also been studied, and has been shown to increase film thickness because of increased surface roughness. [45] Other studies have also shown that drying in between deposition steps can result in thinner film on the contrary; [46] hence, the effect of drying in between steps is system dependent.

As mentioned before, LbL deposition is very effective in building nanometer thick film with control over its morphology and surface properties. It is also a gentle aqueous assembly technique where small biomolecules like proteins, polysaccharides, DNA, etc. can be incorporated. [1] Additionally, this process is not limited to only a particular substrate. The film properties have been found to be independent of the substrate used, so the PEM film can be constructed on surfaces of any shape, size, and material. Furthermore, LbL deposition is not limited to only electrostatic assembly; hydrogen bonding, biological interactions, and even covalent crosslinking have been successfully utilized for construction of PEM films. [33,47] Other than dipping as shown in Figure 1-1, LbL deposition can also be done with misting [48,49] and spin coating; [50] both assembly methods have been shown to be very effective in depositing conformal coating onto substrates. With the highly versatile properties of PEM films, LbL technology has

been applied to countless applications, including drug delivery, membranes and electrodes for energy applications, biosensors, electrochromic devices, etc. [2,3,6,8,47,51,52]

1.2.1 Layer-by Layer Applications in Bactericidal PEM film

PEM films made using the LbL technique have been developed to be bactericidal. Thus far, no literature has reported the use of PEM film to inactivate viruses; hence, the application for PEM film presented in this thesis work is novel and exciting. Some of the more common polymers and metals incorporated into PEM films for bactericidal activity include silver ions, [53, 54] silver nanoparticles, [55,56] titania (TiO_2), [56] chitosan, [57,58] dextran (anti-adhesive), [57] etc.

Li *et al.* created a two-level bactericidal coating with polyelectrolyte and nanoparticle multilayer deposition; the film kills bacteria by releasing embedded silver ions (chemical-releasing killing) and via immobilized quaternary ammonium salt (contact killing). The film was constructed via LbL deposition using PAH and PAA as the polyelectrolytes. Then, a cap region made of PAH and SiO_2 nanoparticles is added on top of the bilayers. The cap region is then modified with a quaternary ammonium silene, OQAS. Silver ions are loaded inside the PAH/PAA bilayers. The system exhibits very high bactericidal activity in the beginning from the release of the silver ions, and significant antibacterial activity (~ 90%) after the depletion of the silver ions. [53] The disadvantage of this type of PEM film is it is releasing a biocide into the environment, and this is not always desirable.

Antibacterial coating using hydrogen-bonded multilayers containing silver nanoparticles have also been investigated. Efficacy of the film against Gram positive (*S.epidermidis*) and Gram negative (*E.coli*) bacteria was tested using the Kirby-Bauer disk diffusion test; the zone of inhibition (ZoI) increases as the number of bilayers deposited increase. It is also reported that incremental increase in the ZoI requires exponential increase in the amount of silver ions

released. [59] Bactericidal coating made of poly (L-lysine)/hyaluronic acid (PLL/HA) multilayer films and micrometer-sized liposome aggregates loaded with silver ions were created by Malcher *et al.* The encapsulated silver nitrate was released by increasing temperature over the transition temperature of the vesicles (34°C). A 4-log reduction in the number of viable *E.coli* bacterial cells was observed. [54] One of the disadvantages of this approach is that the embedded silver agents will eventually be exhausted, leading to limited functional lifetime. More importantly, silver salts have been shown to be cytotoxic to tissues at high local concentration. [60]

Some PEM films were designed to limit bacterial adhesion and viability by modifying the chemical and physical properties of the material surface. Lichter *et al.* built PEM thin films comprised of poly (allylamine) hydrochloride (PAH) and poly (acrylic acid) (PAA) over a range of conditions to explore the physicochemical and mechanical characteristics of material surfaces controlling adhesion of *Staphylococcus epidermidis* bacteria and subsequent colony growth. They found that adhesion of viable *S. epidermidis* was directly correlated to the stiffness of the polymeric substrate; however, it was independent of the roughness, interaction energy, and charge density of the material. Similar trends were observed for wild type and actin analogue mutant *E.coli* suggesting that these results were not confined to only specific bacterial cells. [61] These results bring about an additional parameter that can be designed into PEM films to enhance its microbicidal activity as PEM films can be built on virtually any type of surfaces of various shapes and sizes.

Of course there have also been PEM films that are developed to release antibiotics over a period of time; antibiotics (e.g., gentamicin, vancomycin, etc.) have been incorporated into biocompatible PEM films that erode under physiological conditions (37°C, pH 7.4). [4, 14] Unfortunately, one of the biggest issues with release of small hydrophilic drug is controlling its

release over extended periods of time; for example, the film developed by Chuang *et al.* was unable to control the burst release of gentamicin at early times resulting in all the drugs being released in less than 24 hours. [14] Recent improvement in the architecture of the film by Moskowitz *et al.* shown release of the drug over weeks, but the initial burst release is still present. [2]

Most of the bactericidal coatings developed thus far involve leaching a bactericidal agent into the environment; this may not be a desirable trait especially when the leached agent is toxic to us as well. Especially with antibiotics, the likelihood of generating resistance strains of bacteria is high when compared to antimicrobial materials designed to kill microbes on contact; however, the release of a bactericidal agent sometimes is beneficial, especially when there is a serious infection when a high dosage is needed to eradicate the infection, preventing the infection from spreading.

1.2.2 Layer-by-Layer Applications in Drug Delivery

PEM films can be easily incorporated on the surfaces of medical implants to provide localized drug delivery. [2] These PEM films can be tuned to release these therapeutic agents under specific conditions, such as under physiological conditions (37°C and pH 7.4), presence of enzymes, [62] or just via simple diffusion. Also, since usually the amount of material incorporated into PEM films increases with the number of layers deposited, the amount of material loaded is highly tunable. Tunable dosage in drug delivery is a very attractive characteristic because currently many treatment options overload the body with the hope of a small amount of the drug being delivered to a specific area of the body. The possibility of localized drug delivery with PEM films opens up many new applications in the biomedical area, especially in the treatment of cancer, as most of the chemotherapy drugs are harmful to the noncancerous cells.

The first generation drug delivery using PEM film has focused on diffusion based delivery of drugs; drugs are deposited in nondegradable PEM films, and the drugs are released via simple diffusion. This often results in a burst release of the drug at early times, followed by residual release of drug and the entire release ending in just a few hours. Since this process is diffusion controlled, there is no way of tuning the delivery time or dosage from these nondegradable films. This issue brought about the idea of degradable films where the release of the drug is based more on surface erosion of the PEM film rather than drug diffusing through the nondegradable PEM film. [3, 14, 63] An example of this system is shown in Figure 1-2 where the release of multiple agents are illustrated; the agent deposited closest to the top of the degradable film theoretically will release first, followed by the next agent underneath it and so on.

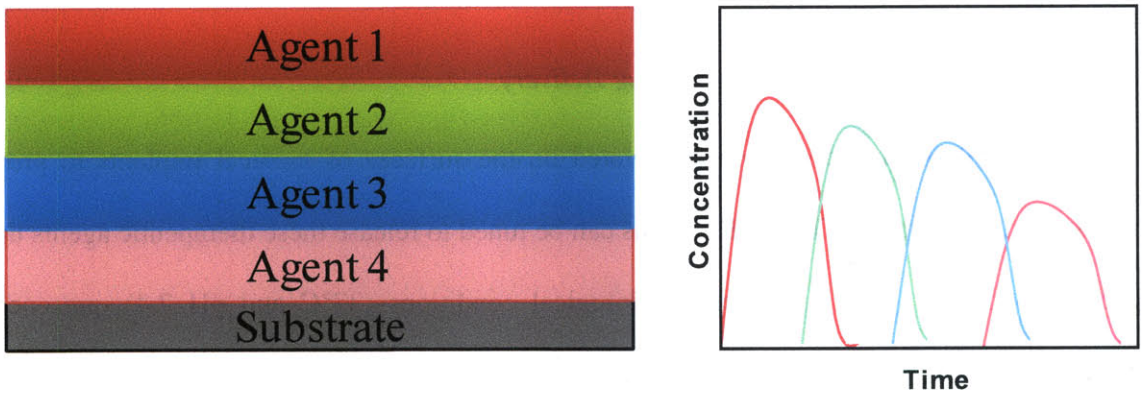

Figure 1-2: Multiagent release from a degradable thin film (Note: thickness of film and substrate are not drawn to scale).

One of the most attractive degradable polymers for the design of these multiagent PEM films is poly (β-aminoesters) (PBAEs). Lynn and Langer first considered these polymers for applications in gene transfer vectors. [64, 65] Figure 1-3 shows the step-growth Michael-type

addition of a bis (secondary amine) monomers to diacrylate esters, to form the three PBAEs: Polymer 1, 2, and 3.

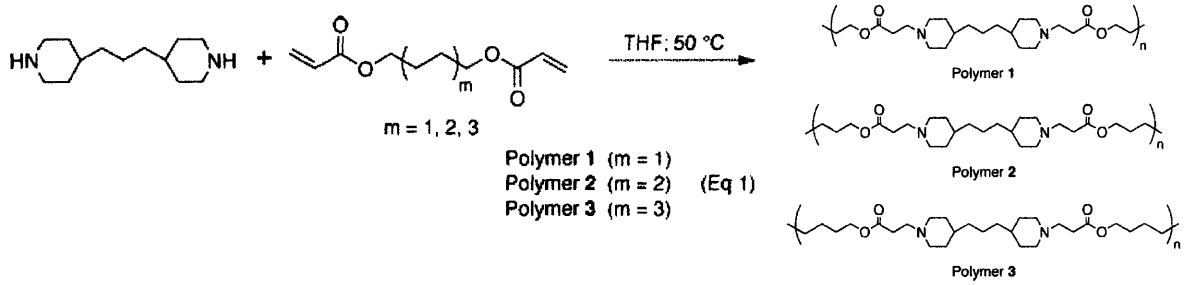

Figure 1-3: Synthesis and structure of poly(β-aminoesters), polymer 1, 2, and 3. [64]

These polymers have been found to be highly biocompatible and noncytotoxic, so are their degradation products. [65] They are cationic at physiological pH (7.4), thus can be hydrolytically degraded because of the presence of ester bonds on the polymer backbone. The polymer will degrade over time in aqueous environment. Poly 1 has been shown to effectively incorporate and release model drugs, heparin etc. for nearly 17 hours at physiological pH. [63] Lysozyme (a model protein), [15] and gentamicin (an antibiotic), [14] diclofenac (an anti-inflammatory) [3] have also been shown to effectively incorporate and release from these degradable films in a surface erosion governed manner. Research in Hammond Lab at MIT has shown that longer release times of dextran sulfate were observe with increasing hydrophobicity of the PBAEs; the increase in hydrophobicity of the PBAEs made it more difficult for water to cleave the ester bonds on the PBAEs backbone, thus delaying the surface erosion of the PEM film; however, increasing the hydrophobicity above a threshold value causes rapid release of dextran sulfate. Phase segregation and bulk film destabilization occurred beyond this threshold

value of hydrophobicity. Drug release times ranged from few hours up to twelve days using PBAEs of various degree of hydrophobicity. [66]

In order to consider PEM film as drug delivery system, some of the important factors that need to be considered are: sequential delivery of drugs, time span of delivery, and incorporation of a wide range of drugs. One of the unresolved problems of these PEM films is interdiffusion between the layers of the film. In reality, the layers in the PEM film are highly interpenetrated and interdiffusion of the loaded agents actively occurs. [33] Due to the long dipping time required in LbL assembly, previously deposited layers can diffuse through the swelled film, rather than being kinetically locked in place. Interdiffusion in the film leads to nonsequential release of drugs in the film. Several solutions have been proposed to solve this problem; some of them include using higher molecular weight polymer, and the use of barrier layers. [67] The use of less time intensive LbL assembly techniques such as misting, [49,68] or spin coating [69] are also likely to help rectify this issue.

1.3 Current Research in Permanent Microbicidal Coatings

A new, non-releasing antimicrobial system has emerged recently from the Klibanov Lab at MIT. This approach utilizes a positively charged hydrophobic polymer at a particular molecular weight and charge to kill bacteria. This polymer can either be covalently attached (first-generation) [70] or "painted" onto surfaces using a cotton swab (second-generation). [71] The first generation coatings involve covalently attaching the long hydrophobic polymeric chain to a material surface; the polymers investigated include poly (4-vinyl-*N*-hyxylpyridinium) (*N*-hexyl-PVP) and *N, N* – hexyl, methyl poly (ethylenimine) (*N, N* – hexyl, methyl PEI), as shown in

Figure 1-4. The second generation coatings use non-covalent hydrophobic interaction (like oil paints) to create these microbicidal coatings; the hexyl moieties in the polymer is replaced with dodecyl moieties to greatly increase the intermolecular hydrophobic interactions to make sure that the polymer does not leach from the surface. It has been shown in a previous paper that if the *N, N* – hexyl, methyl- PEI is used in the "painting" process instead of the *N, N* – dodecyl, methyl-PEI (Figure 1-4), the polymer leaches from the surface. [72] These polymers have been tested against some of the most common pathogenic bacteria (*S.aureus* and *E.coli*) and influenza viruses, and thus far the most effective polymer in killing both bacteria and viruses is the linear *N, N* – dodecyl, methyl-PEI (DMLPEI) (Figure 1-4). [71] The proposed mechanism for killing bacteria for this polymer is by rupturing the bacterial cell membranes. Bacterial cell membrane has a net negative charge; so there is an initial electrostatic interaction between the positively charged surface and the bacterial cell membrane. Next, the hydrophobic side chains can then diffuse through the lipid membrane undermining their integrity. [73,74] Preliminary cytotoxicity of this polymer against mammalian cells has also been tested; mammalian cells toxicity had been tested using COS-7 cells where cell viability has been shown to decrease moderately for both control and painted wells although painted wells have lower viabilities compared to control. [75]

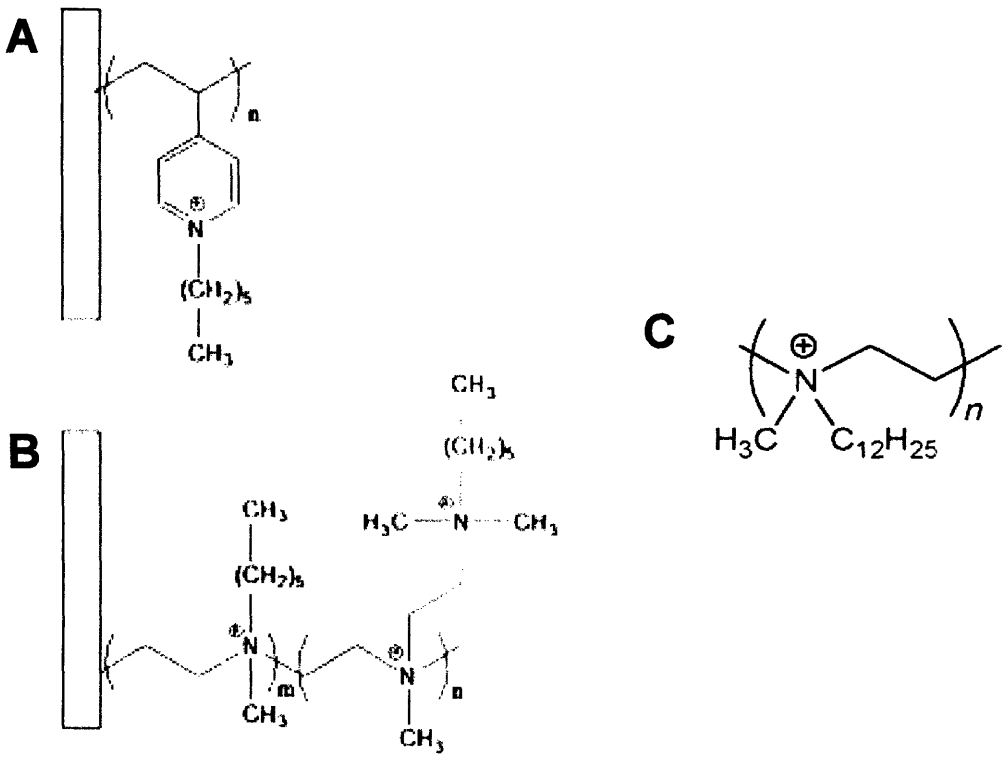

Figure 1-4: Schematic representation of A) poly(4-vinyl-N-hexylpyridinium), and B) branched N-hexyl, N-methyl – polyethylenimine as first generation microbicidal coatings. C) linear *N, N* - dodecyl, methyl-poly(ethylenimine) "paint" as second generation microbicidal coatings.

Some of the disadvantages of the "painting" process used to make these microbicidal coatings are that it cannot be used to coat geometrically complicated objects easily and since the polymer is adhering to the surface via hydrophobic-interactions, there may be possibility that the coating will peel off easily from the surface. It also leaves oily residue on the surface painted. In this thesis work, the linear *N, N* – dodecyl, methyl PEI polycation is incorporated into PEM films using the LbL technique. Contrary to the previous discussed "painting" technique, these PEM films are held together by electrostatic interactions, and are usually robust and adhere to surfaces very well. Plus, this technique has the ability to coat substrates of various geometries

conformally, and they are also only nanometer in thickness, as opposed to the "painted" film, which are on the order of micrometer in thickness. [31,75]

Contact killing antimicrobial surfaces other than the ones developed in Klibanov laboratory have also been investigated. Chemical vapor deposition (CVD) and deposition of PEM film via LbL assembly are two ways of creating multifunctional coatings. Previously, researchers have demonstrated that vapor phase (CVD) and solution phase synthetic platforms (LbL assembly) can be integrated to create multifunctional coatings, such as surfaces that are both hydrophobic and antimicrobial. [76] LbL films built with polyallylamine and poly(4-styrene sulfonate) have been shown to be bactericidal; [77] although the resultant films show high activity against Gram positive bacteria, they are not as effective against Gram negative bacteria. Recent studies have also reported various successful covalent attachments of polymeric microbicidal materials onto various surfaces (e.g., glass, paper, metal, etc.); [78,79] in most of the cases, the biocidal polymer contained cationic groups, such as quaternary ammonium salts (QAS) [79-82] or alkyl pyridinium. [73,78,83] Covalent attachment usually involves a multi-step synthesis process involving various chemicals; in this thesis work, the simple LbL assembly is used to incorporate the antimicrobial polycation into a PEM film to impart a surface with antimicrobial property.

1.5 Thesis Overview

In this thesis, the groundwork for designing a multifunctional platform film technology for use as surface coatings for various medical applications is established. This film technology will impart a surface with long-term resistance towards biofilm formation via a permanent microbicidal base coating and tunable release of therapeutic agents via a completely degradable LbL top film for added medical functionality. Also, the microbicidal film presented in this thesis

work has been shown to resist protein adsorption from undiluted blood plasma as well; this anti-fouling property of the film is an added bonus on top of the microbicidal functionality that the film already possess. I think that this platform film technology is broadly applicable and versatile enough to satisfy various thin films medical implant coating applications. In addition, the microbicidal / antifouling film itself can also be applied to various practical applications including commonly handled objects (e.g., keyboards, doorknobs, elevator buttons, etc.), filtration membranes, food packaging, and many more.

Though several methods exist in constructing thin film coatings, only layer-by-layer deposition allows molecular control over morphology of films necessary to achieve subtle surface film properties to maximize the microbicidal and antifouling properties. Films built with this method are in the nanometer range and the surface properties of the films can be tailored by changing the polymers, and/or assembly conditions during buildup.

In chapter two, the fabrication rules and design parameters to create the permanent microbicidal films were explored. In chapter three, a multifunctional film technology combining the microbicidal film with controlled release of drugs via a degradable LbL film was investigated. In chapter four, the antifouling property of the permanent microbicidal film was extensively investigated. Finally, in chapter five, the mechanism in which the microbicidal film kills bacteria and inactivate influenza viruses were examined via electron microscopy and various other methods. The efforts put into this thesis work have laid the foundation for future work involving the multifunctional platform film technology, especially in moving the technology towards commercialization.

Chapter 2: Design of Permanent Contact Killing Microbicidal Films using Layer-by-Layer (LbL) Technology

Reproduced in part with permission from "Bactericidal and Virucidal Ultrathin Films Assembled Layer by Layer from Polycationic N-alkylated Polyethylenimines and Polyanions" by Wong, S. Y., Li, Q., Veselinovic, J., Kim, B. S., Klibanov, A. M., Hammond, P. T. *Biomaterials 31* (14), 4079-4087, 2010. 10.1016/j.biomaterials.2010.01.119, © 2010 Elsevier

2.1 Introduction

Everyday items handled by people (e.g., doorknobs, handles, keyboards, and elevator buttons) are inhabited by various bacteria and viruses, some of which can spread disease. If such objects could be made microbicidal without altering their functionality and appearance, additional means of managing the spread of disease would result. Bacteria such as *Staphylococcus aureus* and *Escherichia coli* are among the most common human pathogens, and the rise of their antibiotic-resistant strains, e.g., methicillin-resistant *S. aureus* (MRSA), has become a serious problem. Furthermore, annually 5% to 20% of the U.S. population is infected with the influenza (flu) virus; as a result, over 200,000 people are hospitalized and about 36,000 people die each year. [12] The flu problem is even more serious when a new strain of the virus, such as the so-called swine flu (H1N1), becomes infectious to humans. Many bacterial and viral diseases can spread from person to person via contact with commonly handled objects; therefore, if their surfaces can be made bactericidal and virucidal, the extent of this spread would be

reduced. In particular, eliminating live bacteria on surfaces of medical implants, thus preventing biofilm formation would be a major advancement in the biomedical field.

Existing bactericidal coatings typically incorporate microbicidal agents like silver ions, [53, 55, 59] antibiotics, [14] or other drugs, [84] that leach into the environment. A disadvantage of this approach is that the embedded agents will eventually be exhausted, leading to limited functional lifetimes. Furthermore, leachable coatings are not desirable when the leached microbicidal agent is toxic or can lead to resistant microbes.

Recently, a new, non-releasing microbicidal strategy has been developed. [72, 78, 85-87] This approach utilizes hydrophobic polycations, either covalently attached as a result of a multi-step derivatization procedure or deposited (painted) onto surfaces to disrupt the bacterial membranes and inactivate influenza viruses on contact. [53, 73, 88, 89] Although the hydrophobic polycations can be physically applied to surfaces from solution, [72] this "painting" process cannot easily coat geometrically complex surfaces and at least micron-thick films are required for maximal bactericidal activity. [90] Also, these polymeric films can peel off or be scraped off the surface. To address these potential shortcomings, in the present study we employed the layer-by-layer (LbL) self-assembly approach. [31, 91]

With LbL technology, surfaces of various shapes can be coated with conformal ultra-thin films whose surface properties can be systematically controlled through film composition and morphology. [33, 52] LbL technology involves sequential adsorption of multivalent species (molecules, polymers, nanoparticles, etc.) with complementary functional groups utilizing electrostatic or other non-covalent interactions, such as hydrogen bonding. [32, 47, 92] Owing to its ease of application and low environmental impact, LbL technology has found a broad range of

applications, including biomedical materials, [14, 47, 93] membranes and electrodes for energy applications, [6,7,94] and electro- or magnetoresponsive surfaces. [9-11,95]

LbL films are sensitive to assembly (pH and ionic strength) conditions; as a result, their structure and composition depend on the film building process. [38] In addition, the film structure can also be modified post-assembly by exposing the film to conditions different from those used during film assembly. For example, LbL films built from polyallylamine and poly(4-styrene sulfonate) could be made bactericidal by manipulating assembly and post-assembly pH conditions (i.e., lowered pH). [77] Although the resultant LbL films polyelectrolytes result in high activity against Gram positive bacteria, they are not as effective against Gram negative bacteria. Although other bactericidal LbL films have been developed, most of them work by incorporating and releasing such bactericidal agents as silver ions, [53, 55, 59, 96] quaternary ammonium salts, [53] titania, [56] chitosan, [57,97] antibiotics, [2,4,14] antimicrobial peptides, [98] and enzymes. [15] LbL films have also been designed to limit adhesion and viability of bacteria by modifying the chemical and physical properties of the surface. [61]

In this work, we demonstrate that by incorporating polymeric hydrophobic quarternary ammonium salts with high bactericidal activity into LbL films, we can harness the potential of these polycations, while achieving high and broad-spectrum bactericidal activity in nanometer-scale coatings. Finally, we report the first use of LbL films to inactivate influenza virus.

2.2 Materials and Methods

2.2.1 Synthesis of Polymers

Poly(2-ethyl-2-oxazoline) (M_w of 500 kDa), 1-bromododecane, 1-bromohexane, 1-bromobutane, iodomethane, *tert*-amyl alcohol, and other chemicals and solvents were from Sigma-Aldrich. Linear *N,N*-dodecyl-methyl-PEI (DMLPEI) was synthesized as previously described. [71] In short, linear PEI (LPEI) (M_w of 217 kDa) was produced by deacylation of poly(2-ethyl-2-oxazoline); [99] the resultant LPEI was dissolved in water, precipitated with aqueous KOH, filtered, and washed repeatedly with water. The resultant deprotonated LPEI was then alkylated first with 1-bromododecane (96 hr at 95°C) and then with iodomethane (24 hr at 60°C) to produce the end product DMLPEI. Syntheses of linear *N,N*-hexyl-methyl-PEI (HMLPEI) and linear *N,N*-butyl-methyl-PEI (BMLPEI) were similar, except that LPEI was alkylated with 1-bromohexane (24 hr at 95°C) and 1-bromobutane (24 hr at 95°C), respectively. As for *N,N*-dimethyl-PEI (MMLPEI), LPEI was alkylated by addition of iodomethane for 24 hr at 60°C. The structures of these polymers are depicted in Figure 2-1A.

PAA (M_w of 50 kDa; Polysciences) was also used to acylate the $-NH_2$ group of dopamine (DOPA; Sigma); 15% of the carboxyl groups of PAA were functionalized with DOPA (Figure 2-1B).

2.2.2 LbL Film Assembly

LbL films were assembled on rectangular 2.5 cm x 3.0 cm silicon substrates (Silicon Quest International) with a programmable Carl Zeiss HMS slide stainer. Substrates were first plasma-etched in oxygen using a Harrick PDC-32G plasma cleaner on high RF for 1 min and then immediately immersed into a solution of a 1 mg/ml of polycation dissolved in an organic

solvent for at least 10 min. Most of the polycations used in this work only dissolve in organic solvents: DMLPEI was dissolved butanol, HMLPEI in propanol, and BMLPEI in propanol. MMLPEI was the only polycation that was soluble in water. The LbL film was built up by alternating the deposition of a polycation and a polyanion; the latter included PAA, poly(Na 4-styrene sulfonate) (SPS, M_w of 70 kDa; Sigma-Aldrich), poly(Na vinyl sulfonate) (PVS; Sigma-Aldrich), poly(methacrylic acid) (PMA, M_w of 100 kDa; Polysiences), and poly(styrene-*alt*-maleic acid) (PSMA; M_w of 350 kDa; Sigma Aldrich). The polycation solutions used for film construction were at a concentration of 1 mg/ml. Solutions of PAA, PAA-DOPA, PMA, and PSMA used were at a concentration of 2 mg/ml in 0.1 M sodium acetate buffer, pH 5.1. PAA, PMA, and PSMA solutions at pH 3.0 and pH 7.0 were pH adjusted using 1 M HCl and 1 M NaOH, respectively. SPS and PVS solutions were at 2 mg/ml in 0.1 M NaCl and in deionized water, respectively.

LbL films with the bilayer architecture of $(Polycation/Polyanion)_n$ was built, where n is the number of bilayers and polycation and polyanion could be any of those mentioned above. A bilayer would include a deposition of a layer of a polycation, followed by a layer of a polyanion; for example, a 1.5 bilayer film will have a complete bilayer deposited, followed by a layer of polycation on top. The following program was used to build up a bilayer: 20 min of dipping in a polycation solution, followed by three rinses in the organic solvent used to dissolve the polycation (1 min, 30 s, and 30 s, respectively), then three rinses in deionized water (1 min, 30 s, and 30 s, respectively), followed by a 20 min dipping in a polyanion solution, then three rinses in deionized water and three rinses in organic solvent (Figure 2-1C). This program was repeated until the desired number of bilayers was obtained. To be subjected to acid treatment, the built

LbL films were immersed in pH 2.5 water for 3 hr, rinsed vigorously in three separate rinses of deionized water, and dried gently with nitrogen gas.

2.2.3 LbL Film Characterization

Thicknesses of LbL films were measured using a spectroscopic ellipsometer (Woollam M-2000D) and verified using a surface profilometer (KLA Tencor P-16). The surface morphology and roughness of the LbL films were observed using an atomic force microscope (Nanoscope IIIa; Digital Instruments) in tapping mode and a scanning electron microscope (JEOL 6320-HR).

Fourier transformed infrared (FT-IR) spectra of $(DMLPEI/PAA)_{50}$ films with PAA at pH 3.0, 5.0, and 7.0 were acquired using a Nexus 6700 FT-IR (Thermo-Nicolet). Films with such large number of bilayers (50) were used to acquire the data because films typically investigated in this work (less than 4.5 bilayers) did not have sufficient material for the spectrophotometer to detect.

2.2.4 Airborne Bacterial Assay

The bacterial strains used herein were *S. aureus* (ATCC, 25923) and *E. coli* (*E.coli* genetic stock center, CGSC4401). Bactericidal activities of the LbL films were tested based on a previously developed protocol. [100] Briefly, *S. aureus* was grown overnight in cation-adjusted Mueller Hinton Broth II (CMHB) (Difco, BD) and diluted to 5 x 10^6 cells/ml. The diluted bacterial suspension was sprayed onto samples (~10 ml/min) using a gas chromatography sprayer (VWR International, cat. No. 21428-350); samples were incubated at room temperature for 2 min, placed in a Petri dish, and covered with a slab of solid growth agar made from CMHB media and BactoAgar (Difco, BD). The Petri dishes were incubated overnight at 37°C and

bacterial colonies on the surface of the samples were counted by hand if there were a few colonies; alternatively, ten digital images per sample were taken with a 4X objective using a microscope (Axioskop 2 MAT microscope, Carl Zeiss), and the total number of colonies was extrapolated to the whole area of the sample. The same procedure was used for *E. coli* except that it was grown overnight in LB-Miller broth (VWR), diluted to 5 x 10^7 cells/ml, and the agar plates used to incubate the samples were made of 1% LB agar (VWR). Bactericidal activity was calculated by comparing the number of colonies on negative control slides and on the samples. Negative controls used were cleaned silicon substrates. Positive controls were silicon substrates painted with a solution of 50 mg/ml DMLPEI dissolved in butanol as described previously. [71]

2.2.5 Waterborne Bacterial Assay

S. aureus was grown overnight at 37°C in cation-adjusted Mueller Hinton Broth II (CMHB) (Difco, BD); the culture was then centrifuged at 2,700 rpm for 10 min, washed, resuspended in deionized water, and diluted to 10^6 cells/ml. LbL films coated substrates were then incubated with the resultant solution at room temperature for 2 hr to promote bacteria adhesion onto the surface. Samples were rinsed thrice in deionized water and incubated under a solid slab of agar (Difco BD) overnight at 37°C. Bare Si substrate was used as the negative control. The same procedure as in the airborne assay was used for counting the bacterial colonies on the samples and controls. The results were presented as a colony density, which is defined as average number of colonies on sample/average number of colonies on silicon control times 100%; therefore, the colony density of a Si substrate control was always equal to 100%. [78]

2.2.6 Determination of Virucidal Activity

The influenza virus strain used was A/WSN/33 (H1N1); the virus was grown in the Madin-Darby Canine Kidney (MDCK) medium from ATCC. [71] The protocol to test the samples for virucidal activity was that described previously. [100] Briefly, a sample was placed in a Petri dish and a 10 μl droplet of a virus solution (~1.6 x 10^5 pfu/ml) was placed in the center of the sample; a sandwiched system to spread the virus droplet was formed by putting a plain silicon substrate on top of the sample. This system was incubated at room temperature for 30 min; then the top substrate was lifted, and the virus droplet exposed sides were washed thoroughly with PBS. Lastly, a plaque assay was performed to determine whether the samples were effective in inactivating the virus. The virucidal activity was determined by comparing the virus titers obtained from plaque assay of the negative control substrate and of the sample (these control samples were the same as described above for determining bactericidal activities).

2.2.7 Adhesion and Non-leaching Test of LbL Films

The mechanical integrity of the film on surfaces was tested using a 3M Scotch tape which was attached to the film and then removed in one motion. The test was performed on $(DMLPEI/PAA3.0)_{4.5}$ films. The thickness and bactericidal activities of the films before and after the test were measured.

A modified Kirby-Bauer assay described previously was used to test samples for non-leachability: [14] a sample coated side down was placed on *S. aureus* streaked agar plate and incubated overnight at 37°C.

2.2.8 In-vitro Cytotoxicity Assay

Murine pre-osteoblast cell line MC3T3 (ATCC) was seeded on coated (with $(DMLPEI/PAA3.0)_{1.5}$ or $(DMLPEI/PAA3.0)_{2.5}$) and non-coated glass substrates (control) placed in wells of a 6-well plate. 100,000 cells/well was incubated for 24 hr and then labeled with live/dead fluorescent stains (Live/Dead Viability/Cytotoxicity Kit for mammalian cells; Invitrogen). A series of 10 digital images were taken of cells at 10x magnification using a fluorescence microscope (Axioskop 2 MAT microscope, Carl Zeiss). The numbers of live and dead cells were counted on each sample, and the percentage of cell viability was computed relative to control.

2.3 Results and Discussion

2.3.1 Airborne Bactericidal Activity of LbL Films

The polycations used to build the LbL films in this study (Figure 2-1A) varied in hydrophobicity with the length of their *N*-alkyl chain; in contrast to the polyanions used (Figure 2-1B), these polycations were insoluble in water and thus were dissolved in butanol or propanol. The microbicidal activity of the LbL films was examined as a function of the polyanion and the pH of the polyanion aqueous solution during assembly. The polyanion charge density and whether its monomer was a weak or a strong acid, was anticipated to be important because the interactions between the polyelectrolytes govern the availability and density of the positive charges and the conformation of the hydrophobic groups on the surface.

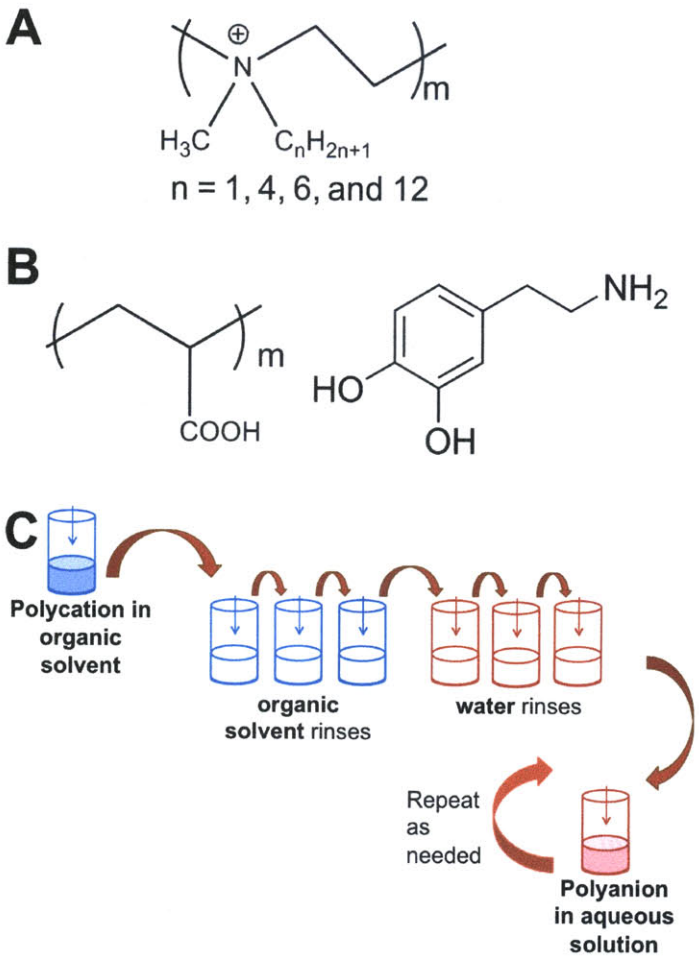

Figure 2-1: A) Structure of microbicidal polycations with various alkyl chain lengths (n = 1, 4, 6, and 12); B) Structure polyacrylic acid (PAA) and dopamine (DOPA) used for acylation between amine group of DOPA and carboxylic group of PAA; C) Schematic of the modified LbL dipping process that alternates between an organic solvent for the polycation and an aqueous solution for the polyanion.

Because LbL assembly typically involves alternation between aqueous solutions, a modified version of the LbL protocol that involved dipping from an organic polycation solution, followed by solvent and then aqueous rinses was introduced, as described in the Experimental Section. Figure 2-2 depicts the growth curves and roughness of $(DMLPEI/PAA)_n$ films built with PAA

solutions at pH 3.0 and 5.0. The films exhibit an initial lag growth phase (thickness not significantly increasing) studied extensively in the LbL literature, [101] followed by a linear growth beyond 4.5 bilayers. The roughness data for the $(DMLPEI/PAA)_n$ films (Figure 2-2) show that for films up to 4.5 bilayers, the thickness and roughness values were statistically the same (from 4 to 10 nm), supporting the initial patchy growth period reported by others. [43] As the number of bilayers was increased further, however, the roughness of the film grew. We observed that the bactericidal activity of $(DMLPEI/PAA5.0)_n$ films rose with increasing number of bilayers; 100% bactericidal activity was achieved at 14.5 bilayers of $(DMLPEI/PAA)_n$ built with PAA at pH 5.0.

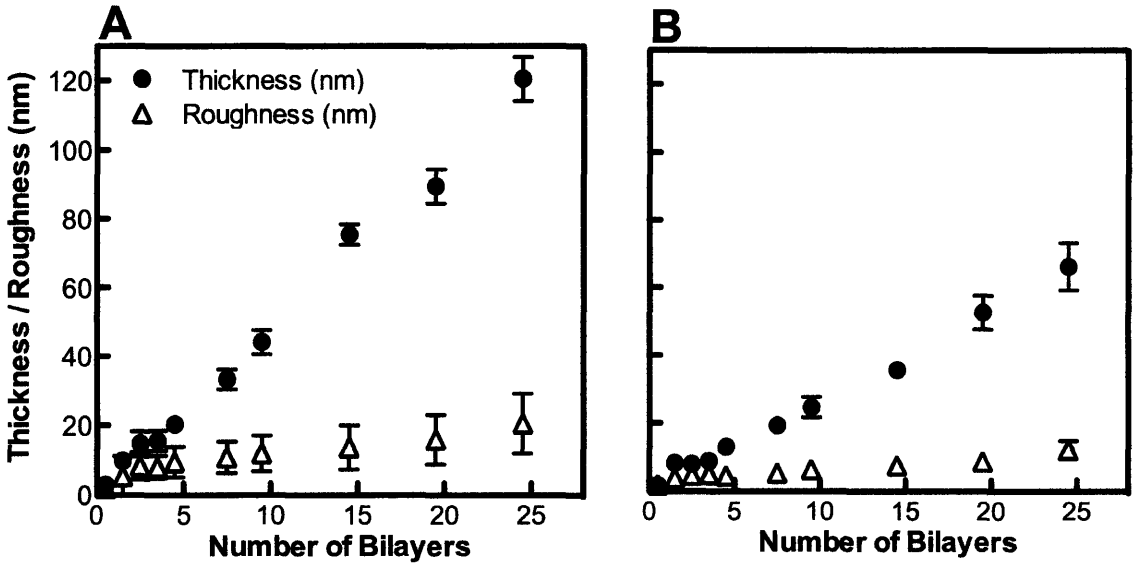

Figure 2-2: Growth curve and roughness of $(DMLPEI/PAA)_n$ prepared with A) PAA at pH 3.0, and B) PAA at pH 5. 0 showing initial patchy growth of the films, and linear growth beyond 4.5 bilayers.

We then investigated the dependence of bactericidal activity on the pH of the PAA solution used during film assembly. As seen in Figure 2-3, by adjusting the pH of the PAA solution used for film deposition the level of bactericidal activity of the films can be changed significantly, achieving complete bactericidal activity with only 1.5 bilayers of deposition for $(DMLPEI/PAA)_n$ with PAA at pH 3.0. We can thus achieve the same level of activity as the microbicidal "painted" films (micron thick) with a much thinner (~10 nm) LbL film using the same microbicidal polycation, DMLPEI. Because the degree of ionization of weak polyacids is highly pH-dependent, the conformation of the PAA chains should also change from a relatively flat and thin random coil at high pH to chain arrangements that take on loops, coils, and brushes forming thicker layers when less charged at low pH. [102, 103] Figure 2-2 shows that LbL films built with PAA at pH 3.0 are thicker than those built at pH 5.0.

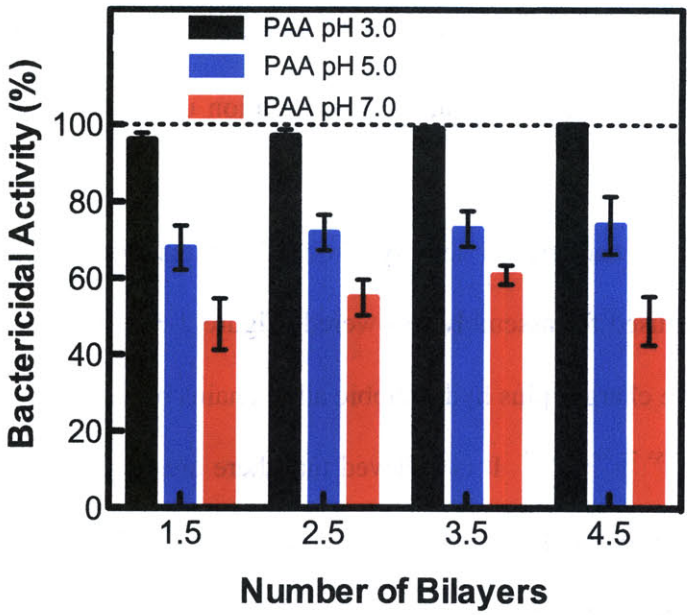

Figure 2-3: Activities of $(DMLPEI/PAA)_n$ LbL films against airborne bacteria; 1.5 to 4.5 bilayers films built with PAA at pH 3.0, 5.0, or 7.0.

When only one layer of the DMLPEI (0.5 bilayer of the film) was deposited on a negatively charged Si wafer, no bactericidal activity was observed. This observation is likely because the negatively charged plasma-treated surface of the Si wafer induced deposition of the DMLPEI layer as a surface-conformal coating, with many of the positive charges tightly associated with the surface negative charges and thus little brush layer generated at the surface. When a PAA at pH 3.0 layer was then deposited, followed by another layer of DMLPEI thus producing a $(DMLPEI/PAA)_{1.5}$ film, the bactericidal activity of the film jumped dramatically to 100% (Figure 2-3). This observation is in agreement with results reported in literature finding that the conformation of the previously adsorbed layer greatly affects the conformation of the next polymer layer. [38, 102] In this case, having a weakly charged PAA layer yields the subsequent

DMLPEI layer with a thicker and loopier brush-like architecture with many of its positive charges available to interact with bacterial cell membranes. Note that only the pH of the polyanion solution could be changed because the polycation used was dissolved in an organic solvent.

The finding that the bactericidal activity of our LbL films against *S. aureus*, increases as the pH of PAA solution used for assembly is lowered (Figure 2-3) is consistent with the current view that mobile positive charges plus hydrophobic alkyl chains of a certain length are necessary for bactericidal activity. [53, 77, 88, 104, 105] It is believed that there are initial electrostatic interactions between the cationic surface and the negatively charged bacterial cell membranes; subsequently, the hydrophobic alkyl chains can diffuse through the lipid bilayer, thus undermining the integrity of the membrane and eventually leading to the death of the bacteria. Previous research has also shown that multiple positive charges are required to permeate cell membranes; [106] the arrangement, accessibility, and mobility of these charged groups on the surface are important as well. [107] A schematic illustrating the likely conformations of the PAA chains and the microbicidal polycation chains is depicted in Figure 2-4A. A transition is observed from thicker and more brush-like PAA layers at low pH that leave more available positive charges on the surface for interaction with the bacterial cell membrane to flat, highly charged PAA layers at higher pH that undergo greater electrostatic interactions with DMLPEI. FT-IR spectra showed in Figure 2-4B support this proposed trend. LbL films made from PAA at pH 3.0, 5.0, and 7.0, showed decreasing intensity of the COOH acid band (C=O stretching of COOH, ν = 1710 – 1700 cm^{-1}) and concomitantly increasing intensity of the COO^- band (asymmetric stretching band of COO^-, ν = 1565 – 1542 cm^{-1}) as the pH of PAA is increased (Figure 2-4B).

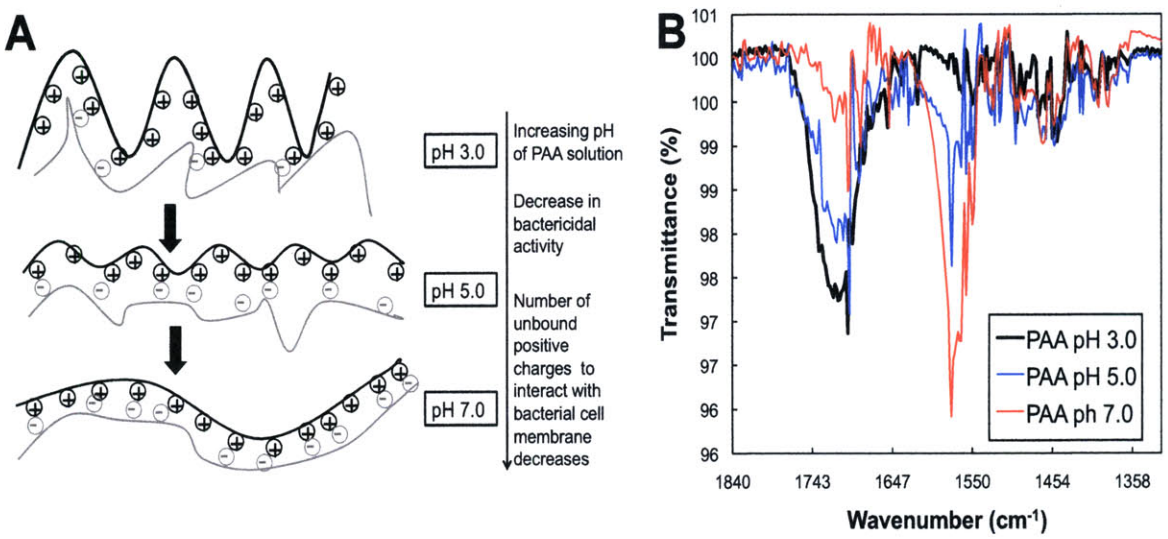

Figure 2-4: A) Schematic representation of the change in conformation of the polymer chains as the pH of the PAA solution used during film assembly is increased. At pH 3.0, the PAA chains are mostly uncharged resulting in a more loopy chain conformation of the polycation DMLPEI, with most of its positive charges available to interact with bacterial cell membranes. As the pH of the PAA solution is increased, the PAA chains become more negatively charged, resulting in more ionic cross-linking with the DMLPEI chains, thus decreasing their number of available positive charges for interaction with bacterial cell membrane; B) FT-IR spectra of $(DMLPEI/PAA)_{50}$ films with PAA at pH 3.0, 5.0, and 7.0 during film assembly. Two distinct bands of the carboxylic acid group of PAA were observed: asymmetric stretching band of COO^- (ν = 1565 - 1542 cm^{-1}), and C=O stretching of COOH (ν □= 1710 - 1700 cm^{-1}).

Our films were found effective against both the Gram positive *S. aureus* and the Gram negative *E. coli* bacteria (Figure 2-5). The difference in the composition of the cell walls of these two types of bacteria should influence the way that positive charges coupled with hydrophobic alkyl chains interact with them. [108] Gram positive bacteria have a simple cell wall consisting of a thick peptidoglycan layer, while Gram negative bacteria have cell walls made out of a lipopolysaccharide layer, a thin peptidoglycan layer, and the periplasmic space. [109] This extra lipopolysaccharide layer is apparently capable of protecting Gram negative bacteria,

making it harder to kill them using just positive charges. [110] In addition, Gram negative bacteria have been shown to change their outer membrane composition to provide extra protection when in contact with quaternary ammonium compounds. [111] Therefore, to exert a broad spectrum bactericidal activity, both positive charges and hydrophobic alkyl chains, as exist in our LbL films, appear necessary.

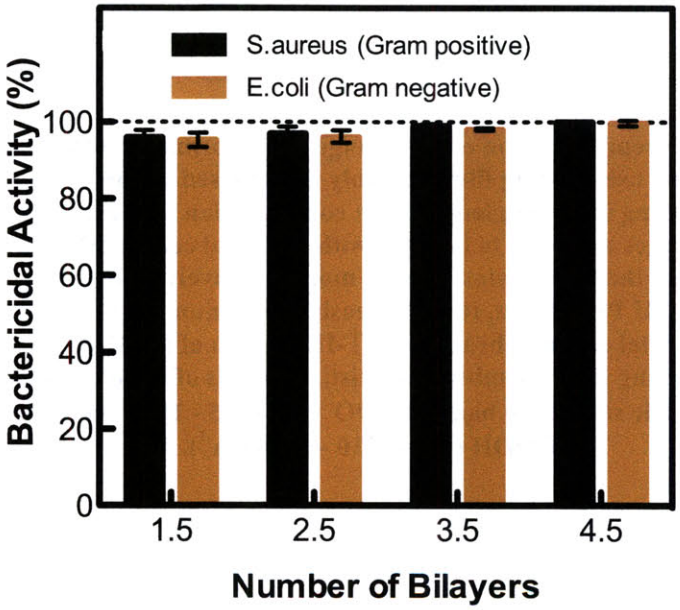

Figure 2-5: Bactericidal activity of 1.5 to 4.5 bilayers $(DMLPEI/PAA)_n$ films against *S .aureus* and *E. coli.*

To further test the view that having mobile positive charges is important for enhanced bactericidal activity, we subjected $(DMLPEI/PAA)_n$ films built from PAA solution at pH 7, to water at pH 2.5, as previously investigated by Lichter and Rubner, who subjected $(SPS/PAH)_n$ films to a low pH, and saw an increase in bactericidal activity of their films. [77] Figure 2-6 shows

that the bactericidal activity of our films increases after exposure of the films to low pH; when the films are exposed to a low pH, some of the carboxylate (COO^-) groups on the PAA chains are protonated to carboxylic (COOH) groups, resulting in conformational changes to the PAA chains, and consequently, the DMLPEI chains. [38] Ultimately, the polymer chains become more mobile with the lowered charge of the PAA chains, leading to less ionic crosslinking with the positive charges on the DMLPEI chains. Thus not only surface coverage (increasing with the number of bilayers) but also the number of mobile positive charges is important for the bactericidal activity of the LbL films.

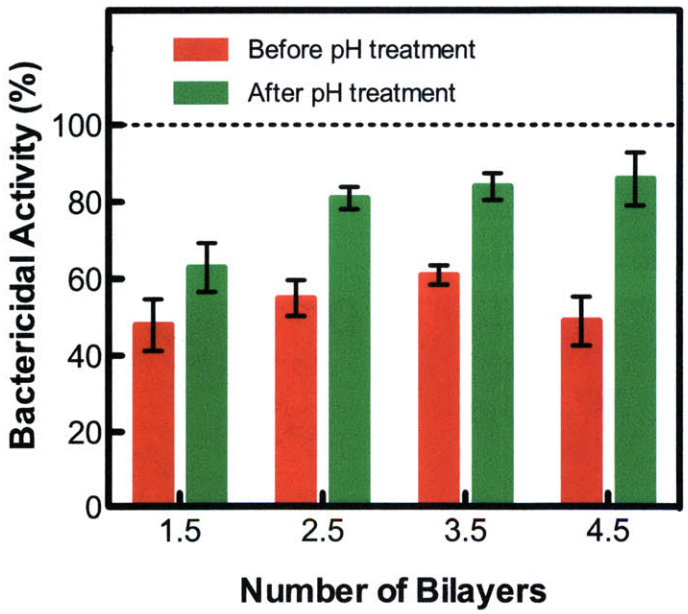

Figure 2-6: Activity of $(DMLPEI/PAA)_n$ films prepared at pH 7.0 before and after pH treatment.

Indeed SEM and AFM images of the films taken before and after the pH treatment (Figure 2-7) reveal that the surface coverage increases, suggesting rearrangements of looser

polycationic chains. After the pH treatment, the roughness of the film decreased from 4.72 ± 1.20 nm to 2.08 ± 0.87 nm. These data indicate that treating $(DMLPEI/PAA)_n$ films built originally with PAA at pH 7.0 post-assembly with a pH 2.5 aqueous solution raised the bactericidal activity of the films, although not to the level of the films originally built at a low pH (namely, PAA solution at pH 3.0); thus the ionic cross-linking within the LbL films is only partially reversible.

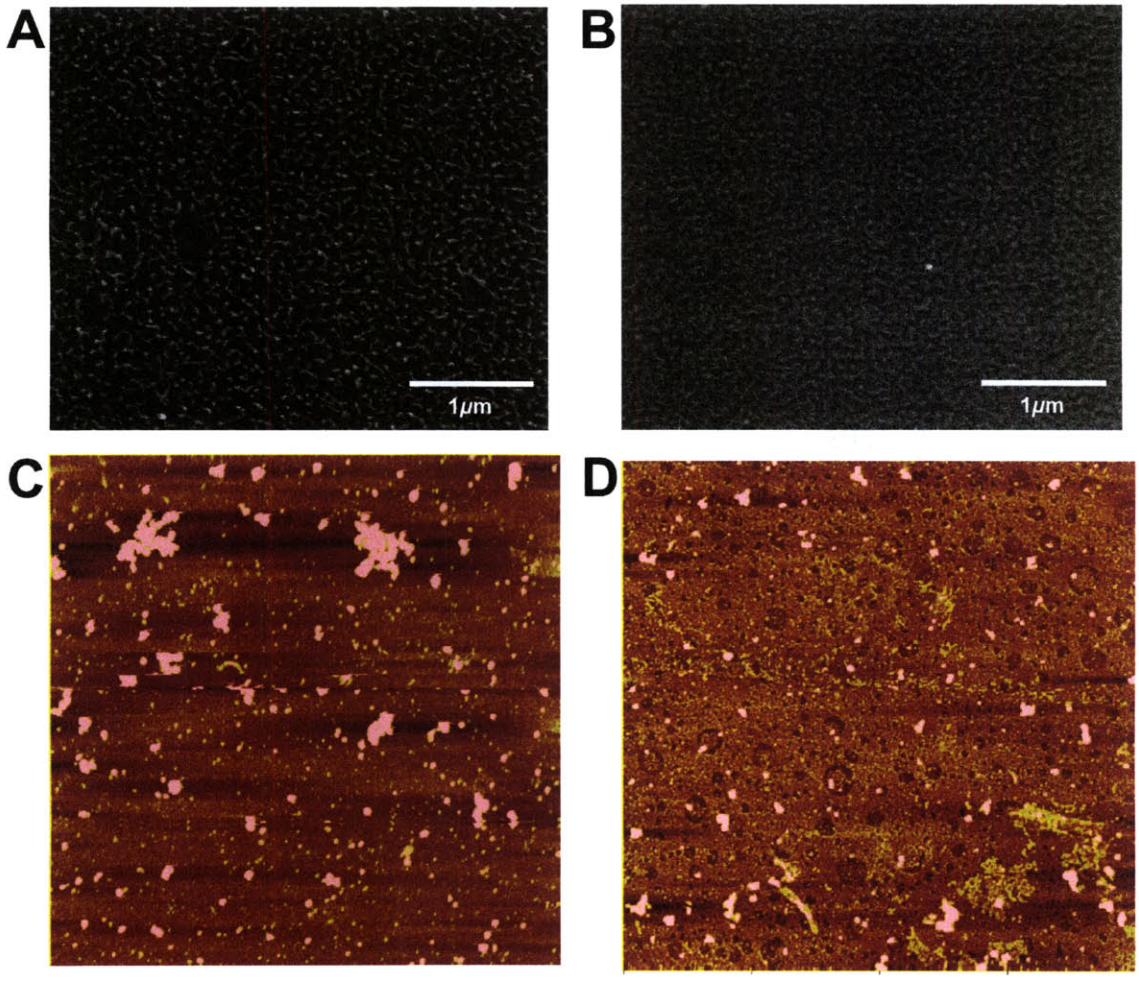

Figure 2-7: SEM images of $(DMLPEI/PAA)_{2.5}$ films prepared at pH 7.0 A) before and B) after pH treatment, showing the increase in coverage of the film post pH treatment. AFM images (10 μm x

10 μm scan) of $(DMLPEI/PAA)_{4.5}$ films prepared at pH 7.0 C) before and D) after pH treatment, also showing more uniform coverage of the film after low pH treatment; z-scale = 25 nm.

By modifying PAA with dopamine (DOPA), the number of carboxylate (COO^-) groups available to form ionic bonds with DMLPEI's positive charges is effectively reduced and the bactericidal activity is increased (Figure 2-8). Functionalizing PAA with DOPA, which reduces the charge density of the PAA chains, presumably results in a loopier PAA chain conformation, as in the case of films built with PAA at low pH assembly conditions, thereby influencing the conformation of the next adsorbed DMLPEI layer and yielding a brush-like layer.

There are also indications of interpenetration between the polyelectrolyte layers in the LbL films discussed here. For example, for the $(DMLPEI/PAA)_2$ and $(DMLPEI/PAA)_5$ films, it did not matter whether PAA or DMLPEI was the topmost layer (Figure 2-8). Instead of forming well-stratified layers, those formed within the LbL films interdigitate, as is typical for polyelectrolyte multilayers. [36]

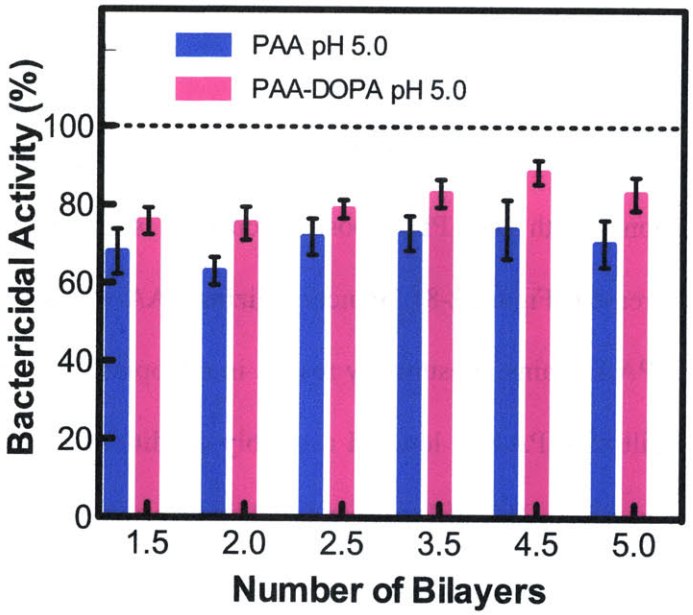

Figure 2-8: Comparison of activity of 1.5 to 5.0 bilayers $(DMLPEI/PAA)_n$ (prepared at pH 5.0) and $(DMLPEI/PAA\text{-}DOPA)_n$ films (also at pH 5.0); figure also shows the comparison of activity of a 1.5 and 2.0 bilayers film and a 4.5 and 5.0 bilayers film illustrating the activities of films with either DMLPEI or PAA as the top most layer. All films were tested with *S. aureus*.

We also found that the bactericidal activity of the LbL films was influenced by the hydrophobicity of the polycation, i.e., the length of its alkyl chains. Using PAA solutions at pH 3.0 and pH 7.0 and polycations with various alkyl chain lengths (Figure 2-9), we found that the bactericidal activity against *S. aureus* varied significantly on the alkyl chain length. For example, films built with linear *N,N*–dimethyl-PEI (MMLPEI, n=1) and *N,N*-butyl,methyl-PEI (BMLPEI, n=4) were significantly less bactericidal than those built with *N,N*-hexyl,methyl PEI (HMLPEI, n=6) and DMLPEI.

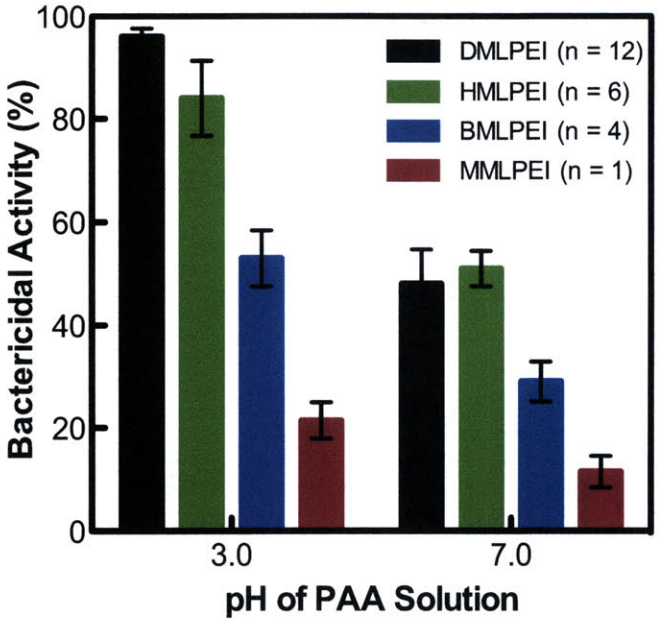

Figure 2-9: Films (1.5 bilayers) were built with polycations of various alkyl chain lengths ranging from methyl (n = 1) to dodecyl (n = 12), with PAA as the polyanion (pH 3.0 and 7.0).

To examine the activity against Gram negative bacteria, for which the size of the alkyl chain is thought to be critical, [77] films made with BMLPEI and MMLPEI as polycations, and PAA at pH 3.0 and pH 7.0 as polyanions were tested against *E. coli*. The bactericidal activity against *E. coli* was found to be lower compared to that against *S. aureus* for $n < 6$ (Figure 2-10). In addition, films built using either linear or branched non-alkylated PEI as a polycation and PAA (at pH 3.0), were impotent against both bacteria. Therefore, hydrophobicity, along with a high positive charge density, is necessary for bactericidal activity.

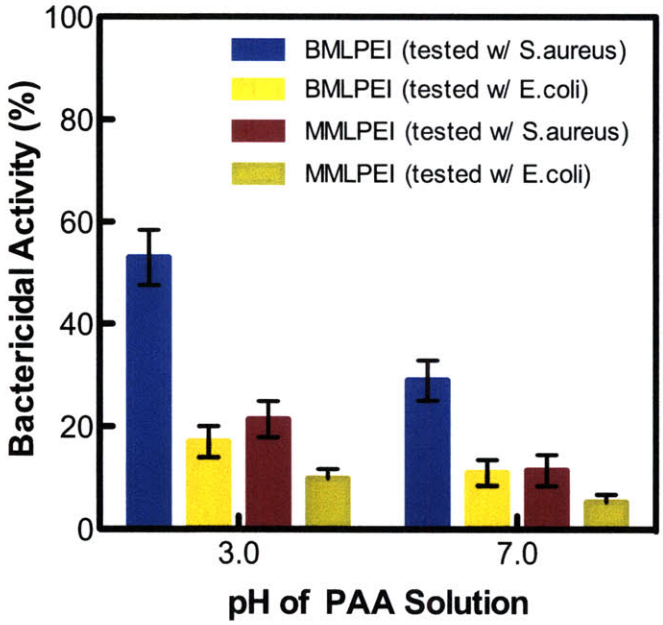

Figure 2-10: 1.5 bilayers MMLPEI (n=1) or BMLPEI (n=4) films built with PAA at either pH 3.0 or pH 7.0 were tested against *S. aureus* and *E. coli.*

Next we examined the dependence of bactericidal activity of the LbL film built with DMLPEI as the polycation on the strength of the acid in the polyanion used. Films built using strong polyacids as poly(4-styrenesulfonate) (SPS) and poly(vinylsulfonate) (PVS) displayed no bactericidal activity. Because strong polyacids are highly ionized, most of the positive charges on the DMLPEI chains should be tightly bound to their negative charges resulting in few mobile positive charges available to disrupt bacterial cell membrane. This effect persisted even when salt was added to the sulfonated polyion solution to reduce the polyanion-polycation electrostatic attraction via ionic screening.

Another interesting observation was that the hydrophobicity of the weak polyacid used for film assembly affected the bactericidal activity as well (Figure 2-11). While LbL films built

with a slightly more hydrophobic poly(methacrylic acid) (PMA) had similar bactericidal activity as those built using PAA, with a much more hydrophobic poly(styrene-*alt*-maleate) (PSMA) the bactericidal activity dropped significantly. The bulky styrene groups of this strong polyacid could change the polyanion-polycation interaction changing the presentation of the polycation on the surface and also interact with the DMLPEI's alkyl chains preventing them from functioning as "brushes" on the surface, thus decreasing the activity of the films.

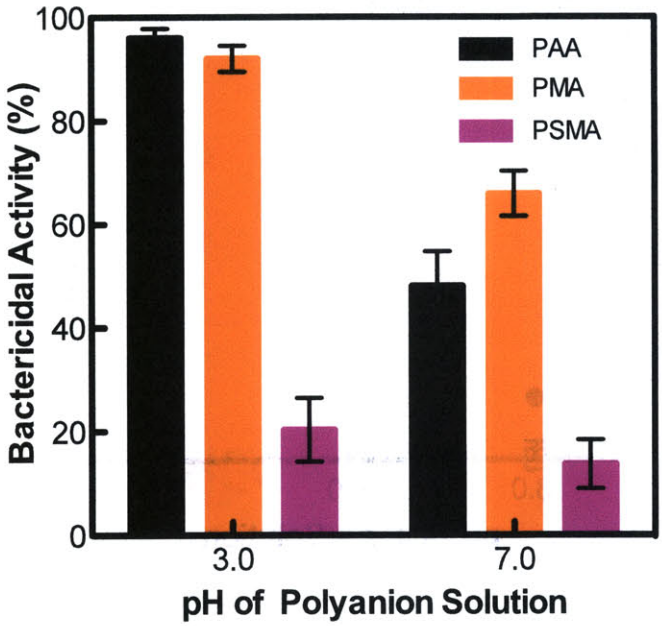

Figure 2-11: Films were built with DMLPEI and three polyanions of varying hydrophobicity; all films were 1.5 bilayers.

2.3.2 Activity of LbL Films Against Waterborne Bacteria

Next we explored the possibility of using our microbicidal LbL films as permanent coatings for biomedical implants to prevent bacterial attachment in aqueous environments. To

this end, 1.5 bilayer and 2.5 bilayer $(DMLPEI/PAA)_n$ films built at pH 3.0, 5.0, and 7.0 were tested against waterborne *S. aureus* and found to be effective in preventing bacterial attachment onto the surface relative to a bare silicon substrate control. As seen in Figure 2-12, the films made at pH 3.0 were most effective in preventing bacteria from attaching to the surface, which is in agreement with our aforementioned airborne results.

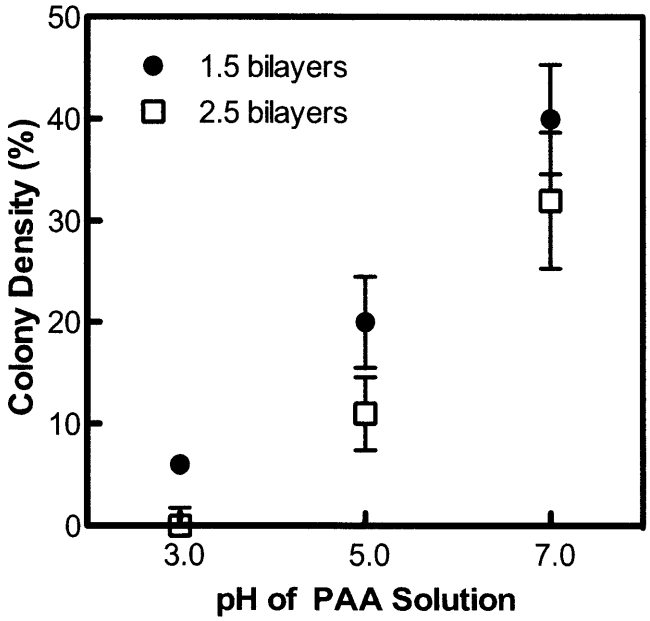

Figure 2-12: Activity of LbL films against waterborne *S. aureus* comparing colony density on a bare silicon control with that on either a 1.5 or a 2.5 bilayer $(DMLPEI/PAA)_n$ films; PAA was at pH 3.0, 5.0, or 7.0; Colony density on control slide is 100%.

2.3.3 Virucidal Activity of LbL Films

The most bactericidal LbL films were tested against Influenza A/WSN/33 (H1N1) virus. This virus has an outer lipid envelope [112] which may be vulnerable to the high density of positive

charges and hydrophobicity presented on the LbL surfaces (as was the case with surfaces "microbicidally painted" with DMLPEI [71,113]).

A 1.5 bilayer $(DMLPEI/PAA3.0)_n$ film was found to be 60% virucidal (Figure 2-13), although it was 100% bactericidal. However, the virucidal activity of the LbL films increased as we increased the number of bilayers, and reached 100% beyond 7.5 bilayers. Since the size of a viral particle (~100nm) is at least 10 times smaller than that of a bacterium (~1μm), the incomplete virucidal activity seen with our films at a lower number of bilayers may be due to the voids on the surface that are large enough to fit a virus but too small for a bacterium (Figure 2-14).

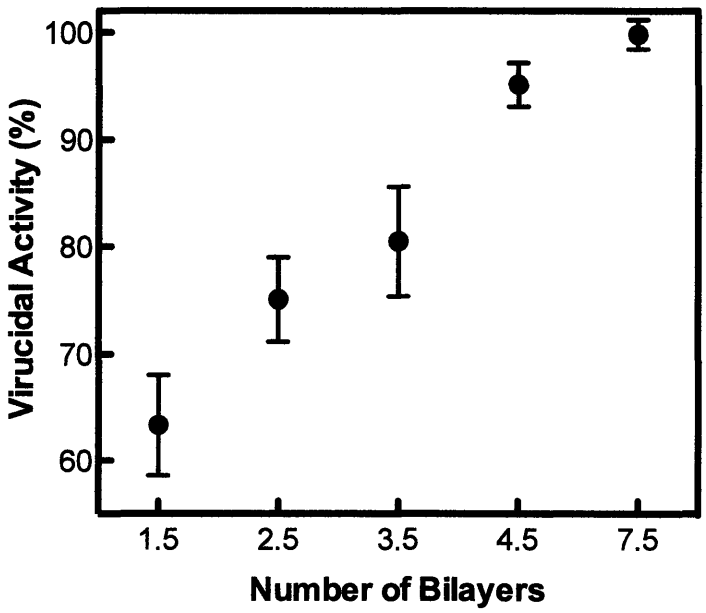

Figure 2-13: Virucidal activity of the $(DMLPEI/PAA)_n$ LbL films prepared from PAA at pH 3.0 against influenza A/WSN/H1N1 virus.

SEM images of the initial layers of our films show that as the number of bilayers increases, the surface coverage of the films increases (Figure 2-14A). At a lower number of bilayers, there are areas on the surface not covered by the film; this patchiness can enable a virus particle (~100 nm) to land on bare surface regions and thus not be inactivated. This bare spot is too small to fit a bacterium (~1 μm), thus 100% bactericidal activity is achieved even for films with low numbers of bilayers.

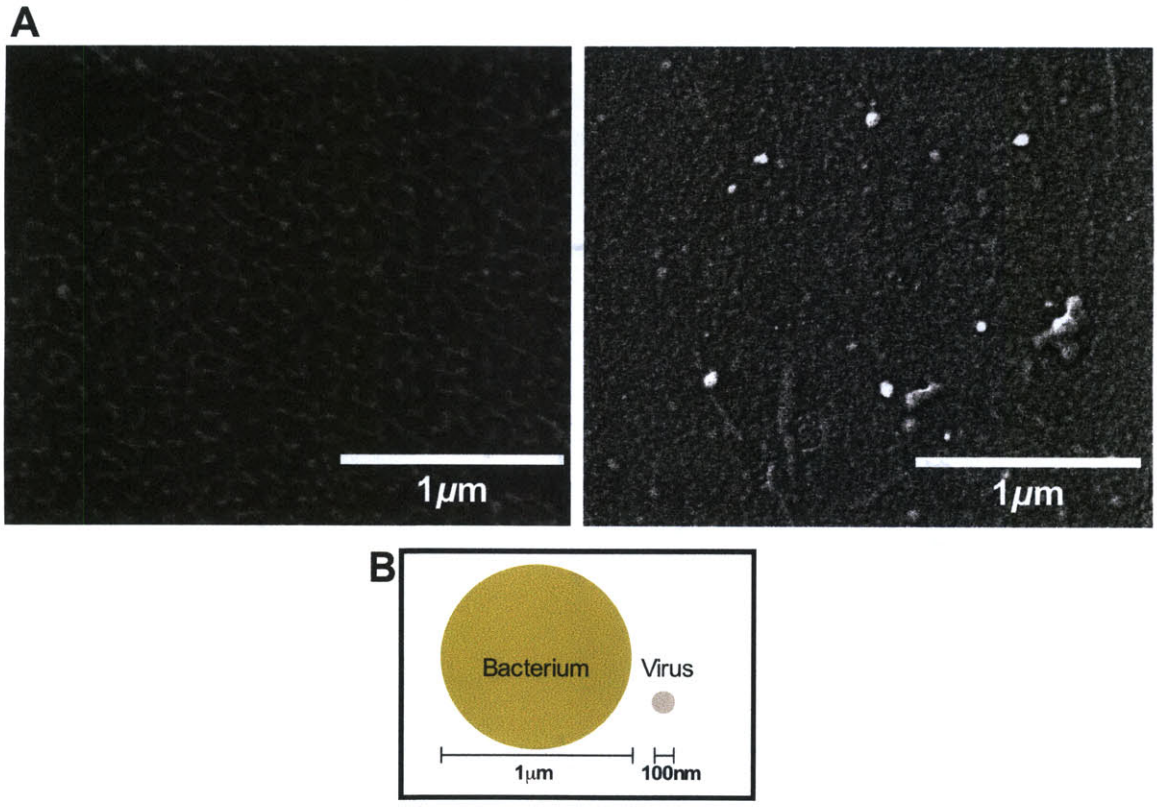

Figure 2-14: A) SEM images of 2.5 and 7.5 bilayers $(DMLPEI/PAA)_n$ films prepared from PAA at pH 3.0, showing the increase in surface coverage of films with increasing number of bilayers; B) Relative size of a bacterium to a virus particle.

2.3.4 Cytotoxicity, Non-leaching and Adhesion Tests of LbL Films

To test the safety of our microbicidal LbL films, we observed mammalian cell viability when seeded on coated surfaces. To this end, an *in-vitro* cytotoxicity assay with Murine pre-osteoblast cells (MC3T3) was performed with $(DMLPEI/PAA)_{1.5}$ and $(DMLPEI/PAA)_{2.5}$ films formed at pH 3.0 using an uncoated substrate as control. The cell viability on our films was found to be indistinguishable from that on the uncoated surface, indicating that there is no apparent cytotoxicity associated with our films from this study (Figure 2-15).

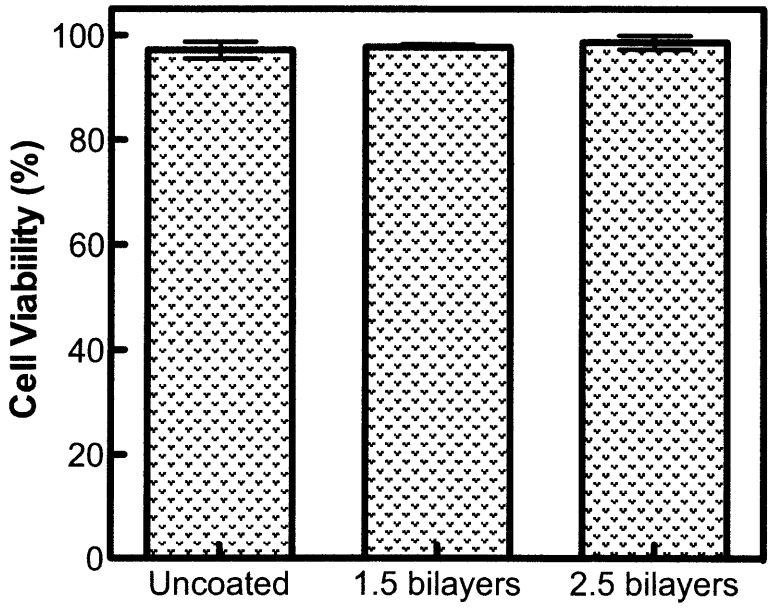

Figure 2-15: Cell viability on uncoated versus film-coated substrate, showing no apparent cytotoxicity on the films.

The proposed mechanism for microbicidal action of DMLPEI is via a direct disruption of the microbes' membrane by hydrophobic polycationic chains upon contact with the film. [74] To

establish whether our LbL films also kill on contact, rather than by leaching the polycation, a modified Kirby-Bauer assay was performed. [14] No zone of inhibition was detected beyond the film boundaries (Figure 2-16) and only bacteria directly in contact with the film were killed.

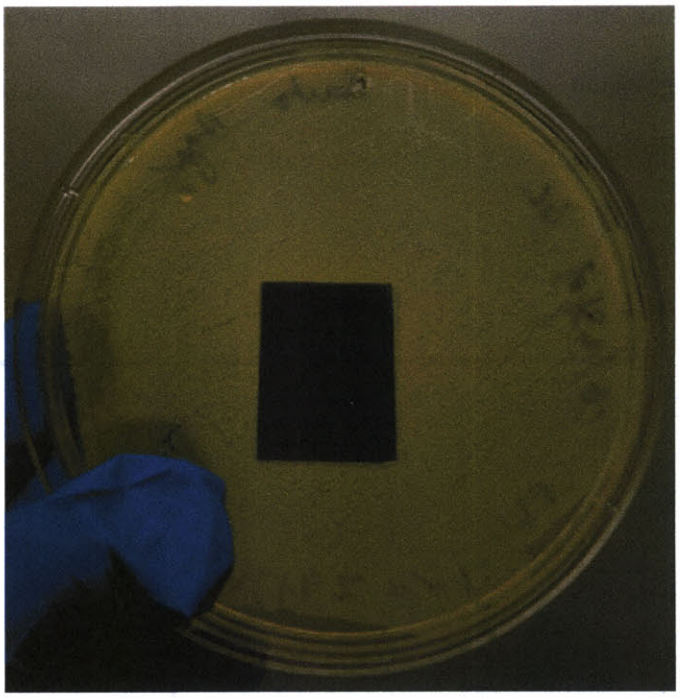

Figure 2-16: Non-leaching test with a $(DMLPEI/PAA)_{1.5}$ LbL film prepared from PAA at pH 3.0 on an agar plate streaked with *S. aurues*. No zone of inhibition is seen beyond the boundaries of the film. Cloudy white area is covered with bacteria colonies.

Finally, attaching a strip of 3M Scotch tape onto the surface of the film and removing it quickly in a single motion tested the mechanical integrity of our LbL films. The films before and after this experiment were tested for bactericidal activity against *S. aureus*. We observed no change in the activity of the $(DMLPEI/PAA)_{4.5}$ films, built with PAA at pH 3.0, demonstrating

their mechanical robustness. We also observed no difference in the measured film thickness before and after the adhesion test (20.3 nm ± 1.5nm).

2.4 Conclusions

We demonstrated herein that microbicidal functionality could be imparted onto surfaces using LbL technology by using the right combination of polycations and polyanions, as well as assembly and/or post-assembly conditions. We found that LbL films that are as thin as 10 nm were lethal to both airborne and waterborne Gram positive and Gram negative bacteria, as well as to a strain of influenza virus. Our films were effective in preventing bacterial attachment to surfaces, and thus indicate promising properties for prevention of biofilms on surfaces. While highly microbicidal, the LbL coatings were also found to be non-cytotoxic to a mammalian cell line based on cell viability assay. Coupled with their mechanical robustness, these properties bode well for practical potential of our LbL films where microbicidal and virucidal functionalities are required.

Chapter 3: Multifunctional Polyelectrolyte Multilayer Platform Film Coating Technology for Various Medical Implant Applications

Reproduced in part with permission from "Dual Functional Polyelectrolyte Multilayer Coatings for Implants: Permanent Microbicidal Base with Controlled Release of Therapeutic Agents" by Wong, S. Y., Moskowitz, J. S., Veselinovic, J., Rosario, R. A., Timachova, K., Blaisse, M. R., Fuller, R. C., Klibanov, A. M., Hammond, P. T. J Am Chem Soc, 132 (50), 17840-8, 2010. 10.1021/ja106288c, © 2010 American Chemical Society

3.1 Introduction

Recently, there has been great interest in developing drug-device combinations for medical applications, [114] including cardiovascular prostheses, [19,20] orthopedic implants, [2,21] stents, [22] biosensors, [115] and electrical leads. [116] The primary causes of implant failures, adverse foreign body response (FBR) and implant-related infection, could benefit from such combination therapies. FBR is initiated by protein adsorption onto the surface, which can trigger an inflammation cascade as a wound healing response to protect the body from foreign objects and may lead to fibrous encapsulation of the implanted device. [24, 117] Localized delivery of anti-inflammatory agents is still the most effective way to control inflammation and subsequent fibrosis. [118] Medical devices can thus be designed in combination with anti-inflammatory agents to achieve direct delivery to the surrounding tissues. Implant-associated infections can occur on any implanted medical device from minimally invasive contact lenses, to temporary urinary

catheters and endotracheal tubes, to permanent cardiac valves and orthopedic implants. [20] Pathogens are generally introduced to the implant surface by exogenous organisms on the skin, non-sterile surgical tools, or the local environment. Again, by designing the medical device with microbicidal functionality should reduce the infection rate. Perhaps most importantly, systemic bacteria circulating in the bloodstream can spontaneously become pathogenic upon attachment to the implant surface at any time (even years) after implantation. This necessitates a drug-device combination that yields long-term prevention of bacterial attachment while being capable of eliminating pre-existing infection. Thus due to considerable benefits from the use of drug-device combinations, the design of a robust platform to incorporate additional therapeutic value into existing medical implants is compulsory.

Implant failure due to device-associated infection adds up to approximately 1 million cases annually. [119] Of these, catheter-associated urinary tract infection accounts for about 40% of all nosocomial infections [120] and orthopedic implant-related infections ring up close to $2 billion in annual treatment procedures despite their lower infection rate. [119] Regardless of the implant type, the basic pathogenic mechanism for infection is that of bacterial colonization of the device surface, which can lead to the development of a biofilm, a matrix of sessile bacteria consisting of about 15% bacterial cells by mass and 85% hydrophobic exopolysaccharide fibers. [24] Biofilms can damage surrounding tissues and generate planktonic bacterial cells spreading infection. [26] The biofilm environment protects the bacteria from being easily targeted by normal therapeutic levels of antibiotics. [26, 121]

Current engineering approaches to biofilm control include the use of drug-device combinations that elute antibiotics locally in an effort to eradicate planktonic bacteria before biofilm formation and employ ultrasonic energy [122] or weak DC field [123] to disrupt an existing

biofilm, hence making it more susceptible to standard treatment. As the search for biofilm-resistant materials continues, the release of local antibiotics from implant surfaces remains the most common strategy for prevention; however, the standard release kinetics of many antibiotic-releasing systems is problematic. Generally, the initial burst-release phase is efficacious in achieving eradication of an existing infection; however, this is often followed by a monotonically decreasing rate of elution that eventually exposes any persistent bacteria to sub-lethal concentrations of antibiotic, hence allowing the development of resistant strains. In theory, having a permanent microbicidal surface coating that does not lose its functionality would prevent bacterial attachment and thus biofilm formation.

Polyelectrolyte multilayer (PEM) films have been studied extensively for applications in drug delivery. [3,14,15] They can be easily incorporated onto the surfaces of implants to provide controlled and localized drug delivery of therapeutic agents. In the present work, films are constructed using the layer-by-layer (LbL) deposition technique, [33] in which oppositely charged species are adsorbed sequentially onto an initially charged substrate. PEM films are simple and economical to fabricate and can be built on most geometries with nanometer scale control over thickness and surface properties. [31,33] Consequently, the amount of material loaded is highly tunable, which is attractive for drug delivery because many treatment regimens overload the body with drug in hope that a small amount of it will actually be delivered to a specific area of the body. Owing to its versatility, LbL technology has been applied to a broad range of fields including drug delivery, [2,3,14,47,92,93] membranes and electrodes for energy applications, [6,7,94] and electro- or magneto-responsive surfaces. [9-11,95]

Previously, we have demonstrated the use of hydrolytically degradable polycations in multilayers for both sustained and designed substantive bolus release of small-molecule drugs

from surfaces. [2, 3] Here we present a bifunctional film technology made of a permanent microbicidal PEM thin film combined with a hydrolytically degradable PEM film capable of incorporating and releasing various therapeutic agents. This architecture imparts the surface of the implant with a microbicidal base film [124] that is biofilm-resistant, with the added advantage of either a bolus delivery of an antibiotic to eradicate infection [2] or sustained delivery of an anti-inflammatory drug to minimize FBR at the implant site [3] as two examples demonstrating the versatility of this platform technology. While previous works have demonstrated multiple functionality in a single construct, [53, 125] thin film technology that exhibits highly adaptable dual functionality, such as long-term biofilm prevention with tunable release of various therapeutic agents depending on the application at hand, as presented in this work, is rare. Most previous dual-action antimicrobial systems exhibit diffusion-based release of a biocide (e.g., silver nanoparticles) and contact-killing or bacteria-repelling capabilities. [53, 125] Therefore, the constructs proposed in this work are promising as next-generation surface coatings for implants.

3.2 Materials and Methods

3.2.1 Materials

Poly(2-ethyl-2-oxazoline) (M_w = 500 kDa), 1-bromododecane, iodomethane, *tert*-amyl alcohol, poly(acrylic acid) (PAA; M_n = 239 kDa), poly(sodium 4-styrenesulfonate) (PSS; M_w = 70 kDa), 3 M sodium acetate buffer (NaOAc; pH 5.2), as well as solvents and common buffers, were from Sigma-Aldrich (St. Louis, MO). PAA (M_w = 50 kDa) and linear polyethylenimine (LPEI; M_n = 25 kDa) were from Polysciences (Warrington, PA). 1,4-Butanediol diacrylate, 1,6-hexanediol diacrylate, and 4,4-trimethylenedipiperidine were from Alfa Aesar (Ward Hill, MA).

Poly (carboxymethyl-β-cyclodextrin) (PolyCD) was from CTD (High Springs, FL). Diclofenac Na salt was from TCI America (Portland, OR) and gentamicin sulfate (GS) and phosphate-buffered saline (PBS; pH 7.4, 137 mM NaCl, 2.7 mM KCl, 10 mM Na_2HPO_4) from Mediatech, Inc. (Herndon, VA). Tritium-labeled gentamicin (^{3}H-GS; 250 μCi total, 1 mCi/mL in ethanol, 200 μCi/mg) was from American Radiolabeled Chemicals (St. Louis, MO). Silicon wafers (test grade n-type) were from Silicon Quest (Santa Clara, CA). Cation-adjusted Mueller Hinton Broth II (CMHB) and BactoAgar were from Difco BD (Franklin Lakes, NJ). Alpha minimum essential medium (α-MEM), fetal bovine serum (FBS), penicillin/streptomycin solution, fluorescein-conjugated albumin from bovine serum (BSA), MTT (tetrazolium [3-(4,5-dimethylthiazol-2-yl)-2,5-diphenyltetrazolium bromide) assay kit, and Live/Dead Viability/Cytotoxicity kit for mammalian cells were all from Invitrogen (Carlsbad, CA). Bovine plasma (IBV-N) was purchased from Innovative Research (Novi, MI). All reagents were used without further purification.

3.2.2 Synthesis of Polymers

Poly(β-amino ester)s Poly 1 and Poly 2 (structures shown in Figure 3-1) were synthesized as previously described. [65] Briefly, a solution of 4,4-trimethylenedipiperidine (34.1 mmol) in 50 mL of anhydrous tetrahydrofuran (THF) was added to the diacrylate monomer (34.1 mmol) dissolved in an equal volume of the same solvent. The reaction mixture was purged with nitrogen and stirred for 48 h at 50°C. Afterwards, the reaction mixture was cooled to room temperature and precipitated into cold hexanes. Polymers were collected via filtration.

Linear *N*,*N*-dodecyl,methyl poly(ethyleneimine) (DMLPEI; structure shown in Figure 3-1) was synthesized as previously described. [71] In short, LPEI (M_w of 217 kDa) was produced in house by deacylation of 500 kDa poly(2-ethyl-2-oxazoline); [99] the product was dissolved in

water, precipitated with aqueous KOH, filtered, and washed repeatedly with water. The resulting deprotonated LPEI was alkylated first with 1-bromododecane (96 h at 95°C) and then with iodomethane (24 h at 60°C) to produce DMLPEI. Polymers were collected and dried under vacuum prior to NMR analyses

3.2.3 Preparation of Polyelectrolyte Solutions for Film Deposition

Solutions of Poly1, Poly2, GS, and PAA were prepared at 2 mg/mL, and PolyCD at 20 mg/mL in 0.1 M NaOAc. Diclofenac powder was dissolved into the PolyCD solution to achieve a final concentration of 1.4 mg/mL, thus yielding complexation of diclofenac with polyCD. Dipping solution of DMLPEI was prepared at 1 mg/mL in 1-butanol. Poly1, GS, and PAA solutions were adjusted to pH 5.0 while those of Poly2 and PolyCD to pH 6.0. For films used in release experiments, the GS solution was spiked with 5 μL of ^{3}H-GS per 50 mL of dipping solution yielding a 0.1 μCi/mL product without significantly changing the concentration of the GS dip bath. LPEI and PSS dipping solutions were prepared at 2 mg/mL in water and adjusted to pH 4.25 and 4.75, respectively, with 1 M NaOH and 1 M HCl. All solutions were prepared with water from a Milli-Q Plus (Bedford, MA) at 18.2 MΩ.

3.2.4 LbL Film Assembly

As previously described, [124] LbL films were assembled on silicon substrates using a programmable Carl Zeiss HMS slide stainer. Substrates were cleaned with methanol and ultra pure water, dried under N_2, and plasma-etched in O_2 using a Harrick PDC-32 G plasma cleaner on high radiofrequency for 1 min, and then immediately immersed into the first polycation solution (i.e., DMLPEI or LPEI) for at least 10 min. Samples were prepared with nondegradable bilayers of either the bactericidal DMLPEI/PAA or the non-bactericidal LPEI/PSS. For the

former, a cascade rinse cycle of three butanol rinse baths (1 min, 30 s, 30 s), followed by three water baths (1 min, 30 s, 30 s) was used after deposition of DMLPEI, and the reverse cycle of water then butanol after PAA. For the latter, a cascade rinse cycle of three water baths (10 s, 20 s, and 30 s) was used after each polyelectrolyte dipping.

For combination films incorporating PolyCD complexed with diclofenac (PolyCD-DIC), 10 bilayers of $(DMLPEI/PAA)_n$ were deposited first, [124] followed by deposition of bilayers of $(Poly2/PolyCD\text{-}DIC)_n$ (where n denotes the number of bilayers), as previously described. [3] The architecture $(DMLPEI/PAA)_{10}(Poly2/PolyCD\text{-}DIC)_{20}$ was used for drug release and film degradation studies. For characterization of the growth of $(Poly2/PolyCD\text{-}DIC)_n$ films on top of $(DMLPEI/PAA)_{10}$ films, $(Poly2/PolyCD\text{-}DIC)_n$ films with n = 5, 10, 15, 20, and 30 bilayers were built (Figure 2).

As for the combination film incorporating GS, $(Poly\ 1/PAA)_5$ was first deposited onto $(DMLPEI/PAA)_{10}$ to facilitate uniform buildup of subsequent GS-containing films. Then deposition of the tetralayer architecture $(Poly1/PAA/GS/PAA)_n$ was performed as previously described.[2] Films with $(DMLPEI/PAA)_{10}(Poly1/PAA)_5(Poly1/PAA/GS/PAA)_{20}$ were used for drug release and film degradation studies. Characterization of the growth of $(Poly1/PAA/GS/PAA)_n$ films on top of $(DMLPEI/PAA)_{10}(Poly1/PAA)_5$ films, was done with n = 5, 10, 15, 20 and 30 (Figure 2). As a control in the efficacy studies comparing films with the bactericidal base layer functionality (i.e., $(DMLPEI/PAA)_{10}$) to those without bactericidal functionality, the architecture $(LPEI/PSS)_{10}(Poly1/PAA/GS/PAA)_{20}$ was used.

3.2.5 Characterization of Film Growth, Degradation and Drug Release

After film deposition, all films were allowed to air dry. For film growth, thicknesses of the $(DMLPEI/PAA)_{10}(Poly2/PolyCD\text{-}DIC)_n$ films were measured using a spectroscopic

ellipsometer (Woollam M-2000D). All thickness measurements were made at five different points on each film and averaged over three separate films. Roughness measurements of films were generated using a surface profilometer (KLA Tencor P-16). Thickness measurements of films were verified using the surface profilometer. In the case of $(DMLPEI/PAA)_{10}(Poly1/PAA)_5(Poly1/PAA/GS/PAA)_n$ combination films, both thickness and roughness measurements were performed by profilometry at four predetermined locations per film using a Veeco Dektak 150 surface profiler and averaged over three separate films.

For drug release and degradation studies with diclofenac combination films, samples were stored at 4°C until use. All measurements were conducted in triplicates. For drug release, each $(DMLPEI/PAA)_{10}(Poly2/PolyCD\text{-}DIC)_{20}$ film was immersed in 1 mL of in a sealed microcentrifuge tube and incubated at 37°C to simulate physiological conditions. At each time point, each film was moved into a new tube with 1 mL of fresh PBS; released drug was quantified with fluorescence spectroscopy (Quantamaster Fluorimeter; PTI, Lawrenceville, NJ). Film degradation was also performed at 37°C in PBS; at various time points, each film was removed, dried under N_2, and thickness measured using a spectroscopic ellipsometer at five different points on the surface of the film. Immediately after measurement, each film was re-immersed in PBS and resealed.

For drug release experiments with combination films incorporating GS, samples were immersed into 20 mL of PBS in a tightly capped Falcon tube maintained at 37°C. Degradation environments were kept sealed to minimize evaporative loss. A 1 mL sample was extracted from the Falcon tube at each predetermined time point and mixed with 5 mL of ScintiSafe Plus 50% (Fisher Scientific, Atlanta, GA) prior to GS quantification. The resulting mixtures were analyzed using a Tricarb Model 2810 TR liquid scintillation counter (Perkin Elmer, Waltham,

MA). The raw data in disintegrations per minute (DPM) were converted directly to μg of drug using the DPM value for the dipping solution (2 mg/mL). Total release from the film at the ith timepoint was calculated by the following equation:

$$m_i = (C_i V_i) + (1\ \text{mL}) \sum_{n=1}^{i-1} C_i$$

where m_i (μg) is the the total cumulative mass of GS released from the film at the time of measurement i, C_i (μg/mL) is the concentration of sample i (which is multiplied by the total volume V_i remaining in the Falcon tube as of the ith measurement), and the summation term adds up the total extensive quantity of gentamicin removed in each of the i-1 former aliquots. Accompanying degradation experiments were conducted by immersing samples into 10 mL of PBS in a tightly capped Falcon tube maintained at 37°C. At each time point, films were removed from the PBS and allowed to air-dry. All dry state thicknesses were determined via profilometry at four locations and averaged over at least three films.

3.2.6 Determination of Activity of Diclofenac Released from Film

In order to determine whether the diclofenac released from $(DMLPEI/PAA)_{10}(Poly2/PolyCD\text{-}DIC)_{20}$ was still active, a cyclooxygenase (COX) enzyme inhibition screening kit was purchased from Cayman Chemicals (Ann Arbor, MI). This assay measures the amount of the highly fluorescent compound resorufin, which is a product of the reaction between hydroperoxy endoperoxide prostaglandin G_2 (PGG_2) and 10-acetyl-3,7-dihydroxyphenoxazine (ADHP). Presence of a COX inhibitor (i.e., diclofenac) would reduce or eliminate the production of resorufin; hence activity of diclofenac can be correlated to the amount of resorufin produced. Samples from the temporal drug release experiment were assayed

against control samples containing no drug, 44 μM drug, and uncomplexed PolyCD (i.e., no diclofenac). The assay was performed according to the manufacturer's specifications.

3.2.7 Bactericidal Activity of Films

The bacterial strains used herein were *Staphylococcus aureus* (*S. aureus*; ATCC 25923) and GS-resistant *S. aureus* (ATCC 33592). After complete degradation of (Poly2/PolyCD-DIC)$_{20}$, the bactericidal activity of the underlying (DMLPEI/PAA)$_{10}$ film was tested using a mediaborne assay [124] and Kirby-Bauer assay, [14] each as previously reported. All experiments were done in triplicate.

Briefly, for the media-borne assay, *S. aureus* was grown overnight at 37°C in CMHB. The culture was then centrifuged at 2,700 rpm for 10 min, washed, resuspended in fresh CMHB media, and diluted to 10^6 cells/mL. Film-coated substrates were compared to blank Si controls by incubating with the bacterial broth at room temperature for 15 min, 30 min, 1 h, and 2 h promoting bacterial adhesion onto the surface. Samples were rinsed thrice in fresh CMHB media and incubated overnight at 37°C under a solid slab of agar made from CMHB media and BactoAgar. In the separate long-term experiment, bacterial solution was incubated at 37°C with either bare Si, or (DMLPEI/PAA)$_{10}$, or (DMLPEI/PAA)$_{10}$(Poly2/PolyCD)$_{20}$ in separate Petri dishes for a period of two weeks. The pH of the bacterial growth medium was about 7.4, which promoted the degradation of the (Poly2/PolyCD)$_{20}$ film on top of the (DMLPEI/PAA)$_{10}$ film. Every three days, the solution in each Petri dish was refilled with 2 mL of fresh CMHB media to replace fluid loss due to evaporation in the incubator, and to provide fresh nutrient for the bacteria to thrive. After the two weeks, each sample was removed and rinsed three times with fresh medium to remove any nonspecifically bound bacteria from the surface. Each sample was then incubated under a slab of agar overnight and bacteria colonies counted as described earlier.

In a separate experiment, to determine if protein adsorption would compromise the microbicidal activity of $(DMLPEI/PAA)_{10}$ films, the films and blank silicon substrates were incubated in 100 μg/mL fluorescein-conjugated albumin solution at 37°C for 1 h. Films were then removed, rinsed thrice in fresh PBS, and imaged via fluorescent microscopy. Films and blank substrates were also incubated in bovine blood plasma at 37°C for 1 h. Both sets of samples were further tested with the mediaborne assay detailed earlier using the 2 h incubation time.

For Kirby-Bauer assay, *S. aureus* was grown overnight at 37°C in CMHB; agar plates were then streaked with exponentially growing *S. aureus* at 10^8 cells/mL. Blank Si, $(DMLPEI/PAA)_{10}$, $(DMLPEI/PAA)_{10}(Poly2/PolyCD\text{-}DIC)_{20}$, and $(DMLPEI/PAA)_{10}$ after complete degradation of $(Poly2/PolyCD\text{-}DIC)_{20}$ were placed film side down on the agar plates and incubated overnight at 37°C.

For films releasing GS, Kirby-Bauer assays were performed with *S. aureus* comparing blank Si, contact-killing $(DMLPEI/PAA)_{10}$, release-killing $(LPEI/PSS)_{10}(Poly1/PAA/GS/PAA)_{20}$, and dual functional $(DMLPEI/PAA)_{10}(Poly1/PAA)_5(Poly1/PAA/GS/PAA)_{20}$ after increasing degradation times of $(Poly1/PAA/GS/PAA)_{20}$. Zones of inhibition (ZOI) were imaged. To further distinguish the unique functionality of the nondegradable, contact-killing $(DMLPEI/PAA)_{10}$ surface, a GS-resistant strain of *S. aureus* was used to perform a separate Kirby-Bauer assay.

3.2.8 Quantification of Blood Plasma Adsorption Using Quartz Crystal Microbalance (QCM)

A Masscal G1 (quartz crystal microbalance) was used for quantification of protein adsorption onto surface of the microbicidal base film relative to an uncoated crystal. Film was deposited onto 1-inch quartz crystals (5-MHz frequency) with gold electrodes (Tangidyne Corp.,

SC). The frequency of the blank crystal was recorded before film deposition; frequency of the film-coated crystal was recorded again after film deposition (dried with N_2). Both blank and film-coated crystals were then incubated in bovine blood plasma (density of approximately 1,025 mg/mL) at 37°C for 1 h; the crystals were then rinse thrice in fresh PBS then dried with N_2. The frequency of the crystals was recorded again after protein adsorption. Upon protein adsorption, the oscillatory motion of the crystal declined, and the decreased resonant frequency was measured. The Sauerbrey equation was used to relate the change in frequency to mass adsorbed per unit area (17.7 ng cm^{-2} Hz^{-1} for 5-MHz crystals). [126] Although the Sauerbrey relation (for rigid layer) is not strictly true for adsorption of protein due to viscoelastic property of the protein adlayer, it can be used as an approximation to compare relative amounts of protein adsorbed between the blank and film-coated crystals. The experiments were done in triplicate.

3.2.9 In-vitro Cytotoxicity Assay: Adhesion and Proliferation of Cells

Films were tested with human pulmonary epithelial cancer cells (A549), murine pre-osteoblast cells (MC3T3-E1), and murine macrophage cells (Raw264.7) which were seeded on $(DMLPEI/PAA)_{10}$ or uncoated glass slides. In all cases, cells were grown in α-MEM supplemented with 10% FBS and 1% penicillin/streptomycin at 37°C with 5% CO_2. Substrates were placed in the bottom of 6-well plates and each well seeded with 150,000 cells and 3 mL of media. To investigate cell adhesion to the surface of our films, two sets of experiments were performed in parallel: cells in media with FBS and without FBS. Cells were cultured for 6 h on substrates, and cell adhesion investigated by examining morphology by light microscopy; for metabolic activity (via MTT assay), the cells were cultured on samples for 3 h in normal growth media, and 3 h in growth media containing 10% MTT. Substrates were transferred to new 6-well plates to quantify only those cells which were adherent to the substrate. One mL of dimethyl

sulfoxide was added to solubilize the resulting purple formazan crystals, 100 μL aliquots from each sample were placed into a 96-well microtiter plate, and absorbance was measured at 570 nm with a 690 nm correction. All samples were measured in triplicate. Cell metabolic activity was calculated relative to the negative control (uncoated glass slide). Proliferation experiments requiring the same experimental procedure were conducted on the same set of films at days 1, 3, and 7 in FBS-enriched media.

3.3 Results and Discussion

3.3.1 Design of Combination Films with Dual Functionality

We set forth to design a dual functional combination film technology that is highly adaptable and broadly applicable to various thin film medical device coating specifications. The charged multilayer film components, shown in Figure 3-1, include poly (acrylic acid), degradable poly (β-amino ester)s (PBAEs), charged poly (cyclodextrins) complexed with diclofenac (PolyCD-DIC), and linear *N,N*-dodecyl,methyl-poly(ethylenimine) (DMLPEI).

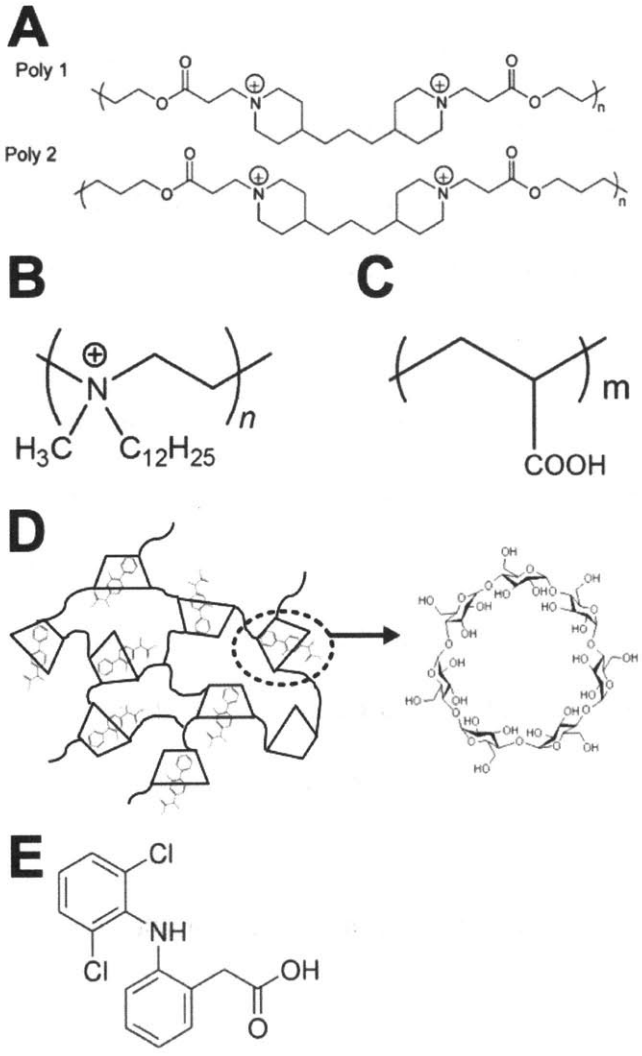

Figure 3-1: A) Structure of hydrolytically degradable poly(β-amino ester)s, Poly1 and Poly2. B) Structure of microbicidal linear *N,N*-dodecyl,methyl-PEI (DMLPEI). C) Poly(acrylic acid) (PAA). D) Schematic of poly(β-cyclodextrin) with drug sequestered in the interior of its monomer unit, as well as a close-up structure of a monomeric β-cyclodextrin. E) Structure of diclofenac.

The dual functional LbL films consisted of a thin permanent (nondegradable) microbicidal base film, $(DMLPEI/PAA)_{10}$, and a hydrolytically degradable top multilayer film incorporating cationic poly(β-amino ester)s[65] Poly1 or Poly2 (Figure 3-1A) capable of releasing

various drugs. The efficacy and versatility of this dual functional film architecture was demonstrated using two examples: (1) the small hydrophilic antibiotic gentamicin to eradicate infection at an implant site, and (2) the small hydrophobic anti-inflammatory drug diclofenac to assist with healing at the implant site. The permanent microbicidal base film was built up via electrostatic interaction between the hydrophobic polycation DMLPEI and PAA as the polyanion.

Poly(β-amino ester)s, such as Poly1 and Poly2, can undergo hydrolytic degradation at physiological conditions and have been incorporated into PEM films as an erodible component for controlled release. [2-4, 14, 15, 66, 127] Hydrolytic degradation of the poly-(beta)-aminoesters is impacted by access of water molecules to the hydrolyzable bond. Poly2, which has a longer alkyl chain length than Poly1 and hence a greater local hydrophobicity around the ester bond, exhibits a slower rate of hydrolysis. [66] Diclofenac, which is a small aromatic molecule is complexed with PolyCD, capable of sequestering hydrophobic drugs in the interior pockets of its cyclodextrin groups, while the negatively charged exterior allowed for stable bilayer growth of $(Poly2/PolyCD\text{-}DIC)_n$. [3] Gentamicin (GS) is a water-soluble aminoglycoside with five protonatable amine groups and therefore can be incorporated into PEM films; [2,14] however, since both it and Poly1 are positively charged at deposition conditions, a polyanion must be included to build up a stable film via electrostatic interactions. PAA was chosen because it promotes incorporation of a large quantity of GS into PEM films. [2] This results in a tetralayer film architecture of $(Poly1/PAA/GS/PAA)_n$. These combination films, schematically depicted in Figure 3-2, can be constructed with high loadings and designed to release gentamicin *ex vivo* and *in vivo* for periods ranging from hours to weeks. [2] It is also possible to construct a GS-releasing film with Poly2 instead of Poly1, and the same applies to the diclofenac releasing films. The

degradation and release kinetics of the film should be different, with faster release for a (Poly1/PolyCD-DIC)$_n$ film and slower release for a (Poly2/PAA/GS/PAA)$_n$ one.

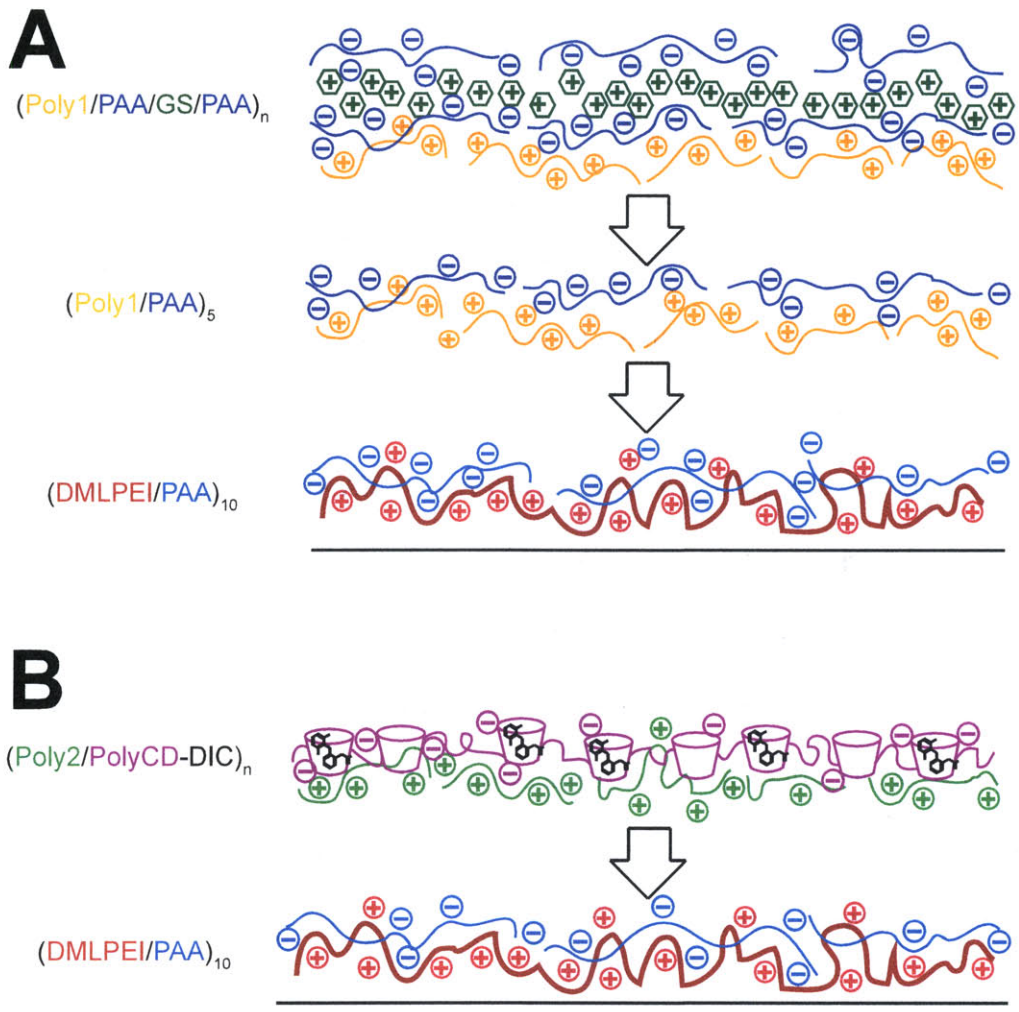

Figure 3-2: Schematic representation of the combination films in this work. A) Gentamicin releasing (Poly1/PAA/GS/PAA)$_n$, and B) diclofenac releasing (Poly2/PolyCD-DIC)$_n$ combination films, built on top of the microbicidal (DMLPEI/PAA)$_{10}$.

3.3.2 Characterization of the Combination Films: Growth, Erosion, and Release

To characterize the hydrolytically degradable films built on top of the microbicidal base film, three critical film characteristics were examined: growth, erosion, and release. The thickness and roughness of the microbicidal base film $(DMLPEI/PAA)_{10}$ — 26 ± 5 and 7 ± 4 nm, respectively, — were measured before buildup of the erodible $(Poly2/PolyCD\text{-}DIC)_n$ or $(Poly1/PAA)_5(Poly1/PAA/GS/PAA)_n$ films. Ten bilayers were used in the base film to achieve 100% microbicidal activity and provide a uniform platform for buildup of the subsequent drug-releasing layers. $(DMLPEI/PAA)_n$ films had previously been shown to exhibit an initial lag growth phase for which the film exhibited complete surface coverage only beyond 4.5 bilayers.[124] The thickness and roughness of the combination films of $(DMLPEI/PAA)_{10}(Poly2/PolyCD\text{-}DIC)_n$ and $(DMLPEI/PAA)_{10}(Poly1/PAA)_5(Poly1/PAA/GS/PAA)_n$ were then measured, and their growth curves are depicted in Figure 3-3A and Figure 3-3B. The $(Poly1/PAA)_5$ adhesion layer was deposited after the microbicidal base film to help initiate and facilitate uniform deposition of the $(Poly1/PAA/GS/PAA)_n$ film. The $(Poly1/PAA)_5$ adhesion layers increased the total thickness and roughness of the growing film to 75 ± 18 and 30 ± 13 nm, respectively. Without the intermediary layers of $(Poly1/PAA)_5$, we observed no film growth of $(Poly1/PAA/GS/PAA)_n$ directly on top of $(DMLPEI/PAA)_{10}$.

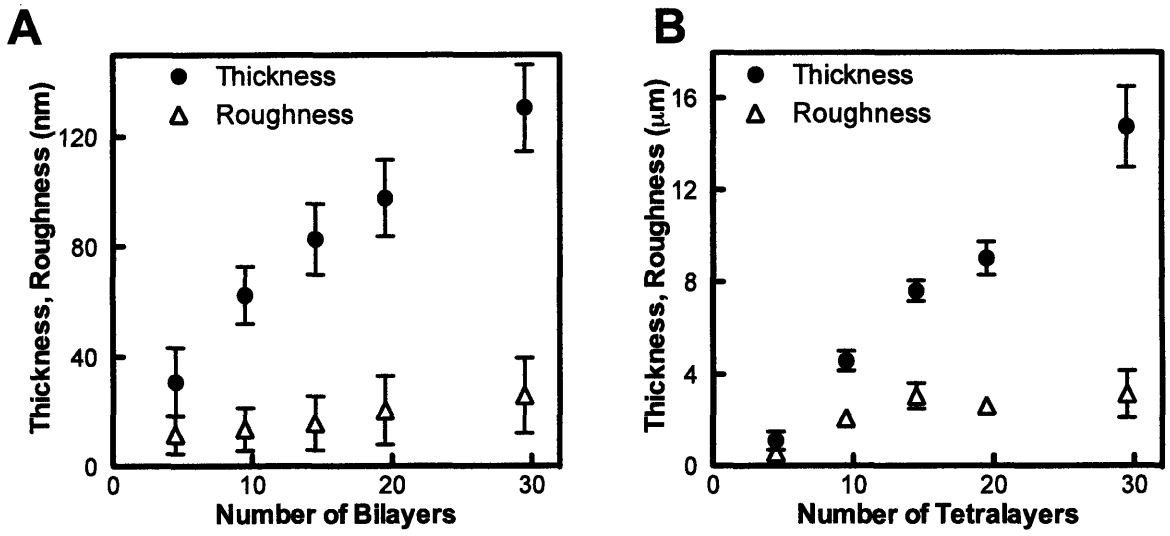

Figure 3-3: Thickness and roughness of A) (Poly2/PolyCD-DIC)$_n$ and B) (Poly1/PAA/GS/PAA)$_n$ films (note difference in y axis scale). All films were made on top of base film (DMLPEI/PAA)$_{10}$.

We hypothesized that the hydrophobic nature of the highly interpenetrated (DMLPEI/PAA)$_{10}$ film (water contact angle of 85° ± 2°) surface reduced the ability of the hydrophilic GS molecules to wet and adsorb onto the surface. Adding the buffer layers (water contact angle of 67° ± 3°) provided a more hydrophilic surface and reservoir for GS molecules to establish themselves within the film. Both sets of combination films exhibited linear growth; films incorporating diclofenac had nanometer-scale thickness (average of 3 ± 1 nm per bilayer), [3] as opposed to the much thicker GS-releasing films (0.50 ± 0.05 μm per tetralayer on average). Roughness of (DMLPEI/PAA)$_{10}$(Poly2/PolyCD-DIC)$_n$ films was relatively small compared to the film thickness. The micron-scale thickness and roughness of the GS-releasing films reported here had previously been observed; [2] we believe that this phenomenon is due to a significant interdiffusion of small, polar GS molecules within the film architecture during assembly, as well as both film dissolution and diffusion that occur during the deposition process. Futhermore, we

observed no turbidity in the dipping solutions throughout the fabrication process, which suggests the absence of aggregates. The film thickness increases faster than the surface roughness during film growth, and the roughness levels off at about 20 bilayers in both cases.

Having established that these combination films could be grown consistently and controllably, their degradation characteristics were investigated in a physiologically relevant environment (PBS, 37 °C). Degradation experiments were conducted with $(DMLPEI/PAA)_{10}(Poly2/PolyCD\text{-}DIC)_{20}$ and $(DMLPEI/PAA)_{10}(Poly1/PAA)_5(Poly1/PAA/GS/PAA)_{20}$ films. Diclofenac-releasing films exhibited a linear degradation profile over a period of 10 days (Figure 3-4A), which is characteristic for stable, surface-based erosion of degradable LbL films. [3] Degradation of GS-releasing films was also linear, but complete film erosion occurred within three to four hours (Figure 3-4B). The much faster erosion rate of the gentamicin-releasing film was due to the fact that the small molecular size of GS allows out-diffusion of drug from the film and subsequent destabilization of the assembled layers. For this reason, the mechanism for GS release is a combination of rapid small molecule diffusion, followed by film destabilization and polymer erosion. On the other hand, the $(Poly2/PolyCD\text{-}DIC)_n$ thin films are composed of two alternating polyelectrolytes that do not exhibit out-diffusion and for which the primary mechanism of erosion is Poly2 degradation. As mentioned before, these combination films were designed to provide sustained release of anti-inflammatory drug over days or bolus-style release of antibiotics over hours to address an existing infection. The resulting degradation profiles clearly align with the desired properties of each combination film.

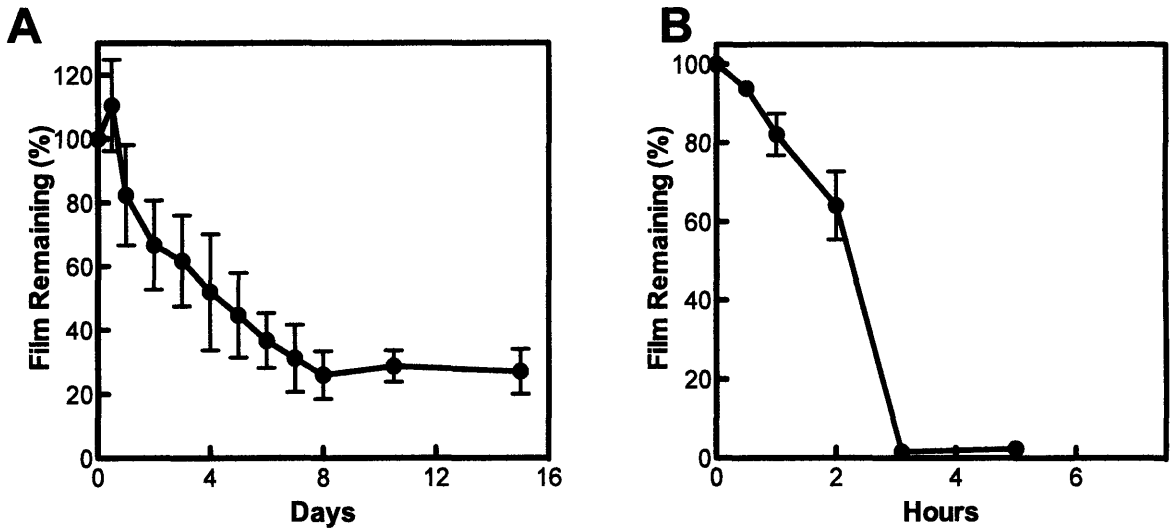

Figure 3-4: Degradation curves for A) (Poly2/PolyCD-DIC)$_{20}$ and B) (Poly1/PAA/GS/PAA)$_{20}$ films (note difference in x axis scale). All films were made on top of base film (DMLPEI/PAA)$_{10}$.

Release studies were performed with the same film architectures as in the degradation experiments. A major advantage of LbL systems is that the quantity of drug incorporated into each film can be tuned according to the total number of deposited layers thus making the LbL technology platform a versatile way to address many applications and drug delivery specifications. Approximately 8 μg/cm^2 of diclofenac was incorporated into (DMLPEI/PAA)$_{10}$(Poly2/PolyCD-DIC)$_{20}$, with sustained release over 10 days (Figure 3-5A). The GS-releasing (DMLPEI/PAA)$_{10}$(Poly1/PAA)$_5$(Poly1/PAA/GS/PAA)$_{20}$ films incorporated about 70 μg/cm^2 of the antibiotic and released over a timeframe similar to film degradation, with approximately 90% delivery during the first 2.5 h (Figure 3-5B); this burst release of antibiotic is critical to address an existing infection at an implant site by preventing re-propagation and biofilm formation. It should be noted that the underlying (DMLPEI/PAA)$_{10}$(Poly1/PAA)$_5$ film, without the topmost (Poly1/PAA/GS/PAA)$_{20}$ film, can load 6.3 ± 0.8 μg/cm^2 of GS via

absorption, showing that the small GS molecules are able to diffuse through the underlying layers of film.

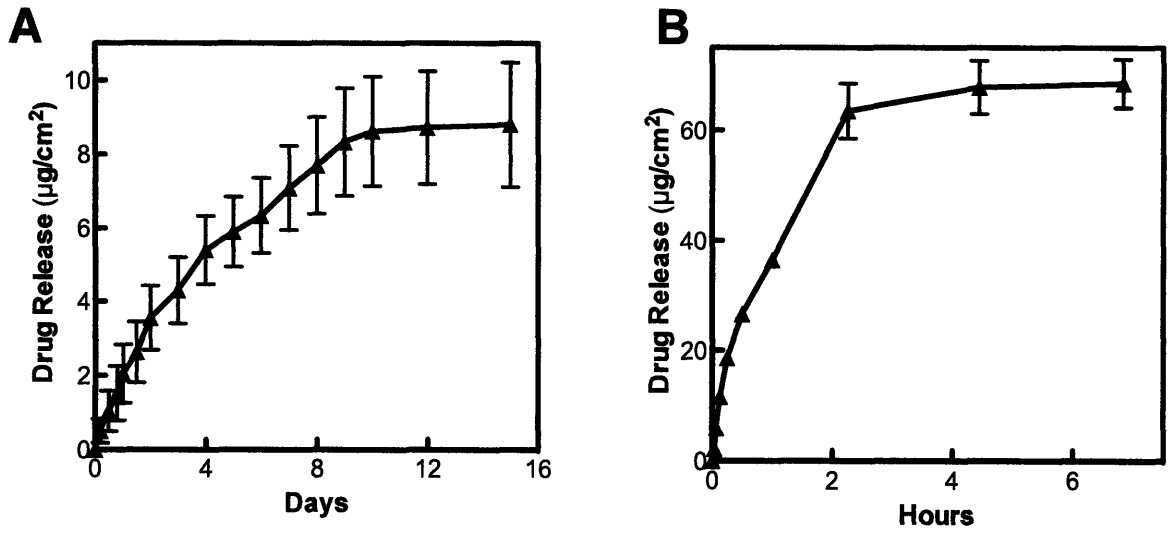

Figure 3-5: Drug release curves for A) (Poly2/PolyCD-DIC)$_{20}$ and B) (Poly1/PAA/GS/PAA)$_{20}$ films (note difference in x and y axis scales). All films were made on top of base film (DMLPEI/PAA)$_{10}$.

3.3.3 Activity of Drug Released from Combination Films

To confirm that the diclofenac, which was complexed with polyCD was still active after release, the inhibition of cyclooxygenase (COX) enzyme was investigated. COX is one of the enzymes responsible for the formation of prostaglandins, which affect inflammation and rate of return to homeostasis. [128, 129] As seen in Figure 3-6, release samples taken from a (DMLPEI/PAA)$_{10}$(Poly2/PolyCD-DIC)$_{20}$ film eluted from day 1 through day 9 (separate non-cumulative released samples) were effective in inhibiting the activity of COX when compared to the standard of uncomplexed diclofenac solution. This result showed that the activity of

diclofenac was not altered upon complexation with polyCD and can be maintained at levels sufficient to achieve complete COX inhibition in cell assays. Previous studies have shown that a significant amount of diclofenac released from this film construct remains complexed with polyCD, followed by its slow dissociation into solution. [3]

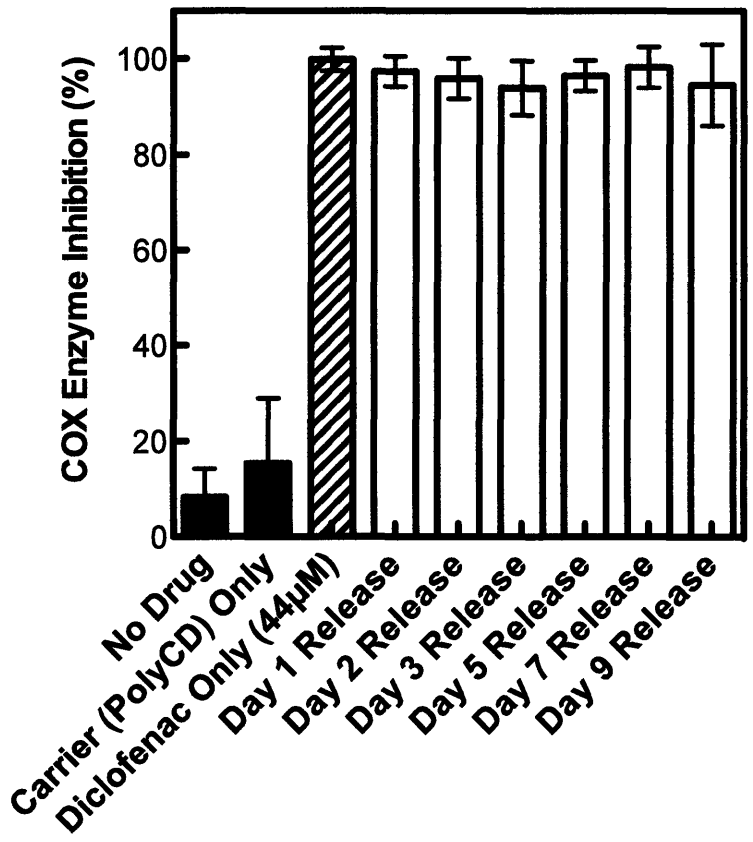

Figure 3-6: Percentage of COX enzyme inhibition showing that diclofenac released from $(DMLPEI/PAA)_{10}(Poly2/PolyCD\text{-}DIC)_{10}$ is still active. The released samples from day 1 to day 9 represent non-cumulative drug released from the film.

The microbicidal activity of the dual functional combination films with underlying DMLPEI base layers, namely $(DMLPEI/PAA)_{10}(Poly1/PAA)_5(Poly1/PAA/GS/PAA)_{20}$, was tested via Kirby-Bauer assays and compared to a control GS-releasing multilayer without an underlying antimicrobial base, namely $(LPEI/PSS)_{10}(Poly1/PAA/GS/PAA)_{20}$ (Figure 3-7). Zones of inhibition (ZOIs) were observed at 0 min, 15 min, and 2 days. Each time corresponds to the duration for which the sample was immersed in phosphate buffered saline (PBS) at 37°C prior to plating for the Kirby-Bauer assay. At early times (0 and 15 min), the ZOI of these two films are nearly identical. After 2 days, a smaller ZOI exists around the combination films; however, the control film no longer exhibits any ZOI. Since the microbicidal base film is non-erodible, it only kills bacteria directly in contact with it; the ZOIs around the erodible GS films are the direct result of GS released from the films, confirming its activity. As GS is eluted from the films, the ZOI gradually decreases. There appears to be more GS available for elution in the combination film, as observed by the ZOI at day 2, likely due to the added GS loading achieved via absorption of GS into the microbicidal base layers and the intermediate Poly1/PAA layers used to construct the film.

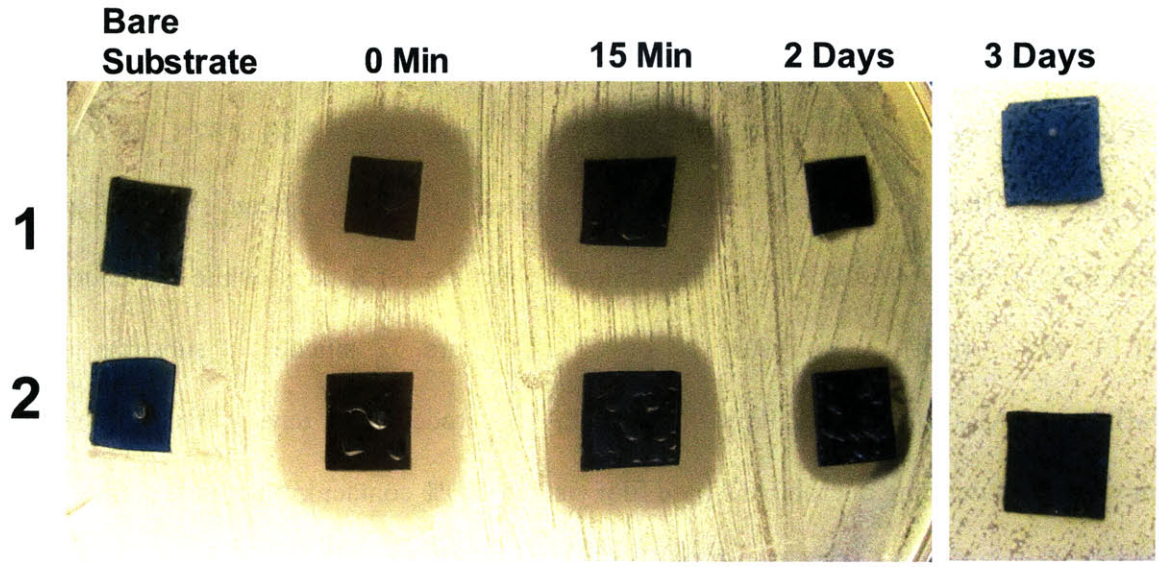

Figure 3-7: Kirby-Bauer assays of gentamicin (GS) releasing films eroded for various time periods, ranging from 0 min (as built) to 3 days; Row 1 represents GS films built on $(LPEI/SPS)_{10}$ base films and Row 2 those built on microbicidal $(DMLPEI/PAA)_{10}$ base films. Figure also shows a decrease in the size of zone of inhibition as time increases.

3.3.4 Bactericidal Activity of the Permanent Microbicidal Base Film

After the hydrolytically degradable top films were completely eroded, the newly exposed microbicidal $(DMLPEI/PAA)_{10}$ base films were shown to be still efficacious against *S. aureus* using Kirby-Bauer assays. Based on these assays and film degradation and elution curves, there is no more drug eluting from the film at day 3. As seen in Figure 3-7, the 3-day samples with the microbicidal base film show 100% direct contact killing of *S. aureus;* there is no ZOI present, but the region underneath the film indicates no bacterial growth on the surface of the substrate. On the other hand, the system with the standard base film of $(LPEI/SPS)_{10}$ exhibits no measurable efficacy in preventing bacterial growth on the surface relative to the uncoated silicon substrates. To further distinguish the unique functionality of the microbicidal base film from that

of any remaining GS, a GS-resistant strain of *S. aureus* was used to determine the efficacy of a completely eroded $(DMLPEI/PAA)_{10}(Poly1/PAA)_5(Poly1/PAA/GS/PAA)_{20}$ film *versus* $(LPEI/PSS)_{10}(Poly1/PAA/GS/PAA)_{20}$ (Figure 3-8) after immersion in PBS at 37°C for four days. The top row (left to right) of Figure 3-8 consisted of a bare silicon substrate and the $(LPEI/PSS)_{10}(Poly1/PAA/GS/PAA)_{20}$ film following erosion for 4 days, while the bottom row (left to right) consisted of a bare silicon substrate and $(DMLPEI/PAA)_{10}(Poly1/PAA)_5(Poly1/PAA/GS/PAA)_{20}$ eroded for 4 days. The 4-day released film with the underlying microbicidal base film yielded 100% contact killing, with similar results obtained for underlying $(DMLPEI/PAA)_{10}$ films exposed after complete degradation of the diclofenac-releasing films (Figure 3-9).

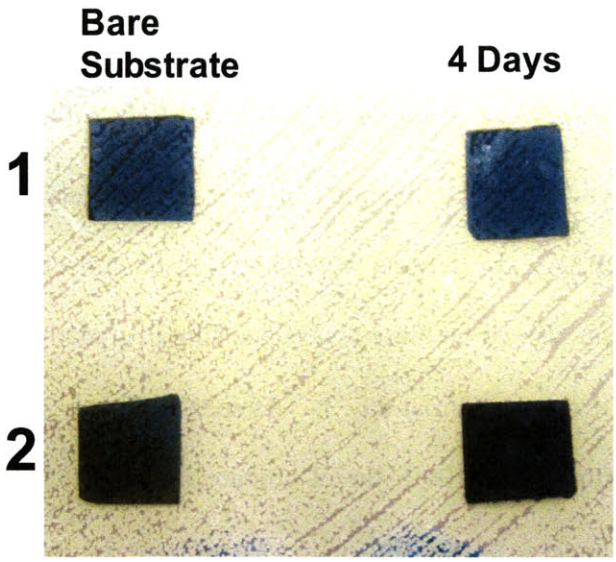

Figure 3-8: Row 1 represents GS films built on $(LPEI/SPS)_{10}$ base films and Row 2 those built on microbicidal $(DMLPEI/PAA)_{10}$ base films. Films eroded for 4 days and tested with GS-resistant bacteria to confirm the microbicidal base film functionality; the result shows that the microbicidal $(DMLPEI/PAA)_{10}$ base film (bottom right sample) is effective in killing the bacteria, while the $(LPEI/SPS)_{10}$ base film (top right sample) is not.

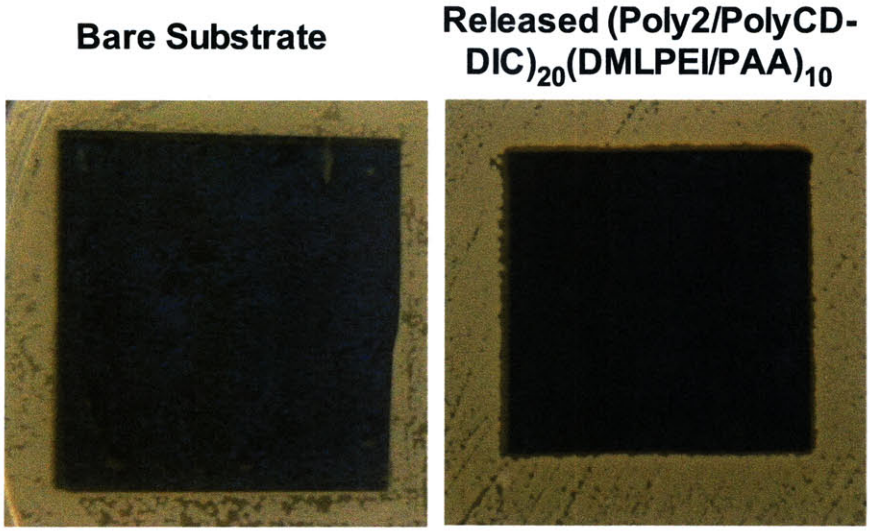

Figure 3-9: Similar results were obtained for (Poly2/PolyCD-DIC)$_{20}$(DMLPEI/PAA)$_{10}$ films that had been allowed to undergo complete drug release before testing, showing that microbicidal base film remains active. Note that the dark (black) colored substrate surfaces are bacteria-free, while the lighter beige colored substrate surfaces correspond to contamination by bacteria colonies (each dot corresponds to a colony forming unit).

As mentioned earlier, biofilm formation on the surface of an implant is a major cause of implant failure. Therefore, it is advantageous to prevent the formation of biofilms on the surface of medical implants in the first place. To this end, (DMLPEI/PAA)$_{10}$ films with completely eroded top films were tested against media-borne *S. aureus* and found to be effective in preventing bacterial attachment relative to blank silicon substrates (Figure 3-10). These film-coated substrates prevented colonization of their surfaces by bacteria for periods of time ranging from 15 min to 2 weeks, whereas bacteria significantly colonized blank silicon substrates after just a 15-min incubation.

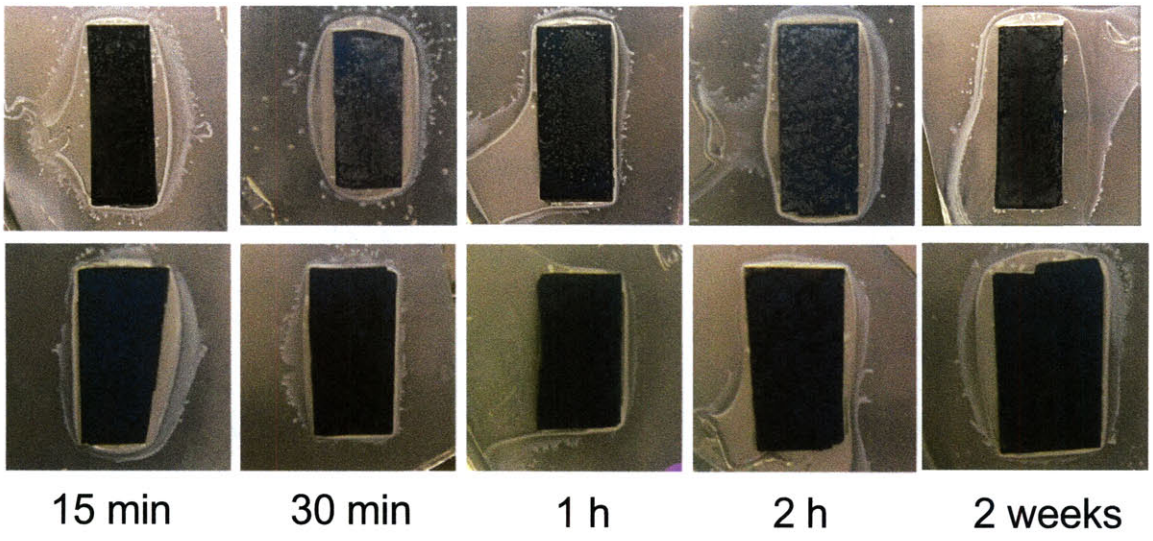

Figure 3-10: Mediaborne assay with *S. aureus* with increasing time of incubation in bacterial solution; top row shows bare substrates completely colonized by bacteria (light beige colored dots); bottom row shows $(DMLPEI/PAA)_{10}$ films with degradable top films completely eroded with no sign of colonization by bacteria (black colored substrate).

Another major issue with implants is protein adsorption from blood plasma onto implant surfaces, initiating a foreign body response; this is a common problem with medical implants which can happen within seconds of implantation[23] and elicit inflammatory responses. [23, 25, 130] Therefore, cells at the surface of biomaterials are not necessarily in direct contact with the material itself. To test whether the microbicidal functionality of our base film would be compromised by protein adsorption, $(DMLPEI/PAA)_{10}$-coated quartz crystals and blank crystals were incubated in solutions of bovine blood plasma for 1 h; the adsorption of protein was quantified using quartz crystal microbalance (QCM), and we found that almost no protein was adsorbed onto the surface of $(DMLPEI/PAA)_{10}$ coated crystals relative to blank crystals: 4.0 ± 1.0 $\mu g/cm^2$ on film-coated crystals versus 89.5 ± 14.2 $\mu g/cm^2$ on blank crystals (i.e. 22 times more adsorption of protein on blank crystals). This result was further confirmed with adsorption

of fluorescently tagged albumin on film-coated and blank glass slides (Figure 3-11). No albumin adsorption onto the surface of $(DMLPEI/PAA)_{10}$ coated films was observed whereas the blank glass slides were completely biofouled. This finding suggests that these films may prevent at least some common protein adsorption, likely due to a combination of hydrophillic and hydrophobic groups that present molecular-scale heterogeneities on the surface of the $(DMLPEI/PAA)_n$ system. [131, 132]

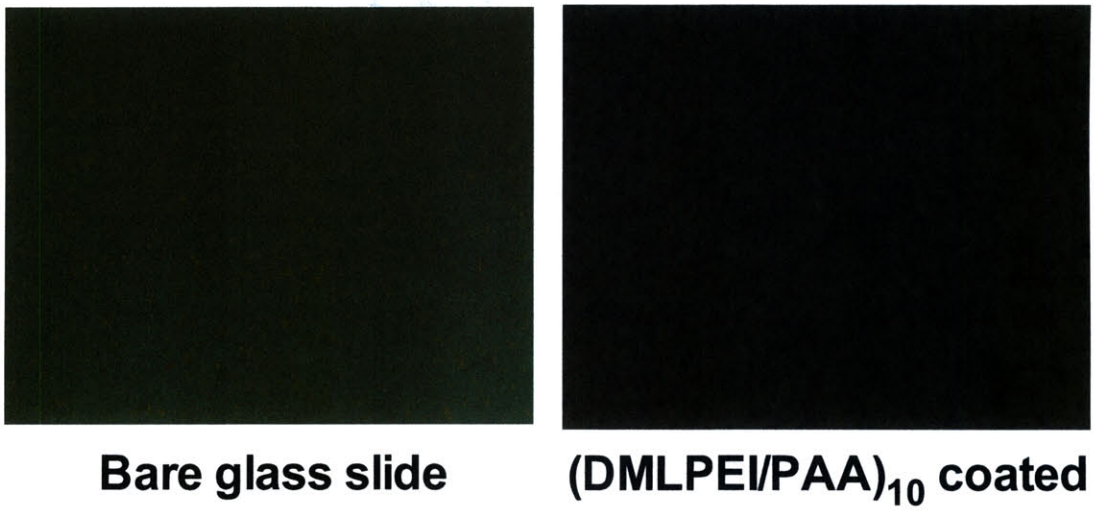

Figure 3-11: Fluorescently tagged albumin adsorption onto bare glass slide and $(DMLPEI/PAA)_{10}$ coated glass slide.

The protein-treated samples and controls made on silicon wafers were tested with the mediaborne assay (with a 2-h incubation time); film-coated substrates were still effective in preventing bacterial attachment (95 ± 3 % clear), while the blank substrates were heavily colonized (Figure 3-12). More importantly, protein-treated samples that were tested with the mediaborne assay for a period of 2 weeks remained highly effective in preventing bacterial

colonization; 88 ± 2% of the surface remained bacteria-free. Thus the permanent microbicidal base film functionality was not heavily compromised even in the presence of blood plasma and still prevented formation of biofilms.

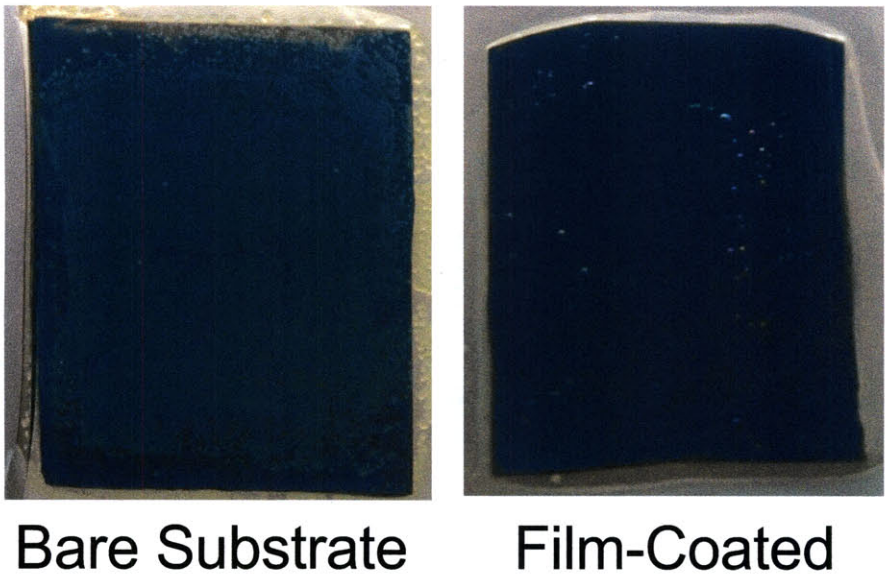

Figure 3-12: Mediaborne assay with *S. aureus* comparing bare substrate and $(DMLPEI/PAA)_{10}$ film after incubation in blood plasma for 1 h. The bare substrate shows complete colonization by bacteria (beige colored dots), while film-coated substrate remains uncolonized (black colored substrate).

3.3.5 Cytotoxicity, Adhesion and Proliferation of Cells on Films

To investigate the cytotoxicity and interaction of cells with our films, murine pre-osteoblast cells (MC3T3-E1) and human pulmonary epithelial cancer cells (A549) were seeded onto glass coated with $(DMLPEI/PAA)_{10}$ and uncoated glass as a control. There was no difference in cell adherence to film-coated substrates relative to uncoated glass slides in media with or without serum (Figure 3-13). The use of serum-free media ensured that the cells were

exposed to the surface of the films and not a protein-coated surface. An MTT assay, which measures metabolic activity of cells, was compared to cell morphology data and found to be consistent. Cell viability on the permanent microbicidal films was indistinguishable from that on blank glass slides, indicating no apparent cytotoxicity associated with these films.

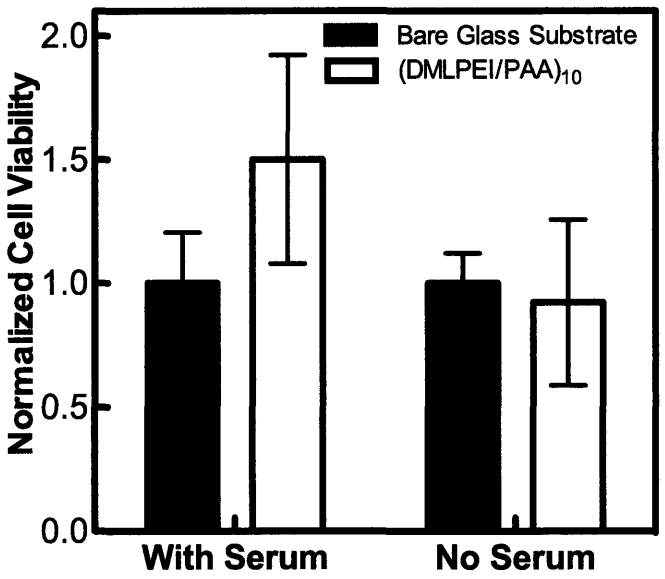

Figure 3-13: Cell viability of films relative to bare glass substrates indicating no apparent cytotoxicity of the films. Cells were grown in media with or without serum. Note that the difference in cell viability shown is not statistically significant (t-test p values of 0.36 and 0.84 for data with serum and without serum respectively).

Cell proliferation was investigated with $(DMLPEI/PAA)_{10}$ films. MTT assays of cells seeded and cultured on films for 1, 3, and 7 days show no difference in cell metabolic activity compared to that on blank glass substrates (Figure 3-14), which was again consistent with cell

morphology observations (Figure 3-15). We have shown that while bacterial cells were not able to colonize surfaces coated with our films even after a 2-week incubation in concentrated bacterial solution, mammalian cells both attached and divided normally on the microbicidal $(DMLPEI/PAA)_{10}$ films.

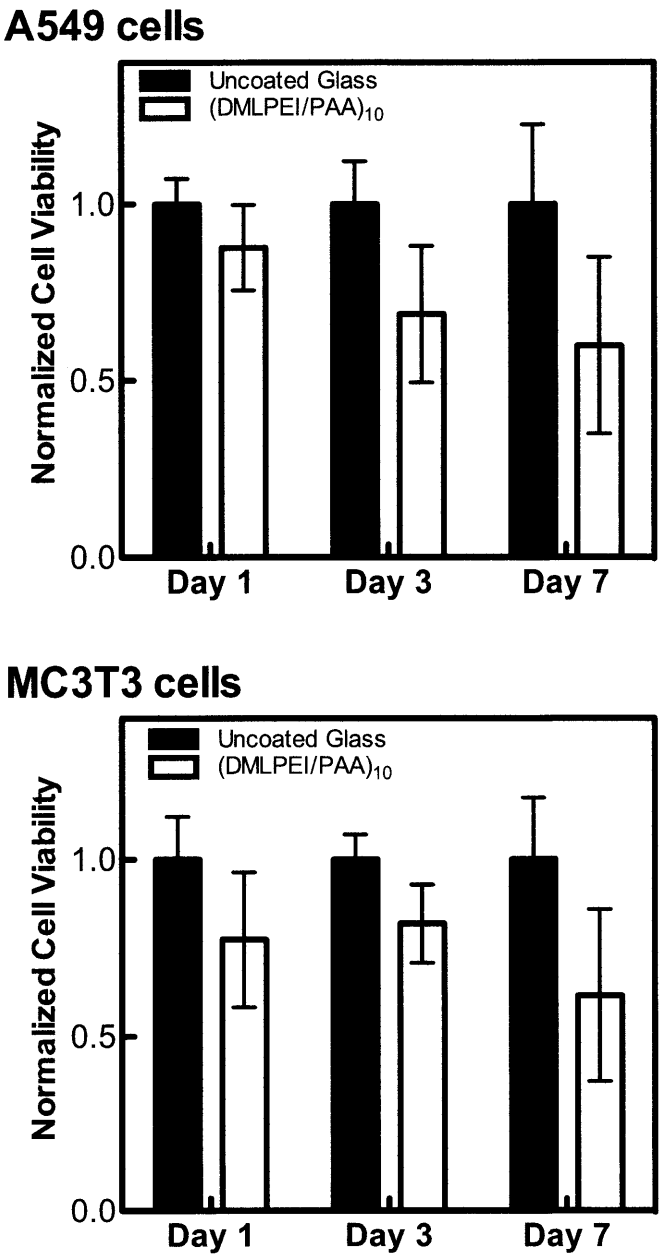

Figure 3-14: Viability of A549 (epithelial) and MC3T3 (osteoblast) cells on $(DMLPEI/PAA)_{10}$ coated glass slides after culturing for 1, 3, or 7 days.

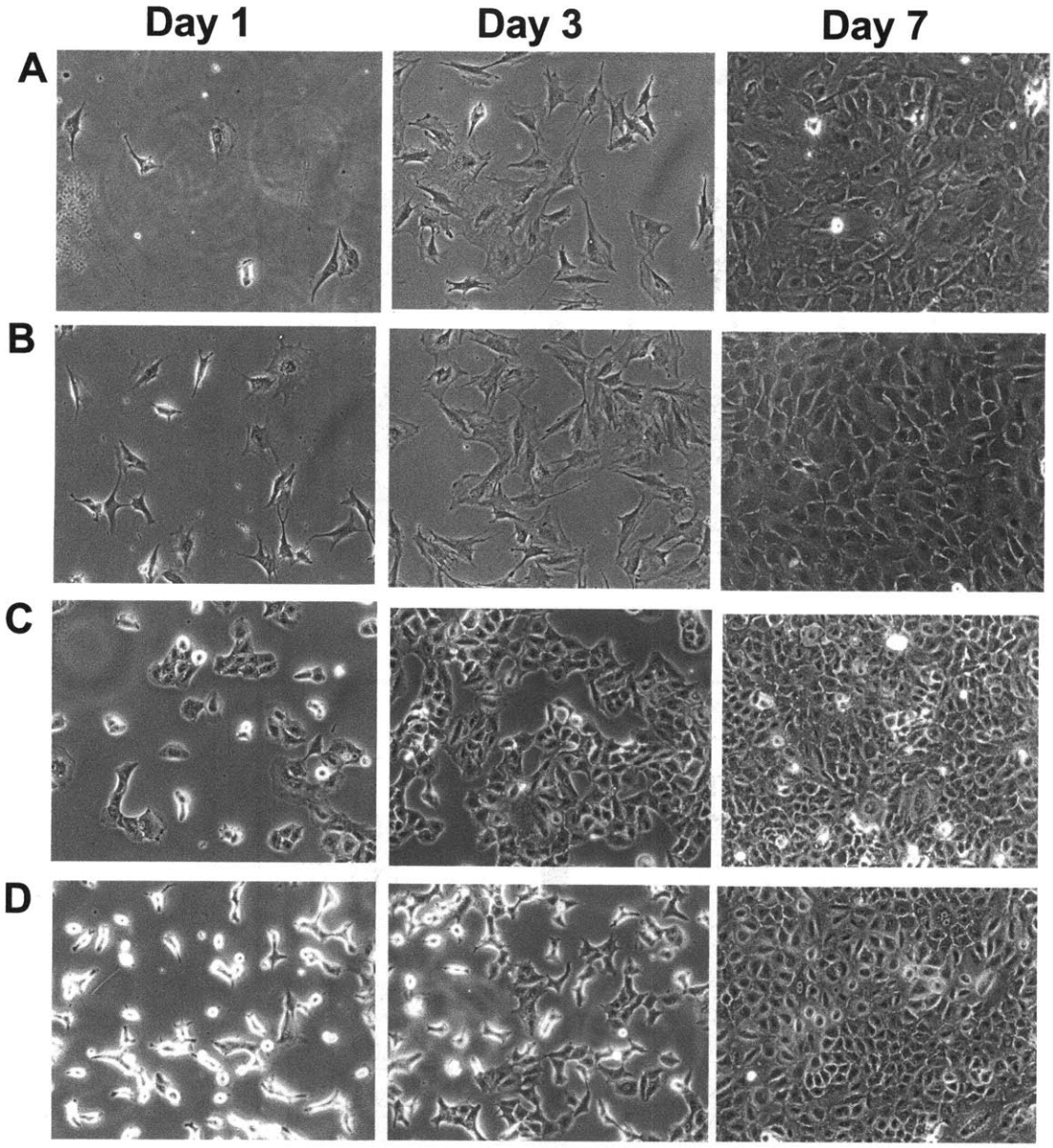

Figure 3-15: Proliferation (day 1, 3, and 7) of MC3T3-E1 cells on A) bare glass substrates and B) $(DMLPEI/PAA)_{10}$ films; proliferation of A549 cells on C) bare glass substrates, D) $(DMLPEI/PAA)_{10}$.

Cytotoxicity of the films was also tested against a primary cell line, namely a murine macrophage cell line (Raw264.7); cell metabolic activity (Figure 3-16) on the microbicidal film was slightly lower when compared to cells seeded on bare glass substrate on day 1, day 3 or day

6. Previously, we found no difference in cytotoxicity when mammalian cells (i.e., osteoblasts and epithelial cells) were seeded on the film-coated substrate relative to the uncoated substrate (Figure 3-14 and Figure 3-15); by using macrophages, one of the cell types involves in an immune response, the cells can assess the cytotoxicity of foreign biomaterials more effectively.

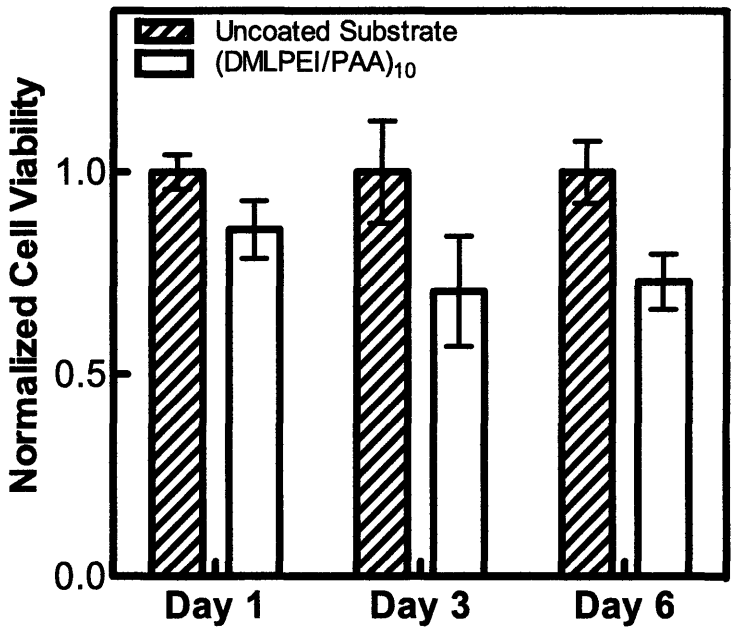

Figure 3-16: Cell viability of macrophages (Raw264.7) on bare substrate versus film-coated $(DMLPEI/PAA)_{10}$ coated substrate on day 1, 3, and 6.

Cell proliferation pictures, as shown in Figure 3-17 also showed slightly higher density of cells on bare glass substrates especially on day 3 and day 6; although both cell viability assay and cell proliferation show slight cytotoxicity on the surface of the film-coated substrate, majority of cells were still able to adhere and proliferate on the film surface.

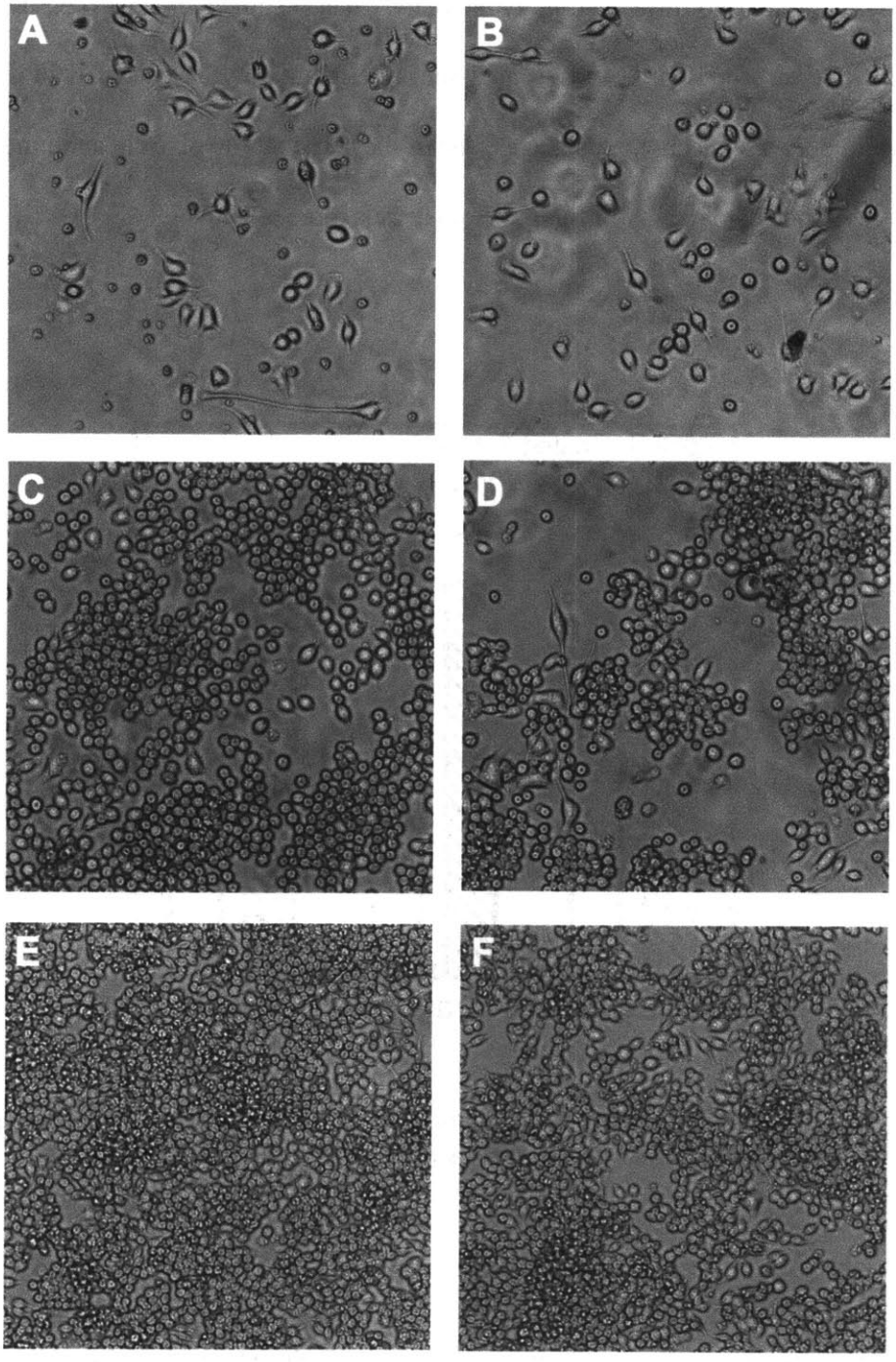

Figure 3-17: Proliferation of macrophages (Raw264.7) on bare glass (left column) and film-coated glass (right column); A) and B) are day 1 pictures; C) and D) are day 3 pictures; E) and F) are day 6 pictures

3.4 Conclusions

The sustained capability of the underlying microbicidal film to resist biofilm formation, even in the presence of highly resistant strains of bacteria, suggests the potential of these systems as implant coatings. Here, we propose the use of the microbicidal base film $(DMLPEI/PAA)_{10}$ as a long-term surface coating for medical implants to prevent bacterial attachment, with the added versatility of tunable release of therapeutic agents via a degradable LbL top film to provide an additional medical functionality. The combination film technology has been demonstrated in this work with the paired use of an antibiotic-releasing or the diclofenac-releasing film to provide localized drug delivery the implant site and treat an infection or minimize FBR by inhibiting the formation of inflammatory mediators. When each film is gone, the microbicidal base film would serve as a long-term implant coating preventing bacterial attachment and biofilm formation. This dual functional platform film technology appears broadly applicable and versatile enough to satisfy a variety of thin film medical device coating specifications.

Chapter 4: Mechanistic Investigation of Protein Resistance in Microbicidal Polyelectrolyte Multilayer Films

Reproduced in part with permission from "Drastically Lowered Protein Adsorption on Microbicidal Hydrophobic/Hydrophilic Polyelectrolyte Multilayers" by Wong, S. Y., Han, L., Timachova, K., Veselinovic, J., Hyder, M. N., Ortiz, C., Klibanov, A. M., Hammond, P. T. Submitted to *ACS Nano*, © 2011 American Chemical Society

4.1 Introduction

Biofouling can generally be described as an undesired attachment of biomolecules (e.g., proteins) or organisms (e.g., bacteria, algae, plants) on wetted surfaces in an aqueous environment; this is a major problem in many applications, including biomedical implants, [20, 24, 133] hospital equipment, [134] biosensors, [115, 135] food packaging, [29] water filtration membranes, [27] marine equipment, [28] in vitro diagnostics, [136] and so on. Protein adsorption on surfaces often reduces the sensitivity and efficacy of the devices. In addition, protein adsorption, and the subsequent formation of a layer of protein on surfaces, especially in biological implants, creates an environment suitable for bacterial colonization, and eventually forms a biofilm. [24] The two primary causes of implant failures are the adverse foreign body response (FBR) and implant-related infection. FBR begins with protein adsorption onto the implant surface, which then triggers an inflammation cascade as a wound healing response to protect the body from foreign objects; this can eventually lead to fibrous encapsulation of the implanted device. [24, 117] On the other hand, implant-associated infections can happen on contact lens, catheters, prosthetic devices, and orthopedic implants. [20] Current treatment methods for infection include surgical

replacement of the infected implant, along with broad-spectrum antibiotic therapy, often incurring additional health care costs. [137] This becomes a serious concern when the infection is caused by an antibiotic-resistant strain (e.g., methicillin-resistant Staphylococcus aureus (MRSA)); [133, 138] therefore, if surfaces can be made to simultaneously resist protein attachment and bacteria colonization, the percentage of implant failure related to FBR and infection can be drastically reduced.

Protein adsorption onto a surface is a complex and not well understood phenomenon; broadly, it can be discussed in terms of two limiting mechanisms: adsorption by electrostatic (charge-charge) interactions and hydrophobic interactions. Of course, a combination of these two effects may occur, and other non-specific interactions via hydrogen bonding and dipolar mechanisms also play a role. Currently, the few materials that effectively resist protein adsorption from complex biological fluids include poly(ethylene glycol) (PEG), [139, 140] oligo(ethylene glycol) (OEG) self-assembled monolayers (SAMs), [141] zwitterionic-based materials,[142] and various hydrophilic biomacromolecules (e.g., dextran, mannitol). [143, 144] It is believed that long PEG polymers resist protein adsorption because of steric repulsive forces when the chains are compressed by protein molecules approaching the surface; [145, 146] however, PEG is susceptible to oxidation damage over time and loses its function in biological media. [141, 147] Recent studies show that OEG SAMs attract a tightly bound water layer around the OEG chains, which is responsible for repulsive hydration forces against protein adsorption. [148, 149] Other hydrophilic polymers also generate steric repulsion plus hydration based on similar mechanisms to PEG. Zwitterionic-based and mixed charge surfaces are believed to introduce a dense hydration layer via water binding around close packed ionic groups. [143, 144, 150, 151] In addition to these hypotheses, surfaces with molecular-scale heterogeneities on a length-scale

relevant to the fouling protein have also been shown to interfere with adsorption. [131, 132, 152-154] It is believed that a set of residues on the surface of a protein forms the initial contact with the surface; once this initial contact is made, cooperative effects from neighboring residues make additional contact. [154] If a surface can be designed with heterogeneities on the length-scale relevant to a protein, this initial adsorption event could be disrupted. Mixed SAMs that undergo curvature-driven phase segregation on metal nanoparticles, resulting in domains as small as 0.5nm, have shown excellent resistance to protein adsorption. [132, 155] Mixed SAMs on flat surfaces with domain size of tens of nanometers have shown that proteins adsorb preferentially on the hydrophobic regions; [156] mixed SAMs have also been shown to have superior antifouling capability compared to either of the respective pure SAMs. [157] The drawback of SAMs is the need for carefully prepared substrates, the limited types of substrates that can be coated, and their stability, which can be challenged under long term exposure to water alkalinity or acidity.

In this work, we assembled thin polyelectrolyte multilayer (PEM) films, alternating deposition of a hydrophobic *N*-alkylated poly(ethylenimine) and a hydrophilic poly(acrylic) acid, which we have shown in previous work resulting in highly active microbicidal thin films. [124] We examine the protein adsorption behavior on these films as a means of determining the primary mechanism that leads to very low protein adsorption on these systems. Films are constructed using the layer-by-layer (LbL) deposition technique, [33] in which multivalent species with complementary functional groups are adsorbed sequentially onto a substrate. PEM films are simple and inexpensive to fabricate and can be built on most geometries with molecular scale control over thickness and surface properties. [31, 33] Due to its versatility, LbL technology has been applied to various applications including drug delivery, [2, 3, 14, 47, 92, 93, 158] membranes and electrodes for energy applications, [6, 7, 94] and electro- or magneto-responsive surfaces. [9-11, 95] In

our previous work, we have demonstrated that the films made with the hydrophobic *N*-alkylated poly(ethylenimine) and poly(acrylic) acid showed broad-spectrum contact-killing antimicrobial activity against both Gram positive and Gram negative bacteria; films were effective in preventing bacterial colonization from turbid bacteria solution for at least two weeks, while also preventing adsorption of at least certain types of protein. [124, 158] Here, we extend the investigation of the antimicrobial film to include its potential as an antifouling surface coating. This film architecture will impart the surface of the implant with contact killing antimicrobial and antifouling properties.

4.2 Materials and Methods

4.2.1 Materials

Poly(2-ethyl-2-oxazoline) (M_w = 50 kDa or 500 kDa), 1-bromododecane, iodomethane, 1-bromooctadecane, 1-bromohexane, 1-bromobutane, *tert*-amyl alcohol, 3 M sodium acetate buffer (NaOAc; pH 5.2), as well as solvents and common buffers, were from Sigma-Aldrich (St. Louis, MO). Poly(2-ethyl-2-oxazoline) (M_w = 5kDa), PAA (M_w = 5kDa, 50 kDa, and 225 kDa) and linear poly(ethylenimine) (LPEI; M_n = 25 kDa) were from Polysciences (Warrington, PA). Phosphate-buffered saline (PBS; pH 7.4, 137 mM NaCl, 2.7 mM KCl, 10 mM Na_2HPO_4) is from Mediatech, Inc. (Herndon, VA). Silicon wafers (test grade n-type) were from Silicon Quest (Santa Clara, CA). Quartz crystals (5-MHz frequency) with gold electrodes were from Tangidyne Corp. (Greenville, SC). Q-Sense quartz crystal sensors, QSX 303 were from Biolin Scientific Inc. (Lithicum Heights, MD). Glass substrates used to build films on and standard particles for flat surface cell zeta measurement were from Beckman Coulter Inc. (Brea, CA).

Cation-adjusted Mueller Hinton Broth II (CMHB) and BactoAgar were from Difco BD (Franklin Lakes, NJ). Bovine plasma (IBV-N) was purchased from Innovative Research (Novi, MI). All reagents were used without further purification.

4.2.2 Synthesis of Polymers

Linear *N,N*-dodecyl,methyl poly(ethylenimine) (DMLPEI; structure shown in Figure 1) was synthesized as previously described. [71, 113] In short, LPEI (M_w of 2.2kDa, 21.7kDa or 217 kDa) was produced in house by deacylation of 5kDa, 50kDa, or 500 kDa poly(2-ethyl-2-oxazoline); [99] the product was dissolved in water, precipitated with aqueous KOH, filtered, and washed repeatedly with water. Complete deacylation was confirmed by NMR. The resulting deprotonated LPEI was alkylated first with 1-bromododecane (96 h at 95 °C) and then with iodomethane (24 h at 60 °C) to produce DMLPEI. Syntheses of linear *N,N*-octadecyl-methyl-PEI (OMLPEI), *N,N*-hexyl-methyl-PEI (HMLPEI) and linear *N,N*-butyl-methyl-PEI (BMLPEI) were similar, except that LPEI was alkylated with 1-bromohexane (24 h at 95 °C) and 1-bromobutane (24 h at 95 °C), respectively. As for *N,N*-dimethyl-PEI (MMLPEI), LPEI was alkylated by addition of iodomethane for 24 h at 60 °C.

4.2.3 Preparation of Polyelectrolyte Solutions for Film Deposition

Solutions of PAA were prepared at 2 mg/mL in 0.1 M NaOAc, and were adjusted to pH 3.0, 5.0, and 7.0 with 1 M HCl or 1 M NaOH. Dipping solution of DMLPEI (in 1-butanol), HMLPEI (in 1-propanol), BMLPEI (in 1-propanol), OMLPEI (in 1-butanol), and MMLPEI (in deionized water) were prepared at 1 mg/mL. LPEI dipping solution was prepared at 2 mg/mL in water and adjusted to pH 4.25, with 1 M NaOH and 1 M HCl. All solutions were prepared with water from a Milli-Q Plus (Bedford, MA) at 18.2 MΩ.

4.2.4 LbL Films Assembly

As previously described, [124] LbL films were assembled on silicon substrates using a programmable Carl Zeiss HMS slide stainer. Substrates were cleaned with methanol and ultra pure water, dried under N_2, and plasma-etched in O_2 using a Harrick PDC-32 G plasma cleaner on high radiofrequency for 1 min, and then immediately immersed into the first polycation solution (i.e., DMLPEI, HMLPEI, LPEI, etc.) for at least 10 min. LbL films with the bilayer architecture of $(Polycation/Polyanion)_n$ were built, where n is the number of bilayers, the polycation could be any of the ones mentioned above, and the polyanion was polyacrylic acid (PAA) in most cases. A bilayer would include a deposition of a layer of the polycation, followed by a layer of the polyanion; a cascade rinse cycle of three organic solvent rinse baths (1 min, 30 s, 30 s), followed by three water baths (1 min, 30 s, 30 s) was used after deposition of the polycation, and the reverse cycle of rinse water then organic solvent after PAA dipping. Films for surface zeta potential measurements were built using the same protocol except that they were built on glass substrates instead of silicon substrates.

4.2.5 Film Characterization

After film deposition, all films were allowed to air dry. For film growth, thicknesses of the films were measured using a spectroscopic ellipsometer (Woollam M-2000D). All thickness measurements were made at five different points on each film and averaged over three separate films. Roughness measurements of films were generated using a surface profilometer (KLA Tencor P-16). Thickness measurements of films were also verified using the surface profilometer. The surface roughness and composition heterogeneity of the films were measured via tapping mode atomic force microscopy (AFM) in ambient conditions using a Multimode AFM with an *E* scanner (Veeco, Santa Barbara) and a SuperSharpSilicon AFM probe tip (SSS-

NCHR, NanoSensors, Neuchatel, Switzerland). Scanning electron micrographs (SEMs) were obtained using a JEOL KSM-6700F at 250,000× magnification.

The advancing and receding contact angles of films were measured using the "add and remove volume" method with a ramé-hart model 590 goniometer. This method required the addition of the drop volume (~ 5 μL) slowly to the maximum volume permitted without increasing the three-phase line; this resulting contact angle is the advancing angle. Volume is then removed from the maximized drop volume without reducing the three-phase line. The resultant angle is the receding angle. The contact angle hysteresis is calculated by subtracting the receding angle from the advancing angle. Hysteresis characterizes the surface topology of the film, which can help in understanding surface heterogeneity.

Surface zeta potential of glass substrate coated with film was determined using the Beckman Coulter DelsaNano C instrument with a flat surface cell. The cell constant of an uncoated glass was determined in 10 mM NaCl. The stock standard monitor particles were also diluted 100 times in 10 mM NaCl. The sample coated glass substrate is then placed in the flat surface cell and standard monitor particles were injected into the cell, and surface zeta measurement was performed. Measurements were taken in triplicate on three different samples.

In order to simulate interactions between the charged proteins and the films, adhesion interactions were measured between either the $(DMLPEI/PAA)_{9.5}$ or $(DMLPEI/PAA)_{10}$ film, and the AFM cantilever end-attached with spherical SiO_2 glass colloids coated with 2 nm Cr and 50 nm Au (end radius $R \sim 300$ nm, nominal spring constant $k \sim 0.06$ N/m, Novascan, Ames, IA). In order to test the effects of charge on the tip-film interaction, these colloidal tips were functionalized with either carboxyl- or amine-ended self-assembled monolayers (SAMs) by 24 h incubation in 3 mM ethanol solutions of 11-mercaptoundecanic acid ($HS(CH_2)_{10}COOH$, Sigma-

Aldrich) and 2-aminoethanethiol hydrochloride ($HS(CH_2)NH_2 \cdot HCl$, Sigma-Aldrich), respectively. Colloidal force spectroscopy was then performed by enabling the approach of the functionalized AFM tips onto the films up to approximately 40 nN maximum compression force at a constant AFM piezo displacement rate of 1 μm/s in PBS, using a 3D Molecular Force Probe (MFP-3D, Asylum Research, Santa Barbara, CA). The tips were then held at the constant position for a pre-defined surface dwell time *t* before retracting from the film surface at the same AFM piezo displacement rate of 1 μm/s. The maximum adhesion force was then measured from each of the retraction force-distance curves. For each pair of interactions between the film and the functionalized AFM tip, the measurement was repeated for at least $n \geq 25$ different locations, and adhesion forces corresponding to different surface dwell times *t* were investigated at the same location for $t = 0 - 30$ sec.

4.2.6 Quantification of Blood Plasma Adsorption using Quartz Crystal Microbalance (QCM)

A Masscal G1 (quartz crystal microbalance) was used for quantification of protein adsorption onto surface of the film relative to an uncoated crystal. Film was deposited onto 1-inch quartz crystals (5-MHz frequency) with gold electrodes (Tangidyne Corp., SC). The frequency of the blank crystal was recorded before film deposition; frequency of the film-coated crystal was recorded again after film deposition (dried with N_2). Both blank and film-coated crystals were then incubated in bovine blood plasma (density of approximately 1,025 mg/mL) at 37 °C for 1 h; the crystals were then rinse thrice in fresh PBS then dried with N_2. The frequency of the crystals was recorded again after protein adsorption. Upon protein adsorption, the oscillatory motion of the crystal declined, and the decreased resonant frequency was measured. The Sauerbrey equation was used to relate the change in frequency to mass adsorbed per unit area ($C = 17.7$ ng cm^{-2} Hz^{-1} for 5-MHz crystals, n = overtone number). [126]

Although the Sauerbrey relation (for rigid layer) is not strictly true for adsorption of protein due to viscoelastic property of the protein adlayer, it can be used as an approximation to compare relative amounts of protein adsorbed between the blank and film-coated crystals. *In-situ* protein adsorption experiment was done with SiO_2-coated quartz crystal using the Q-Sense E4 system (Biolin Scientific Inc., Lithicum Heights, MD). Frequency changes are directly proportional to mass changes according to the Sauerbrey equation as discussed above. *In-situ* experiments allow us to monitor the time needed for protein adsorption to come to equilibrium. The experiments were done in triplicate.

4.3 Results and Discussion

4.3.1 Design of Antifouling Films

Some of the films investigated in this study have previously been shown to resist adsorption of certain types of protein, while also preventing bacterial colonization from highly turbid bacteria solution for a period of at least 2 weeks. [158] In this work, we extend the study of the films to their ability to resist protein adsorption from bovine blood plasma systematically; we quantitatively examined this phenomenon as a function of the number of bilayers of the film, hydrophobicity of the polycation and polyanion, assembly condition (i.e., pH of solution) of films, net surface charge, and molecular weights of both polycation and polyanion to better understand possible mechanisms of protein resistance.

The charged multilayer film components are shown in Figure 1; the polycations used to build the LbL films in this study (Figure 4-1A) varied in hydrophobicity with the length of their *N*-alkyl chain (ranging from n = 1 to n = 18); throughout this paper, linear *N,N*-dodecyl, methyl

poly(ethylenimine) is abbreviated as DMLPEI, linear *N,N*-octadecyl, methyl PEI as ODMLPEI, linear *N,N*-hexyl, methyl PEI as HMLPEI, linear *N,N*-butyl, methyl PEI as BMLPEI, and linear *N,N*-dimethyl PEI as MMLPEI. The polyanion used is poly(acrylic acid) (PAA) (Figure 4-1B). The bilayer growth of the $(DMLPEI/PAA)_n$ films had previously been reported; [124] the films exhibited an initial patchy growth followed by a linear growth. For example, the thickness and roughness of a $(DMLPEI/PAA)_{10}$ is 25 ± 3 and 6 ± 3 nm respectively.

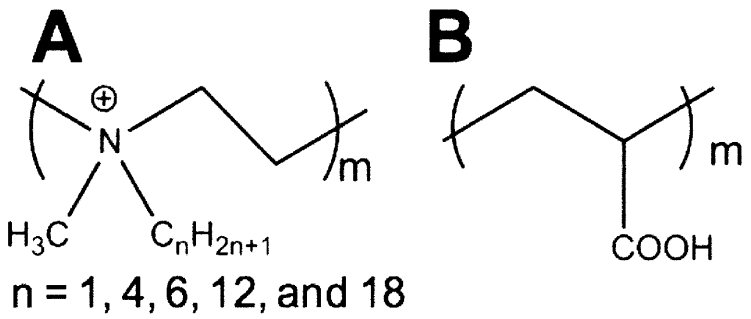

Figure 4-1: A) Structure of polycation with various N-alkyl chain lengths; B) Structure of poly (acrylic acid) (PAA).

4.3.2 Antifouling Activity of Films

We first investigated the antifouling behavior of the $(DMLPEI/PAA)_n$ films with increasing number of bilayers, for cases in which the hydrophobic DMLPEI or the hydrophilic PAA is the topmost layer (Figure 4-2). We observed that the protein resistance of the films improved with an increasing number of bilayers relative to an uncoated substrate, with best performance beyond 5.0 bilayers; below 5.0 bilayers, the film was in a patchy growth regime, during which the polyion layer does not fully coat the substrate, leaving uncovered regions on

the surface.[124] Once the surface was completely coated with film, we saw a significant drop in the mass of protein adsorbed on the surface compared to a silicon control.

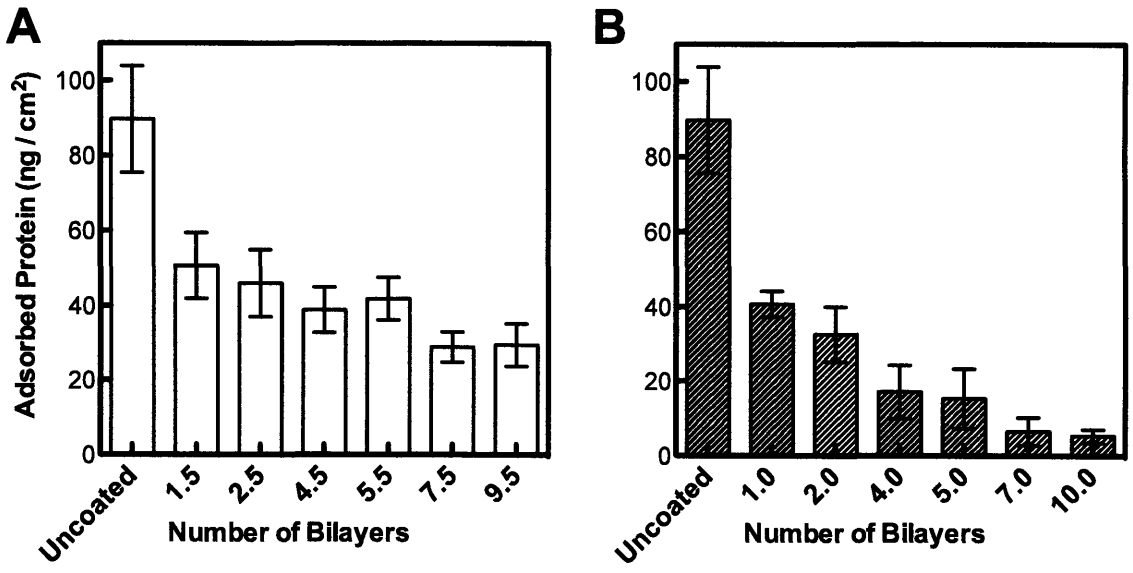

Figure 4-2: Protein adsorption onto surfaces of $(DMLPEI/PAA)_n$ with increasing number of bilayers; A) Odd number of bilayers represents having DMLPEI as the topmost layer; B) Even number of bilayers represents having PAA as the topmost layer.

Overall, we observed significantly less protein adsorbed onto the surfaces of film for which PAA was the topmost layer (Figure 4-2B); 5 ± 2 ng / cm^2 on the 10 bilayers film versus 30 ± 6 ng / cm^2 on the 9.5 bilayers film. Surfaces that adsorb less than 5 ng / cm^2 of protein are considered ultra-low fouling surfaces. [142] The uncoated substrate adsorbed 90 ± 14 ng / cm^2 of protein onto its surface.

Contact angle measurements of the 9.5 bilayers and 10.0 bilayer films indicate contact angles of 96° ± 5° and 85° ± 3° respectively, showing that the films with PAA as the topmost layer are more hydrophilic (Table 4-1). This may be anticipated given that PAA is a highly hydrophilic polymer, and the *N*-alkylated PEI polymers are hydrophobic; however, it is clear that the chains for both surfaces are highly interpenetrated, leading to contact angles that fall between the two extremes of the neat polymers, and yielding only a small difference between the DMLPEI and PAA topped surfaces. LbL films in general have shown to be highly interpenetrated; instead of forming well-stratified layers, the layers interdigitate, as has been shown for several different polyelectrolyte systems. [36, 39, 159] In some multilayer systems, the interpenetration is extensive enough that the topmost layer will present segments at the surface from the underlying polyion. The topmost layer in the case of these LbL films would be expected to present a mixture of the hydrophobic DMLPEI and hydrophilic PAA segments.

In addition, surface zeta potential measurements of the two films showed that the PAA-topped films had a surface charge of -2 ± 2 mV (near neutral), while the DMLPEI-topped film exhibited a surface charge of 40 ± 5 mV (Table 4-1). It is clear from the near-zero surface potential that the PAA-topped films, which exhibit a highly effective protein resistant surface, likely display a mixed-charge surface in which positively and negatively charged groups are equally present. Such LbL films that exhibit a non-reversal of charge with alternating adsorption, have been presented recently in the literature, and indicate that other secondary interactions play a role in film build-up. [160, 161] When only the hydrophobic polycation DMLPEI was directly spincoated onto a substrate, we saw approximately 40 times more protein adsorption (220 ± 28 ng / cm^2) on the surface relative to the $(DMLPEI/PAA)_{10}$ film (Table 4-1). With these observations, we hypothesized that the architecture of the $(DMLPEI/PAA)_{10}$ film built with the

highly hydrophobic DMLPEI and hydrophilic PAA may present molecular to nanoscale surface heterogeneities making it unfavorable for protein to adsorb onto its surface; furthermore, a meaningful role appears also to be due to the presence of a charge neutral surface, minimizing favorable net electrostatic attractions between the film surface and protein.

Table 4-1 Summary of mass of protein adsorbed, surface charge, and contact angle on uncoated and film-coated substrate

Type of Films	Adsorbed Protein (ng / cm^2)	Surface Charge (mV)	Contact Angle (°)
Uncoated Control	90 ± 14	-12 ± 3	0
Spincoated DMLPEI	220 ± 28	55 ± 6	105 ± 6
$(DMLPEI/PAA)_{9.5}$	30 ± 6	40 ± 5	96 ± 5
$(DMLPEI/PAA)_{10}$	5 ± 2	-2 ± 2	85 ± 3

We then examined the dependence of the antifouling activity on the assembly conditions of the film, specifically the change in the pH of the PAA solution; because the hydrophobic polycation DMLPEI was dissolved in 1-butanol, pH of its solution is not changed. As seen in Figure 4-3A, we found no dependence of antifouling activity with changes in pH of the PAA solution during film assembly; films built at the three different pHs of PAA were all effective in retarding protein adsorption. Surface zeta potential measurements of all the films showed near neutral surface charge (Figure 4-3B), while contact angle measurements showed no statistically significant difference in the average angle measured on the surface of all three films: advancing angle = 83° ± 3°, receding angle = 24° ± 4°, hysteresis = 59° ± 2°. Early conclusion from this observation is that while PAA is necessary in the fabrication of the film, it alone may not be the

key player in imparting the films with antifouling activity. As mentioned before, the polycation DMLPEI itself coated on a surface does not have any antifouling property; so PAA adsorption is necessary to create a surface that is heterogeneous with hydrophobic / hydrophilic regions, as well as to produce charge neutrality on the surface. We have shown previously that PAA assembled into films at different pH resulted in films with highly different antimicrobial activity due to the need to present the DMLPEI chain segments as denser, less ionically bound positively charged groups on the surface; [124] however in the case of designing films for antifouling activity, the controlling factor may have more to do with surface heterogeneity than polyelectrolyte chain segment density. The highly hydrophobic DMLPEI and hydrophilic PAA, regardless of their surface charge densities, could still present molecular to nanoscale surface heterogeneities unfavorable for protein adsorption.

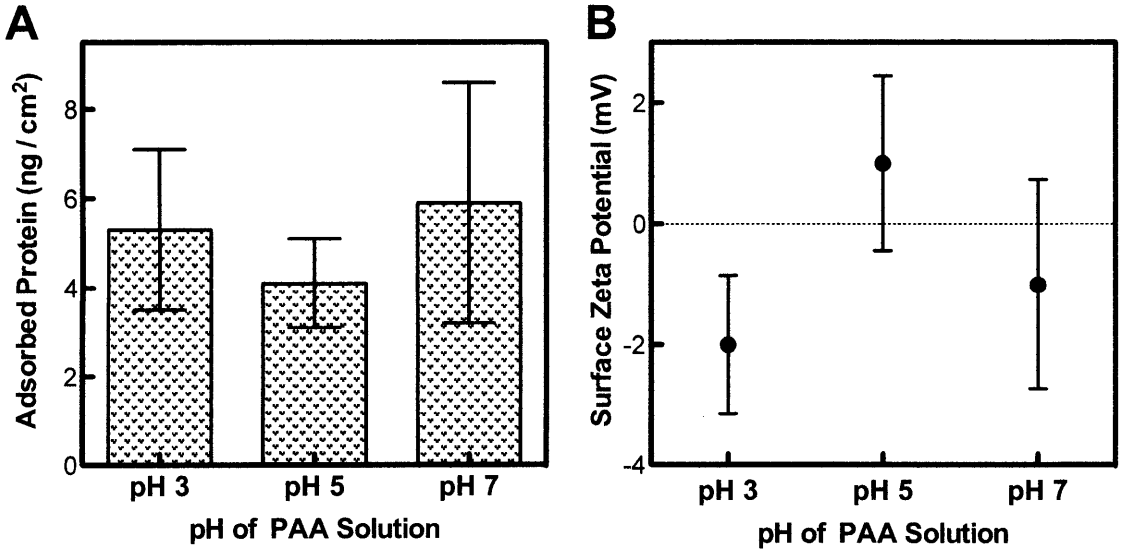

Figure 4-3: A) Protein adsorption onto surfaces of (DMLPEI/PAA)10 films built with PAA at pH 3, 5, and 7; B) Surface zeta potential of (DMLPEI/PAA)10 films built with PAA at pH 3, 5, and 7.

To further investigate the key elements that impart the film with antifouling property, we decided to alter the hydrophobicity of the polycation by varying the *N*-alkyl chain length (n = 1 to n = 18) (Figure 4-4A), while maintaining PAA as the polyanion; hydrophobicity increases with alkyl chain length. Figure 4-4A shows the mass of protein adsorbed onto these films with increasing hydrophobicity of the polycation. Films were also made with linear poly (ethylenimine) (LPEI), the unmodified backbone polymer of the *N*-alkylated polycation. The antifouling activity of the films improved with increasing hydrophobicity of the polycation, until n = 12 and beyond, where the mass of protein adsorbed reached a minimum. This suggests that a certain level of hydrophobicity coupled with the hydrophilicity of PAA is needed to impart the film with optimal antifouling property, presumably creating a heterogeneous surface made up of polymer segments from both the hydrophobic polycation and hydrophilic PAA. Films made with either the hydrophilic LPEI or MMLPEI (n = 1) showed levels of protein adsorption comparable to an uncoated control.

Films also showed increasing contact angle with increasing hydrophobicity of the polycation (Figure 4-4B); more importantly, the hysteresis of the films increased with increasing hydrophobicity of the polycation, showing an increase in surface heterogeneity. Contact angle hysteresis is a macroscopic indication of the presence of regions with contrasting surface properties that could potentially be the hydrophobic and hydrophilic domains suggested previously that resist protein adsorption. Surface zeta potential measurement, as shown in Figure 4-4C increases from – 35 ± 7 mV for the $(LPEI/PAA)_{10}$ film to neutral for the $(ODMLPEI/PAA)_{10}$ film. Interestingly, when we measured the surface charge of the 9.5 bilayers film, the surface remained positively charged (approximately + 40 mV) regardless of the level of hydrophobicity of the polycation (Figure 4-4C). This set of data indicates that at low

hydrophobicity (i.e., LPEI and MMLPEI films), the films behave similarly to classic LbL film, where complete charge reversal happens after each dipping cycle; [33, 162] but, with increasing hydrophobicity, the polycation starts to play a more prominent role in the film buildup. After each polycation-dipping step, the polycation adsorbs giving a positive surface charge; but when PAA adsorbs, PAA only adsorbs enough to neutralize the surface charge without reversing it. Given the hydrophobic nature of the film surface, we hypothesize that the driving force for the adsorption of the hydrophilic PAA chain could be reduced as the underlying surface becomes more hydrophobic. Also, because these films are highly interpenetrated, the film surface presents segments of both polymers; so, when the next hydrophobic polycation layer adsorbs, the polycation adsorbs via hydrophobic interactions with some polycation segments already present on the film surface, thus driving adsorption until the surface achieves a net positive charge again; [161] this process repeats itself with each dipping cycle. In principal, during LbL film assembly, charge reversal happens after every polyelectrolyte-dipping step; in our case, charge reversal doesn't occur after the PAA dipping step. Film deposition onto a surface without charge reversal has been previously reported. [160, 163, 164] This shows that interactions other than electrostatic contribute to the formation of multilayer films; under ordinary circumstances, self-attraction of the polyion backbone will generally lead to charge reversal rather than just simple charge compensation. [161] When these attractive forces are decreased for the polyanion, it serves to neutralize the surface sufficiently for deposition of the next polycation layer. These findings also suggest that the reason why the PAA-topped film is more effective in preventing adsorption of protein, is likely due to its surface being made up of highly interpenetrated segments of both hydrophobic and hydrophilic polymers; just enough PAA is adsorbed to neutralize the surface

charge minimizing protein adsorption via electrostatic attractions, while also presenting a heterogeneous surface consisting of hydrophilic / hydrophobic nanostructures. [131, 132]

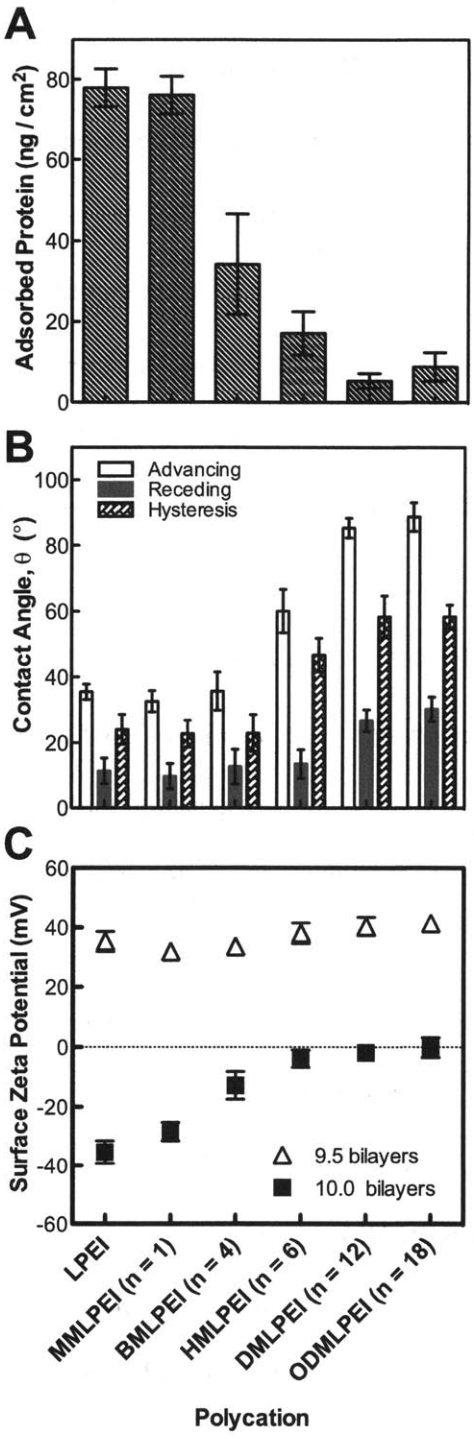

Figure 4-4: A) Mass of protein adsorbed, and B) contact angle measurement of 10 bilayers $(LPEI/PAA)_{10}$ as well as $(XMLPEI/PAA)_{10}$ films made with polycation that varies in their *N*-alkyl chain length (n = 1 to n = 18) ; C) surface zeta potential of 9.5 and 10 bilayers $(LPEI/PAA)_n$ and $(XMLPEI/PAA)_n$ films.

Next we varied the molecular weight of the polycation DMLPEI used to assemble the films again maintaining PAA (MW = 50kDa) at the polyanion; films up to this point were made with 217kDa DMLPEI (Figure 4-5A). When films were assembled with 21.7kDa DMLPEI, the film showed an increase in the mass of protein adsorbed (14 ± 4 ng / cm^2) relative to the film made with the 217kDa DMLPEI (5 ± 2 ng / cm^2). Film that was built with the 2.2kDa DMLPEI had similar protein adsorption behavior as an uncoated substrate. Contact angle measurements of the films showed an increase in the advancing contact angle and hysteresis with increasing molecular weight of DMLPEI used (Figure 4-5B). Surface zeta potential measurement of the PAA-topped $(DMLPEI/PAA)_{10}$ films showed an increase from – 31 ± 5 mV for the 2.2kDa DMLPEI film to – 2 ± 2 mV for the 217kDa DMLPEI film (Figure 4-5C), showing charge reversal on the surface with the lower molecular weight DMLPEI, and not at higher molecular weight DMLPEI. More interestingly, when we measured the surface zeta potential of the DMLPEI-topped $(DMLPEI/PAA)_{9.5}$ films, we saw the opposite trend; the surface charge of the films made with the lower molecular weight DMLPEIs (i.e., 2.2 kDa and 21.7 kDa) were barely positively charged (Figure 4-5C), in contrary as well to previous data showing that polycation-topped films made with 217kDa *N*-alkylated polycation were always highly positively charged (Figure 4-4C). We hypothesized that since the molecular weight of the PAA used was 50 kDa, the smaller molecular weight of the DMLPEI (i.e., 2.2 kDa and 21.7 kDa) when adsorbed onto the PAA-topped surface, they adsorbed only to the point of neutralizing the surface charge. Charge overcompensation does not happen because each of the polymeric chain for the lower molecular weight DMLPEIs is much shorter than the 217kDa DMLPEI; the number of sites for hydrophobic interaction to occur to reverse the surface charge to positive is much smaller.

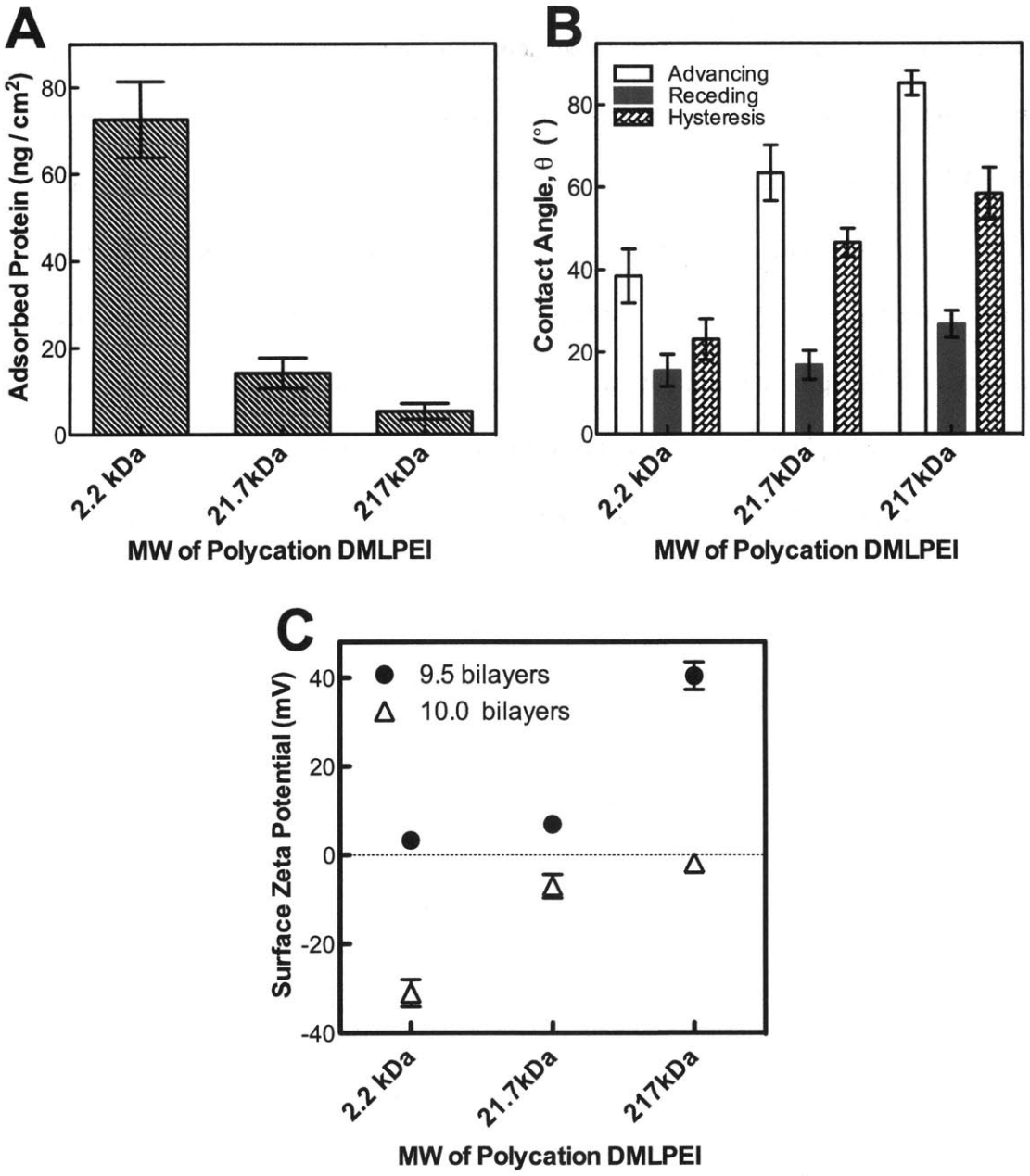

Figure 4-5: A) Mass of protein adsorbed, B) contact angle measurements, C) surface zeta potential of 9.5 and 10.0 bilayers (DMLPEI/PAA)$_n$ films built with DMLPEI of various molecular weight (2.17kDa to 217kDa).

Interestingly, when we examined the influence of molecular weight of PAA to the anti-fouling activity of the film, we saw no dependence on the molecular weight of PAA used during film assembly (Figure 4-6A). Films thus far were built with 50kDa PAA; when films were built with PAA with molecular weight of either 5kDa or 225kDa, we saw similar anti-fouling capability. Contact angle and surface zeta measurements showed statistically insignificant difference among the films (Figure 4-6B and Figure 4-6C). This finding shows that PAA is necessary in build up of the film but the key player in determining the anti-fouling capability of the film is the hydrophobic polycation; but without PAA, the hydrophobic polycation itself does not have the ability to resist protein adsorption.

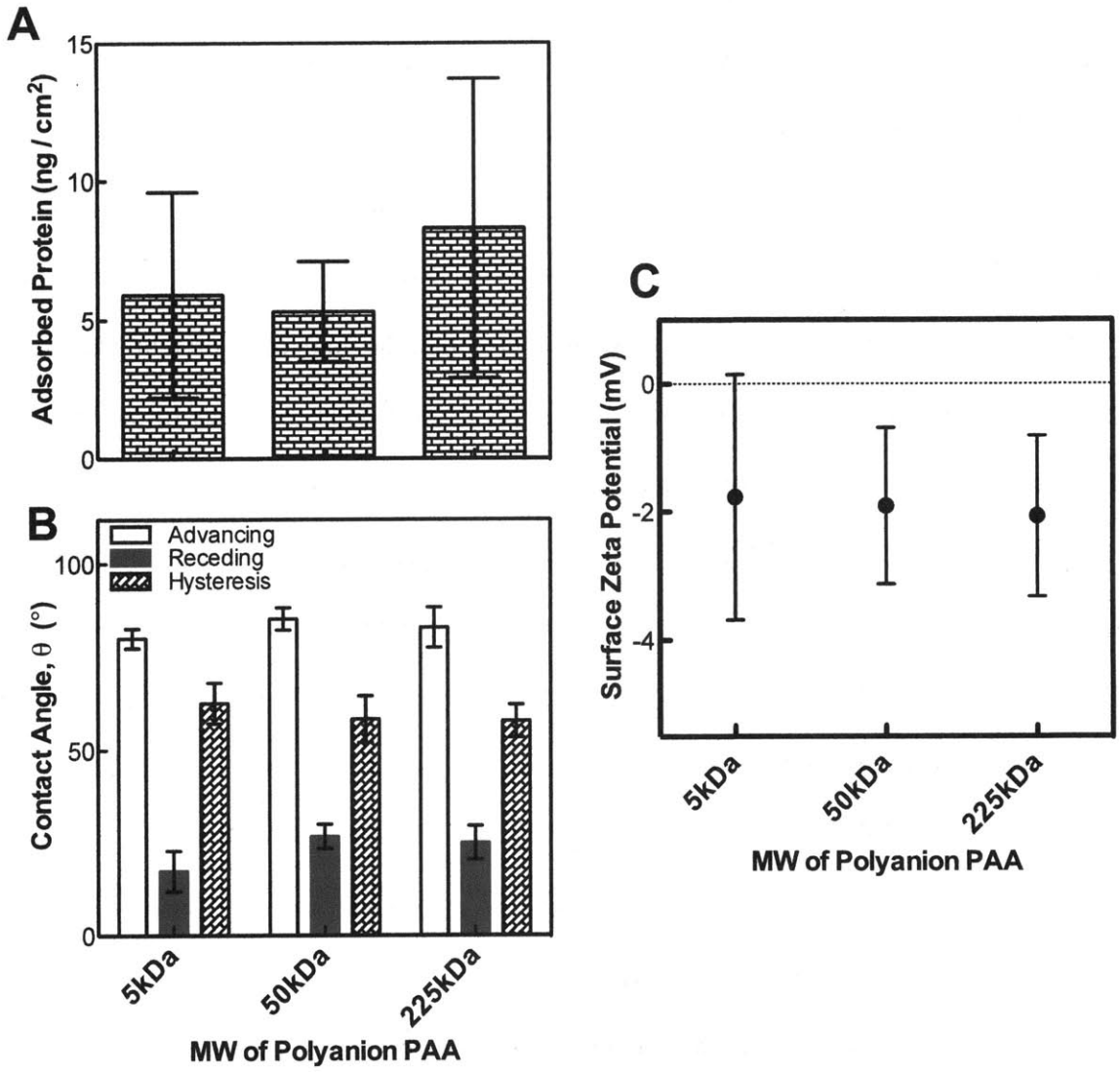

Figure 4-6: A) Mass of protein adsorbed, B) contact angle, C) surface zeta measurement on $(DMLPEI/PAA)_{10}$ films built with PAA with different molecular weight.

All protein adsorption experiments reported thus far were done with undiluted bovine plasma. In order to determine if the charge of protein plays an important role in adsorption behavior, we conducted experiments with either a positively charged protein (i.e. lysozyme) or

negatively charged protein (i.e. pepsin). Results showed that there is no statistically significant difference in protein adsorption behavior on the film regardless of the charge of the protein (Figure 4-7). Consistent with previously obtained data with plasma, the DMLPEI-topped film adsorbed much more protein than the PAA-topped film regardless of the charge of the protein. This result shows that while electrostatic interaction may be one of the factors contributing to the adsorption of protein, it is not the major one in determining the amount of protein adsorbed on the surface of our film; in fact, this set of data implies that the larger tendency of the DMLPEI-topped film to adsorb protein is due in large part to the more hydrophobic nature of the surface. Having the hydrophobic DMLPEI as the final adsorbed layer of polymer creates a surface that consists primarily of the hydrophobic polymer segments; positive surface zeta potential after DMLPEI adsorption shows that enough polycation adsorbs to reverse the surface charge, whereas during the PAA dipping step, only enough PAA adsorbed to neutralize the surface. The PAA-topped film exhibits superior antifouling activity because of its relatively hydrophilic nature when compared to the DMLPEI-topped film, and more importantly, because PAA adsorbs just enough to neutralize the surface charge, the PAA-topped film surface is rich in both the hydrophobic and hydrophilic polymer segments, potentially creating a more heterogeneous surface than a DMLPEI-topped surface, with nanoscale segregation on a length-scale relevant for preventing protein adsorption.

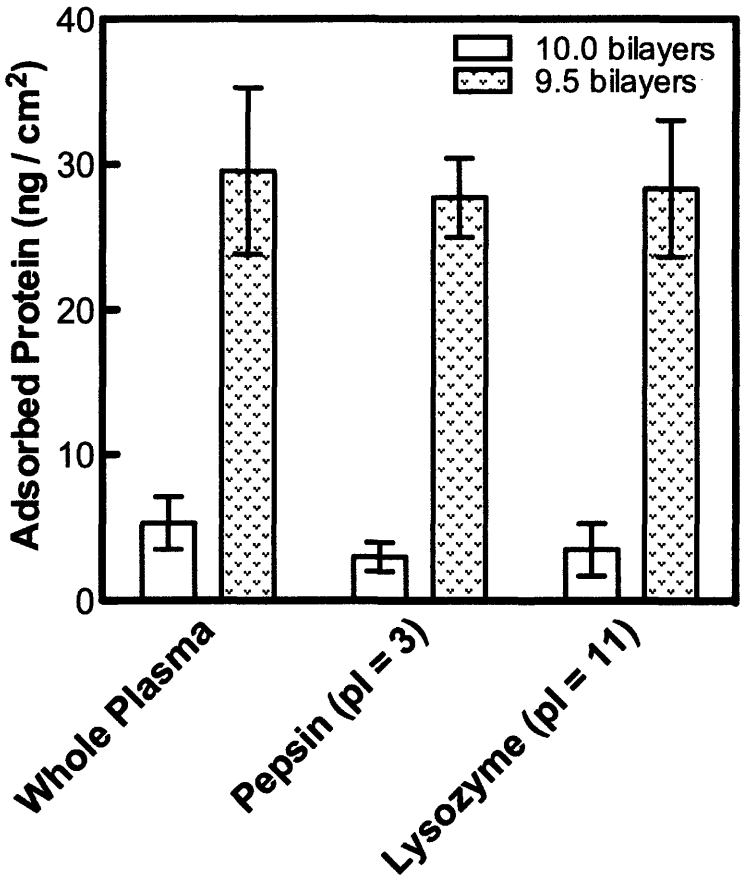

Figure 4-7: Protein adsorption experiment on $(DMLPEI/PAA)_{10}$ and $(DMLPEI/PAA)_{9.5}$ films with plasma, lysozyme or pepsin.

In order to simulate the interactions between either a negatively or positively charged protein with our $(DMLPEI/PAA)_n$ film surface, a carboxyl – functionalized atomic force microscopy (AFM) tip or a amine – functionalized AFM tip, respectively was used to perform a set of adhesion tests. In these adhesion experiments, increasing surface dwell time, t, significantly increased the maximum adhesion forces, $F_{adhesion}$, for both films, via both the

carboxyl – and amine – functionalized tips (Figure 4-8). This increase in $F_{adhesion}$ with t was because a longer surface dwell time would allow a larger degree of interactions between the molecules in contact to take place, such as van der Waals, electrostatic and hydrophobic interactions. More importantly, $F_{adhesion}$ was significantly smaller on the 10 bilayers film than those on the 9.5 bilayers film for both types of tips; however, $F_{adhesion}$ was significantly larger for both films with the amine – functionalized tips, than the carboxyl – functionalized tips (two-way analysis of variance, $p < 0.01$). At the conditions for the experiments were performed (pH 7.4 of PBS), the amine groups on the amine – functionalized tips may not be fully protonated, thus decreasing the overall positive charge of the tip, as compared to the carboxyl groups on the carboxyl – functionalized tip, which would be completely deprotonated (i.e. highly negatively charged); thus this difference is not likely due to a higher charge on the amine functional tips. Since the adhesion was consistently lower on the 10 bilayers film with both negatively and positively charged tips, the adhesion studies suggested that surface interactions were mainly governed by the hydrophobicity, rather than the nature of the charge on the tips and the films. This independent AFM study is in strong agreement with our other experimental data showing that the more hydrophobic and charged surface (e.g., 9.5 bilayers film) preferentially adsorbed more protein via hydrophobic and/or electrostatic interactions with complementary domains on the surface of a protein molecule, while the neutral surfaces (e.g., 10 bilayers film) are very effective in preventing protein adsorption. [139, 141, 165] The surface of the 10 bilayers film could be more heterogeneous with hydrophobic / hydrophilic regions presenting dimensional restrictions for protein to adsorb.

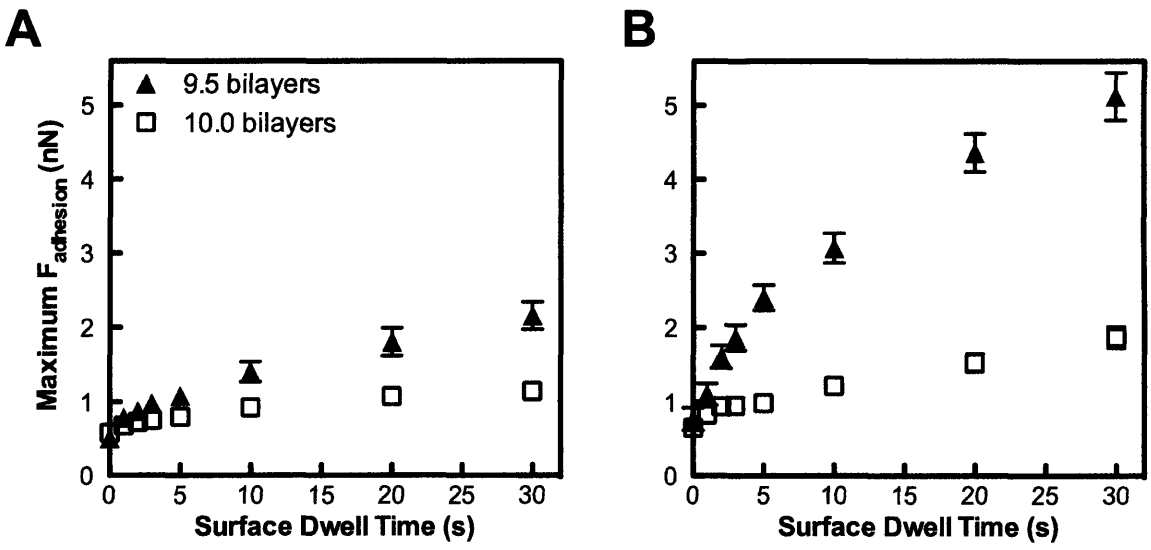

Figure 4-8: AFM adhesion tests with A) COOH-functionalized nano-colloidal tip, and B) NH_2-functionalized nano-colloidal tip on surfaces of $(DMLPEI/PAA)_{9.5}$ and $(DMLPEI/PAA)_{10}$ films. Both sets of data show stronger adhesion on the DMLPEI-topped $(DMLPEI/PAA)_{9.5}$ film, with overall stronger adhesion with the NH_2- functionalized tip.

While charge neutrality and hydrophilicity could help with protein retardation via the recently proposed mixed charge hydration repulsion mechanism, the PAA topped films are still relatively hydrophobic. The AFM adhesion studies also suggest that the zwitterionic/mixed-charge hydration repulsion hypothesis does not apply to our system; during the adhesion experiments, no long range repulsion forces due to the existence of a strong hydration layer was observed (Figure 4-9), as observed in the case for PEG or zwitterionic/mixed-charge materials (Figure 4-10). [145, 150, 151, 166] As previously stated (Table 4-1), the contact angle of the films were approximately 80° for the 10 bilayers film, and 90° for the 9.5 bilayers film, which are contact angles much larger than reported for zwitterionic surfaces (< 20°). [150] In fact, the contact angles

reported on our films are in agreement with the contact angles reported on surfaces that resist protein adsorption because of the existence of nanoscale hydrophobic / hydrophilic domains. [131]

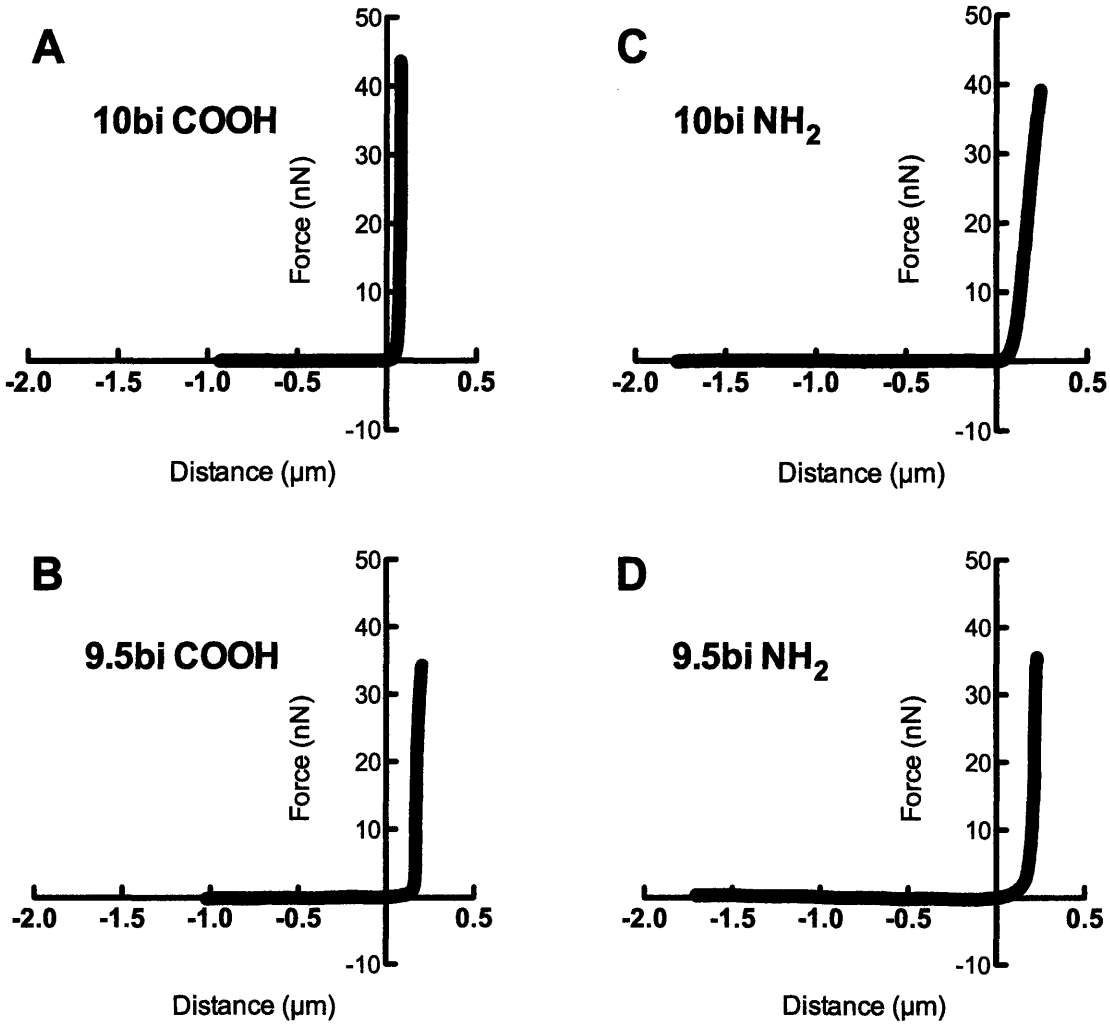

Figure 4-9: Typical approach force curves on 10- and 9.5- bilayers $(DMLPEI/PAA)_n$ films with either COOH- or NH_2- functionalized AFM tip; A) and B) are with COOH – functionalized tips; C) and D) are with NH_2 – functionalized tips.

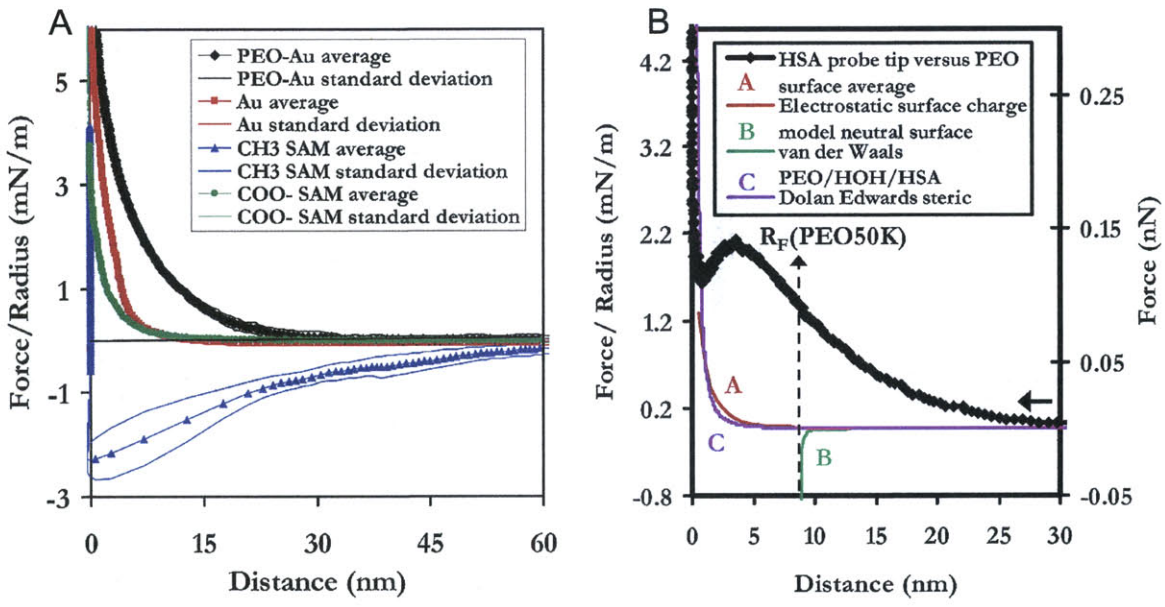

Figure 4-10: Force curves showing repulsion from PEO SAM surfaces, and adhesion on CH_3 SAM surfaces with a HAS (albumin) modified tip; adapted from Rixman et. al. [166]

Shown in Figure 4-11 are scanning electron micrographs (SEMs) of the surfaces of the 9.5 and 10 bilayers $(DMLPEI/PAA)_n$ films, to show the possible existence of nanoscale domains on the surface of our films. The surface of the 10 bilayers film indeed shows domains (~ 10 -20 nm) that are within the length scale that would prevent stable adsorption of proteins.

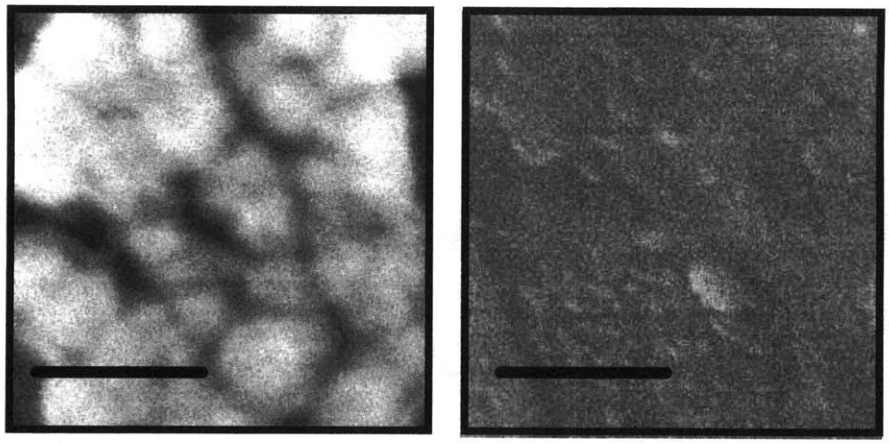

Figure 4-11: SEM images of 10-bilayers (left) and 9.5-bilayers (right) $(DMLPEI/PAA)_n$ films showing existence of nanoscale domains on the surface of the films.

In addition, tapping mode AFM images of the $(DMLPEI/PAA)_{10}$ and $(DMLPEI/PAA)_{9.5}$ films (Figure 4-12) showed that the PAA-topped $(DMLPEI/PAA)_{10}$ film was more rough than the DMLPEI-topped $(DMLPEI/PAA)_{9.5}$ film: R_q = 9.6 ± 1.6 nm versus R_q = 2.0 ± 0.2 nm respectively. The DMLPEI-topped film showed more of a flat layer of the polycation on the surface and less interpenetration of the two polymers (Figure 4-12B), in agreement with the highly positive surface charge of the 9.5-bilayer film (Table 4-1). The phase AFM (Figure 4-12, center top) of the 10-bilayer film shows some phase shift contrast suggesting a smaller-scale segregation; indeed higher-resolution SEM of the film (Figure 4-11, left) shows smaller domain sizes. These AFMs and SEMs suggest some nanoscale segregation of hydrophobic/hydrophilic domains on the $(DMLPEI/PAA)_{10}$ film surface, thereby preventing protein from adsorbing onto the surface, in agreement with previously reported results.[131, 155]

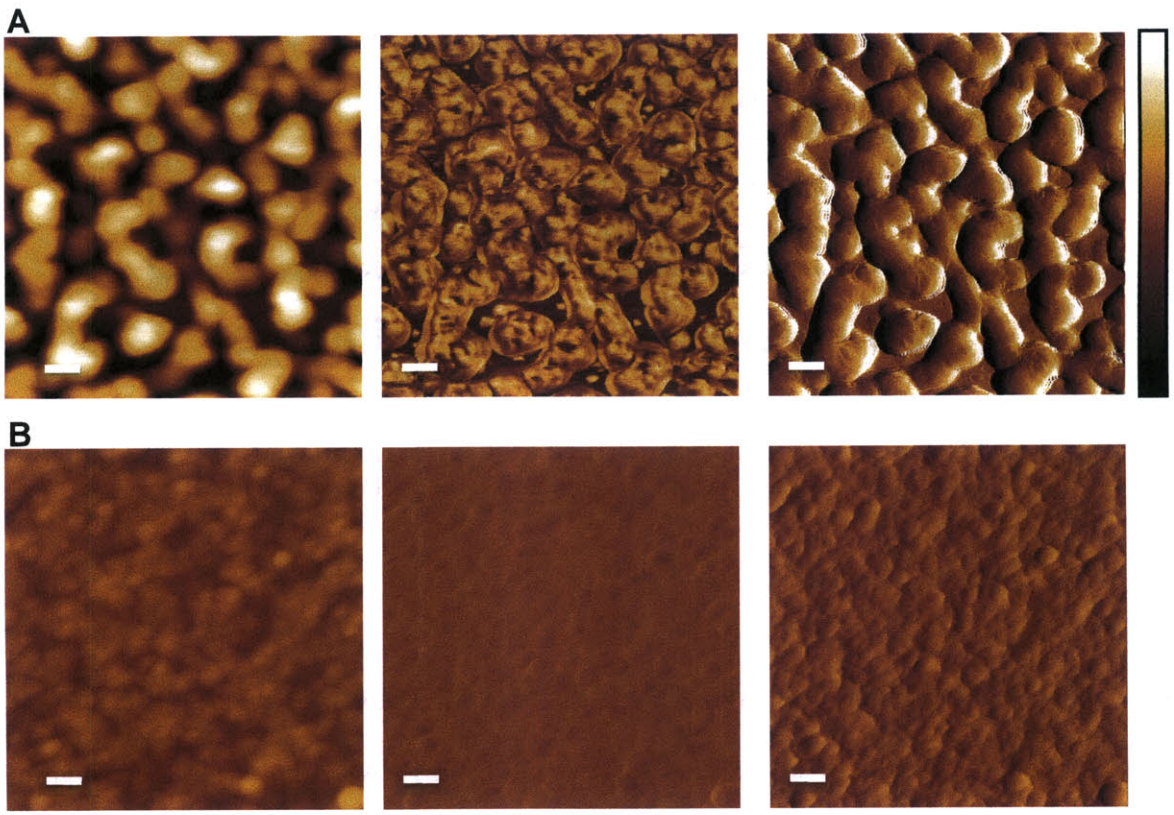

Figure 4-12: Atomic force micrographs of A. $(DMLPEI/PAA)_{10}$ and B. $(DMLPEI/PAA)_{9.5}$ films; scale bar = 50 nm. From left to right is height (color bar = 50 nm), phase (color bar = 50°) and amplitude (color bar = 0.2 V) image respectively.

4.4 Conclusions

The ability of the LbL films investigated herein to resist protein adsorption (and previously reported long-term biofilm formation) suggests their potential use as antifouling coatings for applications ranging from water purification membranes to biomedical implants. We demonstrate that the surface topology of the films could be engineered by carefully choosing

their components and that a fine hydrophobicity/hydrophilicity balance on the surface of the films is needed to create molecular-level heterogeneities unfavorable to protein adsorption. We hypothesize that due to the contrasting nature of the polyelectrolytes making up the films, nanoscale segregation of the polymer segments into hydrophobic and hydrophilic moieties occurs on the surface, thus creating an unfavorable environment for protein adsorption.

Chapter 5: Mechanistic Study of Microbicidal Films

Part of the results discussed within this chapter is adapted from "On Structural Damage Incurred by Bacteria Upon Exposure to Hydrophobic Polycationic Coatings" by Hsu, B. B., Ouyang, J., Wong, S. Y., Hammond, P. T., Klibanov, A. M. Biotechnol Lett 33 (2), 411-416, 2011. 10.1007/s10529-010-0419-1, © 2011 SpringerLink, **and** "Mechanism of Inactivation of Influenza Viruses by Immobilized Hydrophobic Polycations" by Hsu, B. B., Wong, S. Y., Hammond, P. T., Chen, J. Z., Klibanov, A. M. P Natl Acad Sci USA 108 (1), 61-66, 2011. 10.1073/pnas.1017012108, © 2011 P Natl Acad Sci

5.1 Introduction

We have successfully designed a set of contact-killing ionically cross-linked polymeric thin films using the LbL technology. [124] A polycation, linear *N,N*-dodecyl,methyl-polyethylenimine (DMLPEI), with microbicidal activity was layered with a polyanion, such as poly(acrylic acid), to create LbL films highly effective against *Escherichia coli* and *Staphylococcus aureus* (Gram negative and positive bacteria, respectively), as well as influenza A/WSN (H1N1) virus. The dependence of the microbicidal activity on the pH during and post-assembly of LbL film formation, the nature of the polycation and polyanion, the number of layers in the LbL film, and other experimental variables were investigated quantitatively. We demonstrated that microbicidal functionality could be imparted onto surfaces using LbL technology by using the right combination of polycations and polyanions, as well as assembly and/or post-assembly conditions. LbL films as thin as 10 nm, from the series of $(DMLPEI/PAA)_n$ films built with PAA at pH 3 were 100% lethal to both airborne and

waterborne Gram positive and Gram negative bacteria, as well as to a strain of influenza virus. We have also demonstrated that degradable drug releasing films were able to grow on top of the microbicidal film, creating a multifunctional film construct offering permanent microbicidal functionality and controlled drug release. Our films were effective in preventing bacterial attachment to surfaces for at least two weeks, and thus indicate promising properties for prevention of biofilms on surfaces. While highly microbicidal, the LbL coatings were also found to be non-cytotoxic to a couple of mammalian cell lines (i.e., pre-osteoblasts and epithelial cells) based on cell viability assays.

Next, we would like to understand the mechanism by which the LbL coatings inactivate microbes (bacteria and virus), particularly using surface characterization methods (i.e., visualization of microbes with scanning electron microscopy (SEM), and surface chemistry characterization with grazing angle FT-IR). More importantly, we would like to confirm that the formation of LbL film does not alter the mechanism in which the microbicidal polycation inactivates microbes.

5.2 Materials and Methods

5.2.1 Polymer Synthesis

Poly(2-ethyl-2-oxazoline) (M_w of 500 kDa), 1-bromododecane, iodomethane, *tert*-amyl alcohol, and other chemicals and solvents were from Sigma-Aldrich. Linear *N,N*-dodecyl-methyl-PEI (DMLPEI) was synthesized as previously described. [71] In short, linear PEI (LPEI) (M_w of 217 kDa) was produced by deacylation of poly(2-ethyl-2-oxazoline); [99] the resultant LPEI was dissolved in water, precipitated with aqueous KOH, filtered, and washed repeatedly with

water. The resultant deprotonated LPEI was then alkylated first with 1-bromododecane (96 hr at 95°C) and then with iodomethane (24 hr at 60°C) to produce the end product DMLPEI.

5.2.2 LbL Film Assembly and Preparation of Microbicidal "Paint"

LbL films were assembled on silicon substrates (Silicon Quest International) with a programmable Carl Zeiss HMS slide stainer, as previously described. [124] Substrates were first plasma-etched in oxygen using a Harrick PDC-32G plasma cleaner on high RF for 1 min and then immediately immersed into a solution of a 1 mg/ml of DMLPEI dissolved in 1-butanol for at least 10 min. The LbL films were built up by alternating the deposition of DMLPEI and poly (acrylic acid) (PAA); solution of PAA was at a concentration of 2 mg/ml in 0.1 M sodium acetate buffer, pH 5.1.

Microbicidal "paints" were deposited onto silicon substrates from a 50 mg/ml DMLPEI solution using a cotton swab; the paint was then left to dry overnight.

5.2.3 Visualization of Bacteria and Virus with Scanning Electron Microscopy (SEM)

The bacterial strains used herein were *S. aureus* (ATCC, 25923) and *E. coli* (*E.coli* genetic stock center, CGSC4401). The influenza virus strain used was A/WSN/33 (H1N1); the virus was grown in the Madin-Darby Canine Kidney (MDCK) medium from ATCC. [71] The protocol to test the samples for bactericidal and virucidal activity was that described previously. [100] Briefly, *S. aureus* was grown overnight in cation-adjusted Mueller Hinton Broth II (CMHB) (Difco, BD) and diluted to 5 x 10^6 cells/ml. The diluted bacterial suspension was sprayed onto samples (~10 ml/min) using a gas chromatography sprayer (VWR International, cat. No. 21428-350). The same procedure was used for *E. coli* except that it was grown overnight in LB-Miller broth (VWR), diluted to 5 x 10^7 cells/ml. The sprayed samples, including the bare substrate and

film-coated substrates (LbL and paint) were incubated at room temperate for 30 min, and then fixed using a Karnovsky's Fixative kit (Polysciences, Inc.) according to manufacturer's specifications. In short, samples were incubated in a fixing solution of 2% paraformaldehyde plus 2.5% glutaraldehyde in 0.1 M sodium phosphate buffer, pH 7.4 for 2 h and then rinsed for 10 min in phosphate buffer. Next, the samples were incubated in 1% osmium tetroxide solution for 1 h away from light, rinsed with phosphate buffer, and serially dehydrated in 25, 50, 70, and 95% (v/v) ethanol solutions for 10 min each, before final dehydration (in 100% ethanol) thrice, 10 min each. Samples were then freeze-dried in liquid N_2 and sputter-coated (gold/palladium) before imaging with a JEOL JSM-6060 SEM at 11,000× magnification.

Uncoated and film-coated substrates were placed in a Petri dish, and 10 μL droplet of the WSN influenza virus solution was placed in the center before sandwiching with a plain substrate to spread the virus droplet. The sandwich system was incubated at room temperature for 30 min before fixing the samples with Karnovsky's fixative kit, as described above. The fixed samples were then imaged with a JEOL KSM-6700F SEM at 100,000× magnification.

5.2.4 Surface Characterization of Film with Grazing Angle FT-IR (GATR)

Thicknesses of LbL films were measured using a spectroscopic ellipsometer (Woollam M-2000D). Grazing angle Fourier transformed infrared (GATR) spectra of $(DMLPEI/PAA)_{50}$ films with PAA at pH 3.0, 5.0, and 7.0 were acquired using a Nexus 6700 FT-IR (Thermo-Nicolet); LbL film thickness was fixed to approximately 80 nm by varying the number of bilayers constructed for each pH of PAA used.

5.3 Results and Discussion

5.3.1 Mechanism of Killing of Bacteria by Microbicidal LbL Film Compared to Microbicidal "Paint"

We visualized the bacteria upon exposure to the microbicidal surfaces (LbL and paint); shown in Figure 5-1 and Figure 5-2 are scanning electron micrographs (SEMs) of *S.aureus* and *E.coli* respectively upon exposure to bare Si surfaces, Si surfaces coated with the microbicidal LbL film, (DMLPEI/PAA)9.5 with PAA at pH 3.0, or Si surfaces "painted" with DMLPEI. Both strains of bacteria showed drastic morphological change upon exposure to the LbL or "painted" film; these SEMs provided direct evidence of disruption of the microbes' membrane compromising their integrity. The similarity in disruption of the membrane on the LbL versus the "painted" film shows that the construction of the LbL film does not alter the mechanism of killing by the microbicidal polymer DMLPEI. These micrographs showed that bacteria exposed to surface coated with the microbicidal polymer exhibited profound structural deformations, as opposed to the well-defined and smooth morphology seen for the bacteria on bare substrate. [167]

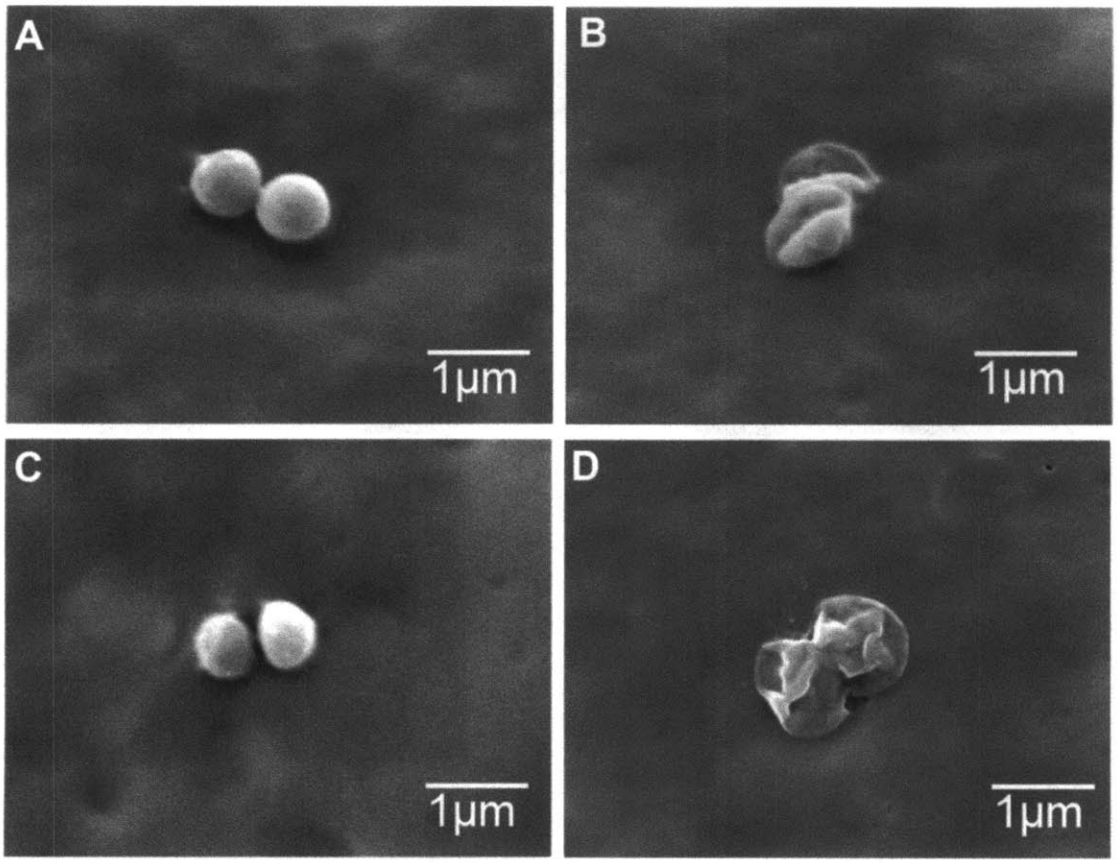

Figure 5-1: SEM images of *S.aureus* on A) bare Si substrate, B) LbL film, C) bare Si substrate, and D) painted film; both types of films show similar morphological damage to bacteria.

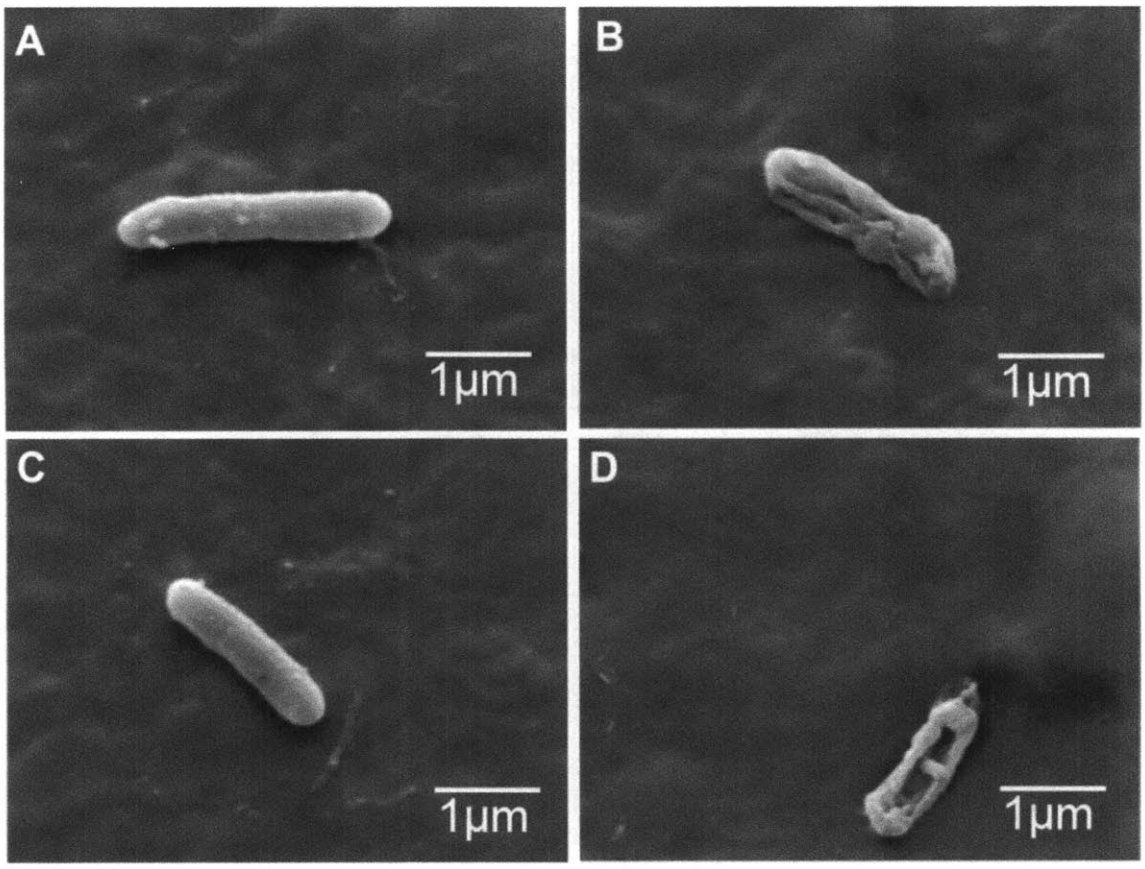

Figure 5-2: SEM images of *E.coli* on A) bare Si substrate, B) LbL microbicidal film, C) bare Si substrate, and D) painted film; both types of films show similar structural damages to bacteria.

Additionally, grazing angle FT-IR spectra (Figure 5-3) of the "painted" and LbL films support this conclusion; the peaks in the spectra show up at the same wave numbers for both types of films, suggesting that the conformation of the polymeric chains is not perturbed from the formation of LbL film. The difference in peak intensity between the "painted" and the LbL film was due to the difference in the amount of material present: "painted" films are micron in thickness while LbL films are nanometer in thickness.

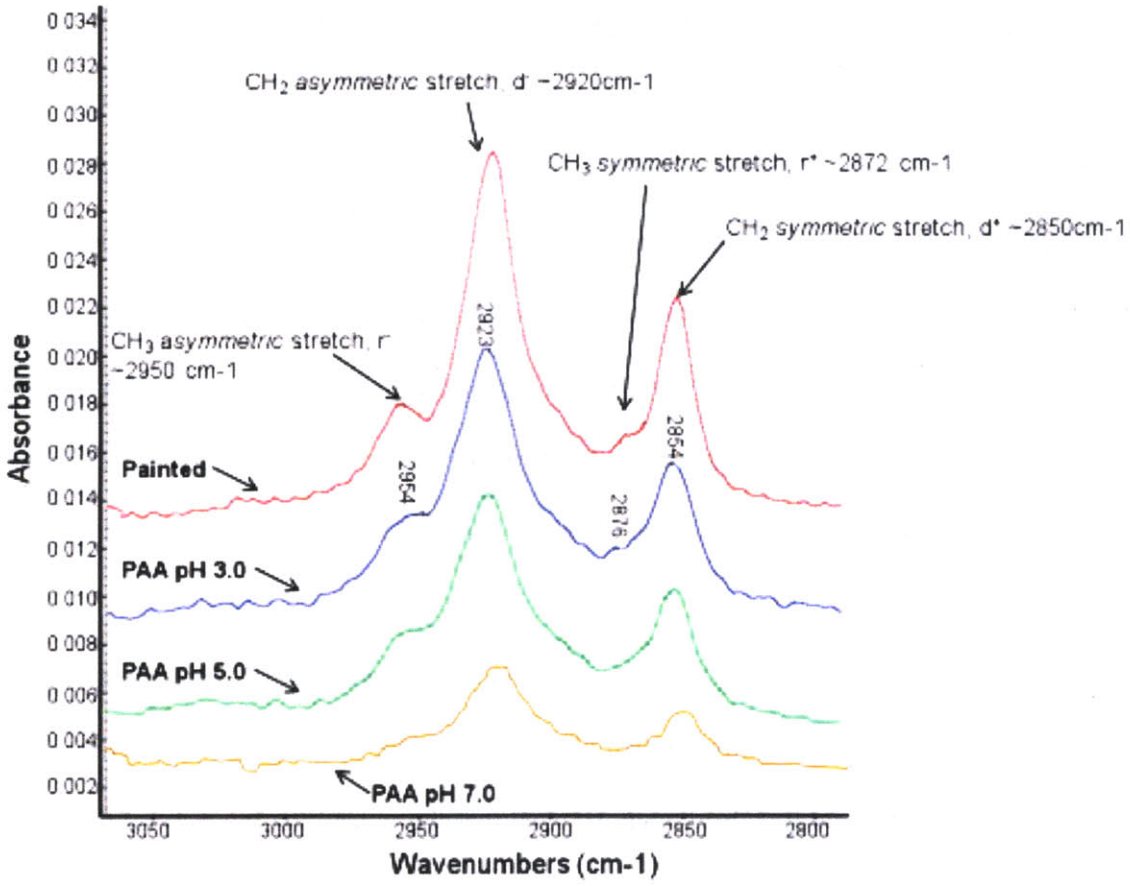

Figure 5-3: Grazing angle FT-IR of painted and (DMLPEI/PAA)n films built with PAA at pH 3, 5, and 7.

The spectra also show that the CH_3 peaks are barely visible on all samples, with decreasing intensity as the pH of PAA increases. In addition, the CH_2 symmetric and asymmetric peaks show up at frequencies between that of a solid crystalline-phase ($CH_3(CH_2)_{21}SH$) and disordered liquid crystalline phase ($CH_3(CH_2)_7SH$). [168] Data from the CH_2 symmetric stretch peak provides information of the local environment of an individual chain; the data indicates that the average local chain environment appears to be in between of a bulk crystalline phase and bulk disordered (liquid) phase. The spectra obtained for our samples

coincide with SAMs of alkanethiols with alkyl chain lengths between n= 7 and n = 11; these SAMs exhibit higher degree of disordering than that of longer chain assemblies (up to n = 21) as a result of a combination of conformationally disordered and thermally disordered alkyl chains because of the presence of gauche kinks and weak interchain interactions, respectively. [168] Also, the CH_2 stretching mode absorption intensity is directly related to the number of CH_2 units per alkyl group; the decrease in the intensity of these peaks with increasing pH of PAA suggests incorporation of less of the microbicidal polycation per layer, which correlates well with the bactericidal activity of the films; recall that the films made with PAA at pH 3 showed the highest level of activity.

Previous mechanistic studies on the microbicidal polycation DMLPEI showed that both airborne and waterborne bacteria were killed upon contact with surfaces functionalized with this polymer; in fact, fluorescent live/dead assay showed that the indeed the integrity of the bacterial membrane was compromised by the hydrophobic polycation. [72, 73] We have confirmed the structural damage to the membrane of these bacteria with these micrographs. The shrunken appearance of the bacteria exposed to the microbicidal surfaces indicates a loss of structural integrity, which is maintained by the cellular wall; this observation suggest interaction between the bacteria's peptidoglycan layer and the microbicidal polycation. Indeed, study examining the quantity of intracellular protein leaked, shows considerable fraction of the total cellular protein is spilled; the quantity and composition of protein exposed is similar to that released using standard lysozyme/EDTA treatment, suggesting both treatments may target the same components on the bacterial cell membranes (Table 5-1). [74] Lysozyme/EDTA treatment is known to release the periplasmic proteins, leaving the cytoplasm relatively intact. [169] Study quantifying the relative amount of periplasmic versus cytoplasmic enzymes leaked shows a disproportionately small

fraction of cytoplasmic enzyme released (Table 5-2). It appears that the outer periplasmic membrane of the bacterium is significantly compromised by the microbicidal polycation, while the cytoplasmic membrane suffers relatively minor damage. [74]

Table 5-1 The protein concentration released into solution by E.coli and S.aureus after various treatments [74]

Treatment	Total protein concentrations (μg/ml)		
	E. coli K12	*E. coli* BAA-196[a]	*S. aureus*
None	0.23 ± 0.03	0.23 ± 0.03	0.20 ± 0.04
N,N-Dodecyl,methyl-PEI coating	0.63 ± 0.03	0.93 ± 0.01	0.53 ± 0.01
Lysozyme/EDTA	0.56 ± 0.05		
French press	15.6 ± 0.6	14.8 ± 0.7	3.2 ± 0.3

Each measurement was performed in duplicate, and the values are given as averages ± standard deviations

[a] The same conditions as with the K12 strain

Table 5-2 The concentration of periplasmic and cytoplasmic enzymes (β-lactamase and β-galactosidase, respectively) released into solution by E.coli after various treatments [74]

Treatment	*E. coli* enzyme concentrations (ng/ml)	
	β-Lactamase[a]	β-Galactosidase[a]
None	0.060 ± 0.001	1.9 ± 0.2
N,N-Dodecyl,methyl-PEI coating	0.11 ± 0.01	9.9 ± 0.6
French press	0.68 ± 0.04	1700 ± 100

5.3.2 Mechanism of Inactivation of Influenza Virus by Microbicidal LbL Film and Microbicidal "Paint"

We then extended the mechanistic study to influenza virus; shown in Figure 5-4 are micrographs of the WSN strain of influenza virus after exposure to either an uncoated substrate or an LbL-coated substrate. Virus particles on a plain uncoated substrate showed no visible structural damage. On the contrary, virus particles exposed to the LbL-coated surface, showed a mixture of either a significantly damaged virus particle (Figure 5-4B) or no visible damage (similar to appearance of virus particle on plain uncoated substrate, Figure 5-4A). This observation is in agreement with result reported for virus particles exposed to the microbicidal "paints" (Figure 5-5). [113] This shows that the formation of LbL film does not alter the way in which the microbicidal polycation inactivates the influenza virus. Virus particles exposed to both types of microbicidal surfaces (LbL and paint) demonstrate very similar structural damages.

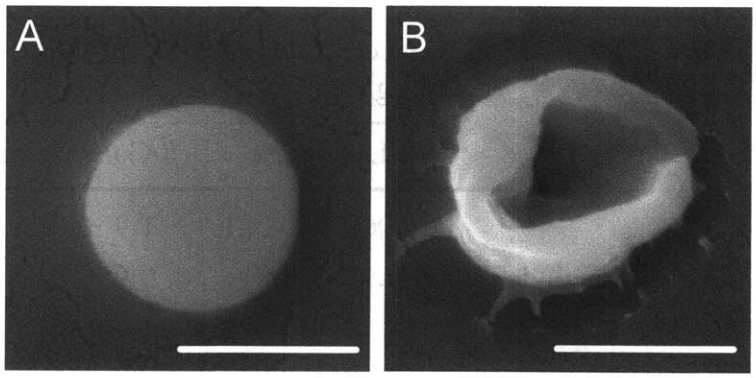

Figure 5-4: SEM images of WSN influenza virus after exposure to A) uncoated Si wafer, B) $(DMLPEI/PAA)_{7.5}$ film coated Si wafer.

Mechanistic study by Hsu et al. on the microbicidal-painted surface reported that virus particles upon exposure to the painted surface irreversibly adhere to it, and then significant structural damages occur leading to inactivation of the virus particles (Figure 5-6). The study has also shown that viral RNA is released into solution, while viral proteins remain intact. [113]

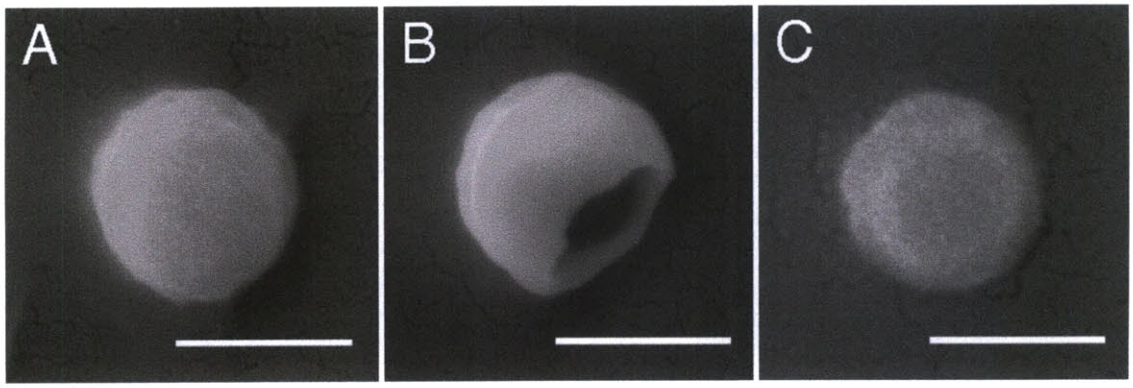

Figure 5-5: SEM images of the WSN strain of influenza virus after exposure to uncoated (A) and DMLPEI-painted (B and C) silicon wafers. A larger fraction of viral particles showed substantial structural damage (B), while a smaller fraction showed no visible damage (C). [113]

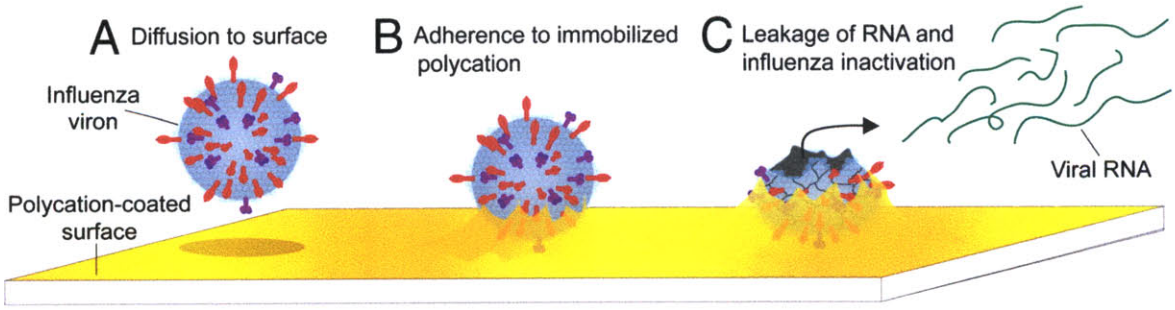

Figure 5-6: Proposed mechanism of influenza virus inactivation by microbicidal coated surfaces. [113]

5.4 Conclusions

We have shown that incorporation of the microbicidal polycation (e.g., *N,N* – dodecyl, methyl PEI) into LbL film does not alter the microbicidal functionality and mechanism in which it inactivates microbes. Both bacteria and viruses membrane were significantly damaged upon exposure to the microbicidal surface, leading to inactivation.

Chapter 6: Conclusion and Future Work

6.1 Thesis Summary

In the past decade, layer-by-layer (LbL) assembly has become an important tool for the design of highly versatile nanomaterials for various applications; more specifically, in the biomedicine field, this technique has been utilized to create surface coatings with various functionalities including delivery of drug agents, mediation of cellular behavior, and many more. The main aim of this thesis work was to use the LbL deposition technique to create a broadly applicable multifunctional platform film technology that would satisfy various thin films medical implant coating applications; this film would impart a surface with long-term antimicrobial / antifouling functionality via a permanent microbicidal base coating, and controlled delivery of therapeutic agents of interest via a degradable multilayer top film. Efforts were focused on maximizing and understanding the factors that influence the microbicidal / antifouling functionality of the polyelectrolyte multilayer (PEM) film; the *N*-alkylated microbicidal polycations previously developed in the Klibanov group at MIT were incorporated into the PEM film via LbL assembly. [71] Hydrolytically degradable multilayer top films previously developed in the Hammond group [2,3] were used to deliver the therapeutics agents because of their ability to provide controlled, and sustained delivery of drugs, while offering temporary surface functionality. When the degradable top film had completely eroded, the surface would then be left with the permanent microbicidal film for long-term prevention of fouling by biomolecules and microorganisms (e.g., proteins and bacteria). The influence of the choice of polyions, assembly and post-assembly conditions to the morphology of layer-by-layer assembled films was

investigated and key challenges were overcome to build the necessary groundwork in designing an ultrathin microbicidal / antifouling coating for various medical implant surface coating applications, as well as numerous other applications including filtration membranes, food packaging, commonly handled objects, and many more.

The design of the ultrathin microbicidal film requires a fundamental understanding of the mechanism of killing of the *N*-alkylated polycation; it kills bacteria or inactivates viruses by rupturing the membranes of the pathogens with its cationic charges and hydrophobic alkyl chains. [74, 113] With this knowledge in mind, we hypothesize that in order for the microbicidal polycation to retain its potency, the polymeric chains have to be incorporated into a LbL film with loose conformations where most of the positive charges and hydrophobic alkyl chains are free to interact with the microbes' membranes. In chapter two, a systematic study in which the choice of polyanion, hydrophobicity of the *N*-alkylated polycation, assembly and post-assembly conditions were investigated to understand the parameters that influence the microbicidal activity of the LbL films. This led to the confirmation of our hypothesis; films that were built with a weakly charged polyanion (i.e., poly (acrylic acid) at an assembly pH below its pKa) showed the maximum microbicidal activity, while films that were built with a highly charged strong polyanion showed no activity. Having a weakly charged polyanion layer yields the subsequent microbicidal polycation layer with loopier brush-like conformations where most of its cationic charges and alkyl chains available to interact with microbes' membranes. As the pH of the polyanion used during assembly increased (i.e., degree of ionization was increased), the microbicidal activity of the films decreased; films built at this assembly condition were highly ionically crosslinked leaving very few positive charges available to interact with microbes' membranes. Importantly, the films showed broad-spectrum waterborne and airborne

microbicidal activity against Gram positive and Gram negative bacteria, as well as the influenza A/WSN (H1N1) virus. The microbicidal film developed herein was used as foundation for work in subsequent chapters.

There has been great interest in developing drug – device combinations for medical applications; one of the biggest unmet needs in this field is the design of a surface coating technology that is versatile enough to be broadly applicable to various medical implications. In chapter three, we designed a multifunctional thin film construct made by combining the microbicidal base film with a hydrolytically degradable top film that offers controlled and localized delivery of therapeutics. We demonstrated the adaptability of the film construct with two degradable film architectures, where each degradable film was built on top of a permanent microbicidal base film: 1) fast (i.e., hours) release of an antibiotic to eradicate infection at the implant site, or 2) sustained (i.e., days) release of an anti-inflammatory drug to cope with inflammation at the implant site due to tissue injury. Both drugs remained efficacious upon release. The microbicidal base film retained its functionality after the degradable films had completely eroded. More importantly, the base film was shown to prevent colonization by bacteria from turbid media for at least two weeks, while remaining biocompatible with a couple of mammalian cell lines. In addition, the microbicidal film was also shown to resist adsorption of at least certain types of protein from blood plasma, opening up many more potential applications for the permanent microbicidal film. This platform technology with multiple functionalities within a single film construct could potentially fill some of the unmet needs in designing bioactive coatings for medical applications.

While investigating the microbicidal film potential when in contact with biologically relevant fluids, for example blood plasma, we discovered that the film also resisted the

adsorption of some proteins. Biofouling by biomolecules and organisms is a major problem in various industries, including food packaging, filtration membranes, marine equipments and so on. This phenomenon usually results in reduction in sensitivity and efficacy of the object. Protein adsorption on surfaces is a complex and not well understood problem. Adsorptions by electrostatic and/or hydrophobic interactions are the main mechanisms in play; of course, other non-specific interactions like hydrogen bonding and dipole interactions also play a role. The few materials that effectively reduce protein adsorption (e.g., poly (ethylene glycol), zwitterionic/mixed-charge materials, and various hydrophilic biomacromolecules) do so by steric repulsive forces or introduction of a dense hydration layer; [139, 142, 144] surfaces with heterogeneities (hydrophobic/hydrophilic regions) on the nanometer length scale have also been shown to resist protein adsorption. [131, 132] With this knowledge, we hypothesized that the surface of our film could present either mixed-charge or molecular-scale heterogeneities that resist protein adsorption because the *N*-alkylated polycation was very hydrophobic, and the polyanion (i.e., PAA) was very hydrophilic opening up the possibility for nanoscale segregation to happen. In order to test the hypothesis, in chapter four the dependence of the anti-fouling activity of the film was investigated extensively by varying the nature of the polycation and polyanion, assembly conditions of the films, and number of layers in the films. We saw that the film adsorbed approximately 20 times less protein relative to an uncoated control. Changing the level of hydrophobicity of the polycation was demonstrated to alter the surface compositions and anti-fouling property of the films. Protein resistance was most marked for films with the polyanion as the topmost layer, and these films showed near neutral surface charge; films with the polycation as the topmost layer, showed highly positive surface charge. A large contact angle hysteresis on the surface of the film was also measured, indicating a heterogeneous surface

topology. In order to simulate interaction of a protein with the film surface, adhesion studies with modified (COOH – or NH_2 – functionalized) AFM tips were performed; both sets of studies showed significantly lower adhesion force on the polyanion-topped film as compared to the polycation-topped film, in agreement with other experimental results. Also, long range repulsion of the modified tip from the surface was not observed, indicating that there was no induced layer of hydration present on the surface of our film, suggesting that the mixed-charge hydration repulsion hypothesis does not apply to our system. SEM images showed nanoscale domains within the range where they would be able to reduce stable protein adsorption on the polyanion-topped film as well. This evidence along with the contact angle hysteresis data showing a heterogeneous surface, we think that the anti-fouling property of our film is mainly due to the existence of molecular-scale hydrophobic/hydrophilic domains on the surface.

In chapter five, we would like to further understand the mechanism by which the LbL coatings inactivate the microbes (bacteria and virus). Various characterization methods were used, including visualization of microbes with scanning electron microscopy (SEM), and surface chemistry characterization with grazing angle FT-IR). More importantly, we would like to confirm that the formation of LbL film did not alter the mechanism in which the microbicidal polycation itself inactivates microbes. We observed that microbes' membranes were significantly damaged upon exposure to the film-coated surfaces. Also, from grazing angle FT-IR experiments, the peaks in the spectra showed up at the same wave numbers for both types of films (LbL and "painted"), suggesting that the conformation of the polymeric chains was only partially extended and was not significantly perturbed by the formation of LbL film.

6.2 Future Work

Several recommendations can be made to further demonstrate the practicality of the multifunctional coatings developed in this thesis work. The *in-vivo* efficacy of the permanent microbicidal / antifouling films should be tested in an animal model designed to study the long-term functionality of these films. More specifically, the potential of the microbicidal film to prevent long-term biofilm formation should be evaluated systematically in an animal model if the technology is to be used as a surface coating for various medical implants applications in future. The dual functional film construct (microbicidal and drug releasing) developed here will also need to be evaluated *in-vivo*, for a specific application. For example, the antibiotic releasing film with the underlying contact killing film will be well suited for localized prevention of infection at an implant site; so, an infection animal model will be ideal for evaluating its efficacy *in-vivo*.

Considering that the microbicidal film also has antifouling functionality, this film can potentially be used as surface coatings for diagnostics and filtration membranes applications where low binding of proteins are important to prevent the loss of functionality of the devices. From this aspect, future work can be focused on coating the films directly on these surfaces and test the efficacy of the films in those contexts. Depending on the application at hand, the duration at which the film needs to be active varies; for example, for one-time use filtration membrane, the antifouling film will need to be functional only, during which the membrane is being used. Of course, if the film is used as surface coating for long-term application, then the functionality of the film with repeated exposures will need to be evaluated.

Especially for use in medical implant applications, the extended lifetime of the films in biologically relevant environment will have to be investigated. Most of the time, an implant will

stay in a person's body for more than 10 years; although the microbicidal / antifouling functionality of the film may not be needed for the entire lifetime of the implant, but it is critical that the film remains active during the period it is needed, and after that, long-term cytotoxicity of the film within a person's body will need to be evaluated.

The mechanical robustness and chemical stability of the films in various environments will need to be considered as well, especially if we are to use the coatings on commonly handled objects. The life span of the film will need to be investigated, to find the best application for the film technology; I imagine that the microbicidal film has great potential as a top coating on an adhesive protective coating, for example on touch screen protector that can be changed easily when it's worn out. As portable personal devices like smartphones, tablets, and many other entertainment consoles become popular, the market for hygienic touch surfaces increases dramatically. Also, the microbicidal film can be very well suited as a top coating on one-time use adhesive bandage, which usually has a shorter lifespan, and not expose to harsh mechanical or chemical environments.

One of the challenges of coating porous substrates (e.g., textiles, membranes, bandages, etc) is to form uniform and conformal coating on the large surface area within the fibers or pores of these substrates. With the conventional dip LbL method, when the porous substrates are immersed in the polymer solution, the subsequent rinse steps cannot effectively remove the nonspecifically bound materials; this results in buildup of non uniform films or worst case no film buildup. In recent years, other methods of LbL assembly has been developed, including spray LbL and spin LbL. [48, 49, 69] Similar to dip LbL method, spray LbL assembles films via electrostatic interactions between the oppositely charged species, but the process times can be reduced more than 25-fold by convectively transporting the materials to the surface, versus

diffusion-based transport of material in dip assembly. [49] Most importantly, spray LbL has been shown to form highly conformal coatings on individual fibers or pores of porous substrates (e.g., textiles, electrospun mats, etc.); this is accomplished by drawing a pressure gradient across the porous substrates during the spray LbL process. The microbicidal films investigated in this thesis work were all built with the dip LbL method; future work looking into other method of LbL assembly, especially spray LbL to deposit the microbicidal film on porous substrates will open up more potential uses of this film technology. A foreseeable challenge to overcome with using spray LbL to assemble the microbicidal film is the solvent disparity between the polycation and polyanion; as mentioned before, the polycation only dissolves in organic solvent, and the polyanion is in aqueous solution. Because the kinetics of film deposition in spray LbL are different from dip LbL, the buildup of film in this solvent disparity situation could be very unpredictable. A systematic study looking into the various parameters (e.g., spray time, speed, distance of sprayer from substrate, etc.) involved in spray LbL will be necessary to ensure successful buildup of functionally active films.

The potential for infection to occur exists virtually everywhere, in surgical procedures, everyday encounters, and many more; therefore, the research presented here has many possible applications in various different industries. Although the research presented here focused on designing films with permanent contact killing microbicidal activity, the knowledge gained and groundwork laid here can be applied to the design of other bioactive film coating. The insights into how microbes are killed by these films could open up new ways of designing films that kill them on contact. The same applies for the information gained in designing films with antifouling activity. The work presented herein will expand the scope of use of multilayer films in various

applications particularly in preventing the spread of infections and fouling of surfaces by proteins, both of which cause billion of dollars in cost annually.

Bibliography

1. Picart, C., Polyelectrolyte Multilayer Films: From Physico-chemical Properties to The Control of Cellular Processes. *Curr Med Chem* **2008,** *15* (7), 685-697.
2. Moskowitz, J. S.; Blaisse, M. R.; Samuel, R. E.; Hsu, H. P.; Harris, M. B.; Martin, S. D.; Lee, J. C.; Spector, M.; Hammond, P. T., The Effectiveness of The Controlled Release of Gentamicin from Polyelectrolyte Multilayers in The Treatment of Staphylococcus aureus Infection in A Rabbit Bone Model. *Biomaterials* **2010,** *31* (23), 6019-6030.
3. Smith, R. C.; Riollano, M.; Leung, A.; Hammond, P. T., Layer-by-Layer Platform Technology for Small-Molecule Delivery. *Angew Chem Int Ed Engl.* **2009,** *48* (47), 8974-8977.
4. Shukla, A.; Avadhany, S. N.; Fang, J. C.; Hammond, P. T., Tunable Vancomycin Releasing Surfaces for Biomedical Applications. *Small* **2010,** *6* (21), 2392-404.
5. Macdonald, M. L.; Samuel, R. E.; Shah, N. J.; Padera, R. F.; Beben, Y. M.; Hammond, P. T., Tissue Integration of Growth Factor-eluting Layer-by-layer Polyelectrolyte Multilayer Coated Implants. *Biomaterials* **2011,** *32* (5), 1446-53.
6. Lee, S. W.; Yabuuchi, N.; Gallant, B. M.; Chen, S.; Kim, B. S.; Hammond, P. T.; Shao-Horn, Y., High-power Lithium Batteries from Functionalized Carbon-nanotube Electrodes. *Nat Nanotechnol* **2010,** *5* (7), 531-537.
7. Argun, A. A.; Ashcraft, J. N.; Hammond, P. T., Highly Conductive, Methanol Resistant Polyelectrolyte Multilayers. *Adv Mater* **2008,** *20* (8), 1539-1543.
8. Argun, A. A.; Ashcraft, J. N.; Herring, M. K.; Lee, D. K. Y.; Allcock, H. R.; Hammond, P. T., Ion Conduction and Water Transport in Polyphosphazene-Based Multilayers. *Chem Mater* **2010,** *22* (1), 226-232.
9. Schmidt, D. J.; Cebeci, F. C.; Kalcioglu, Z. I.; Wyman, S. G.; Ortiz, C.; Van Vliet, K. J.; Hammond, P. T., Electrochemically Controlled Swelling and Mechanical Properties of a Polymer Nanocomposite. *ACS Nano* **2009,** *3* (8), 2207-2216.
10. Lyles, B. F.; Terrot, M. S.; Hammond, P. T.; Gast, A. P., Directed Patterned Adsorption of Magnetic Beads on Polyelectrolyte Multilayers on Glass. *Langmuir* **2004,** *20* (8), 3028-3031.
11. Schmidt, D. J.; Moskowitz, J. S.; Hammond, P. T., Electrically Triggered Release of a Small Molecule Drug from a Polyelectrolyte Multilayer Coating. *Chem Mater* **2010,** *22* (23), 6416-6425.
12. CDC- Seasonal Influenza (Flu) Basics. http://www.cdc.gov/flu/about/disease/ (accessed December 07).
13. Dowdle, W. R., Influenza Pandemic Periodicity, Virus Recycling, and The Art of Risk Assessment. *Emerg Infect Dis* **2006,** *12* (1), 34-39.
14. Chuang, H. F.; Smith, R. C.; Hammond, P. T., Polyelectrolyte Multilayers for Tunable Release of Antibiotics. *Biomacromolecules* **2008,** *9* (6), 1660-1668.
15. Macdonald, M.; Rodriguez, N. M.; Smith, R.; Hammond, P. T., Release of A Model protein from Biodegradable Self Assembled Films for Surface Delivery Applications. *J Control Release* **2008,** *131* (3), 228-34.
16. Schneider, A.; Vodouhe, C.; Richert, L.; Francius, G.; Le Guen, E.; Schaaf, P.; Voegel, J. C.; Frisch, B.; Picart, C., Multifunctional Polyelectrolyte Multilayer Films: Combining Mechanical Resistance, Biodegradability, and Bioactivity. *Biomacromolecules* **2007,** *8* (1), 139-145.
17. Dierich, A.; Le Guen, E.; Messaddeq, N.; Stoltz, J. F.; Netter, P.; Schaaf, P.; Voegel, J. C.; Benkirane-Jessel, N., Bone Formation Mediated by Synergy-acting Growth Factors Embedded in A Polyelectrolyte Multilayer Film. *Adv Mater* **2007,** *19* (5), 693-+.
18. Macdonald, M. L.; Rodriguez, N. M.; Shah, N. J.; Hammond, P. T., Characterization of Tunable FGF-2 Releasing Polyelectrolyte Multilayers. *Biomacromolecules* **2010,** *11* (8), 2053-9.

19. Scheller, B.; Hehrlein, C.; Bocksch, W.; Rutsch, W.; Haghi, D.; Dietz, U.; Bohm, M.; Speck, U., Treatment of Coronary In-stent Restenosis with A Paclitaxel-coated Balloon Catheter. *N Engl J Med* **2006,** *355* (20), 2113-2124.
20. Wu, P.; Grainger, D. W., Drug/device Combinations For Local Drug Therapies and Infection Prophylaxis. *Biomaterials* **2006,** *27* (11), 2450-2467.
21. Lucke, M.; Schmidmaier, G.; Sadoni, S.; Wildemann, B.; Schiller, R.; Haas, N. P.; Raschke, M., Gentamicin Coating of Metallic Implants Reduces Implant-related Osteomyelitis in Rats. *Bone* **2003,** *32* (5), 521-531.
22. Yang, C. M.; Burt, H. A., Drug-eluting Stents: Factors Governing Local Pharmacokinetics. *Adv Drug Deliv Rev.* **2006,** *58* (3), 402-411.
23. Tang, L.; Eaton, J. W., Inflammatory Responses to Biomaterials. *Am J Clin Pathol* **1995,** *103* (4), 466-71.
24. Ratner, B. D., *Biomaterials Science: An Introduction to Materials in Medicine.* 2nd ed.; Elsevier Academic Press: Boston, 2004.
25. Tang, L.; Eaton, J. W., Natural Responses to Unnatural Materials: A Molecular Mechanism for Foreign Body Reactions. *Mol Med* **1999,** *5* (6), 351-8.
26. Costerton, J. W.; Stewart, P. S.; Greenberg, E. P., Bacterial Biofilms: A Common Cause of Persistent Infections. *Science* **1999,** *284* (5418), 1318-22.
27. Herzberg, M.; Elimelech, M., Biofouling of Reverse Osmosis Membranes: Role of Biofilm-enhanced Osmotic Pressure. *J Membrane Sci* **2007,** *295* (1-2), 11-20.
28. Dobretsov, S.; Dahms, H. U.; Qian, P. Y., Inhibition of Biofouling by Marine Microorganisms and Their Metabolites. *Biofouling* **2006,** *22* (1), 43-54.
29. Meyer, B., Approaches to Prevention, Removal and Killing of Biofilms. *Int Biodeter Biodegr* **2003,** *51* (4), 249-253.
30. Decher, G.; Hong, J. D.; Schmitt, J., Buildup of Ultrathin Multilayer Films by a Self-Assembly Process .3. Consecutively Alternating Adsorption of Anionic and Cationic Polyelectrolytes on Charged Surfaces. *Thin Solid Films* **1992,** *210* (1-2), 831-835.
31. Hammond, P. T., Form and Function in Multilayer Assembly: New Applications At The Nanoscale. *Adv Mater* **2004,** *16* (15), 1271-1293.
32. Yang, S. Y.; Rubner, M. F., Micropatterning of Polymer Thin Films with pH-sensitive and Cross-linkable Hydrogen-bonded Polyelectrolyte Multilayers. *J Am Chem Soc* **2002,** *124* (10), 2100-2101.
33. Decher, G., Fuzzy Nanoassemblies: Toward Layered Polymeric Multicomposites. *Science* **1997,** *277* (5330), 1232-1237.
34. Joanny, J. F., Polyelectrolyte Adsorption and Charge Inversion. *Eur Phys J B* **1999,** *9* (1), 117-122.
35. Lowack, K.; Helm, C. A., Molecular Mechanisms Controlling the Self-assembly Process of Polyelectrolyte Multilayers. *Macromolecules* **1998,** *31* (3), 823-833.
36. Schmitt, J.; Grunewald, T.; Decher, G.; Pershan, P. S.; Kjaer, K.; Losche, M., Internal Structure of Layer-by-Layer Adsorbed Polyelectrolyte Films - a Neutron and X-Ray Reflectivity Study. *Macromolecules* **1993,** *26* (25), 7058-7063.
37. Schoeler, B.; Poptoschev, E.; Caruso, F., Growth of Multilayer Films of Fixed and Variable Charge Density Polyelectrolytes: Effect of Mutual Charge and Secondary Interactions. *Macromolecules* **2003,** *36* (14), 5258-5264.
38. Shiratori, S. S.; Rubner, M. F., pH-dependent Thickness Behavior of Sequentially Adsorbed Layers of Weak Polyelectrolytes. *Macromolecules* **2000,** *33* (11), 4213-4219.
39. Dubas, S. T.; Schlenoff, J. B., Factors Controlling the Growth of Polyelectrolyte Multilayers. *Macromolecules* **1999,** *32* (24), 8153-8160.
40. Vandesteeg, H. G. M.; Stuart, M. A. C.; Dekeizer, A.; Bijsterbosch, B. H., Polyelectrolyte Adsorption - a Subtle Balance of Forces. *Langmuir* **1992,** *8* (10), 2538-2546.

41. Houska, M.; Brynda, E.; Bohata, K., The Effect of Polyelectrolyte Chain Length on Layer-by-layer Protein/polyelectrolyte Assembly-An Experimental Study. *J Colloid Interface Sci* **2004,** *273* (1), 140-147.
42. Sui, Z. J.; Salloum, D.; Schlenoff, J. B., Effect of Molecular Weight on The Construction of Polyelectrolyte Multilayers: Stripping Versus Sticking. *Langmuir* **2003,** *19* (6), 2491-2495.
43. Ladam, G.; Schaad, P.; Voegel, J. C.; Schaaf, P.; Decher, G.; Cuisinier, F., In Situ Determination of The Structural Properties of Initially Deposited Polyelectrolyte Multilayers. *Langmuir* **2000,** *16* (3), 1249-1255.
44. Porcel, C.; Lavalle, P.; Decher, G.; Senger, B.; Voegel, J. C.; Schaaf, P., Influence of The Polyelectrolyte Molecular Weight on Exponentially Growing Multilayer Films in The Linear Regime. *Langmuir* **2007,** *23* (4), 1898-1904.
45. Lvov, Y.; Ariga, K.; Onda, M.; Ichinose, I.; Kunitake, T., A Careful Examination of The Adsorption Step in The Alternate Layer-by-layer Assembly of Linear Polyanion and Polycation. *Colloid Surface A* **1999,** *146* (1-3), 337-346.
46. Halthur, T. J.; Claesson, P. M.; Elofsson, U. M., Stability of Polypeptide Multilayers As Studied by In Situ Ellipsometry: Effects of Drying and Post-buildup Changes in Temperature and pH. *J Am Chem Soc* **2004,** *126* (51), 17009-17015.
47. Kim, B. S.; Park, S. W.; Hammond, P. T., Hydrogen-bonding Layer-by-Layer Assembled Biodegradable Polymeric Micelles As Drug Delivery Vehicles from Surfaces. *ACS Nano* **2008,** *2* (2), 386-392.
48. Schlenoff, J. B.; Dubas, S. T.; Farhat, T., Sprayed Polyelectrolyte Multilayers. *Langmuir* **2000,** *16* (26), 9968-9969.
49. Krogman, K. C.; Lowery, J. L.; Zacharia, N. S.; Rutledge, G. C.; Hammond, P. T., Spraying Asymmetry into Functional Membranes Layer-by-layer. *Nat Mater* **2009,** *8* (6), 512-518.
50. Cho, J.; Char, K.; Hong, J. D.; Lee, K. B., Fabrication of Highly Ordered Multilayer Films Using a Spin Self-Assembly Method. *Advanced Materials* **2001,** *13* (14), 1076-1078.
51. Caruso, F.; Niikura, K.; Furlong, D. N.; Okahata, Y., 2. Assembly of Alternating Polyelectrolyte and Protein Multilayer Films for Immunosensing. *Langmuir* **1997,** *13* (13), 3427-3433.
52. Hammond, P. T., Form and Function in Multilayer Assembly: New Applications at the Nanoscale. *Advanced Materials* **2004,** *16* (15), 1271-1293.
53. Li, Z.; Lee, D.; Sheng, X. X.; Cohen, R. E.; Rubner, M. F., Two-level Antibacterial Coating with Both Release-killing and Contact-killing Capabilities. *Langmuir* **2006,** *22* (24), 9820-9823.
54. Malcher, M.; Volodkin, D.; Heurtault, B.; Andre, P.; Schaaf, P.; Mohwald, H.; Voegel, J. C.; Sokolowski, A.; Ball, V.; Boulmedais, F.; Frisch, B., Embedded Silver Ions-containing Liposomes in Polyelectrolyte Multilayers: Cargos Films for Antibacterial Agents. *Langmuir* **2008,** *24* (18), 10209-10215.
55. Yu, D. G.; Lin, W. C.; Yang, M. C., Surface Modification of Poly(L-lactic acid) Membrane via Layer-by-layer Assembly of Silver Nanoparticle-embedded Polyelectrolyte Multilayer. *Bioconjug Chem* **2007,** *18* (5), 1521-1529.
56. Yuan, W. Y.; Ji, J.; Fu, J. H.; Shen, J. C., A Facile Method to Construct Hybrid Multilayered Films As A Strong and Multifunctional Antibacterial Coating. *J Biomed Mater Res B Appl Biomater* **2008,** *85B* (2), 556-563.
57. Yu, D. G.; Jou, C. H.; Lin, W. C.; Yang, M. C., Surface Modification of Poly(tetramethylene adipate-co-terephthalate) Membrane via Layer-by-layer Assembly of Chitosan and Dextran Sulfate Polyelectrolyte Multilayer. *Colloids and Surfaces B-Biointerfaces* **2007,** *54* (2), 222-229.
58. Channasanon, S.; Graisuwan, W.; Kiatkamjornwong, S.; Hoven, V. P., Alternating Bioactivity of Multilayer Thin Films Assembled from Charged Derivatives of Chitosan. *J Colloid Interface Sci* **2007,** *316* (2), 331-343.
59. Lee, D.; Cohen, R. E.; Rubner, M. F., Antibacterial Properties of Ag Nanoparticle Loaded Multilayers and Formation of Magnetically Directed Antibacterial Microparticles. *Langmuir* **2005,** *21* (21), 9651-9659.

60. Alt, V.; Bechert, T.; Steinrucke, P.; Wagener, M.; Seidel, P.; Dingeldein, E.; Domann, E.; Schnettler, R., An In Vitro Assessment of The Antibacterial Properties and Cytotoxicity of Nanoparticulate Silver Bone Cement. *Biomaterials* **2004,** *25* (18), 4383-4391.
61. Lichter, J. A.; Thompson, M. T.; Delgadillo, M.; Nishikawa, T.; Rubner, M. F.; Van Vliet, K. J., Substrata Mechanical Stiffness can Regulate Adhesion of Viable Bacteria. *Biomacromolecules* **2008,** *9* (6), 1571-1578.
62. Serizawa, T.; Yamaguchi, M.; Akashi, M., Enzymatic Hydrolysis of A Layer-by-layer Assembly Prepared from Chitosan and Dextran Sulfate. *Macromolecules* **2002,** *35* (23), 8656-8658.
63. Wood, K. C.; Boedicker, J. Q.; Lynn, D. M.; Hammond, P. T., Tunable Drug Release from Hydrolytically Degradable Layer-by-layer Thin Films. *Langmuir* **2005,** *21* (4), 1603-9.
64. Zhang, J. T.; Fredin, N. J.; Janz, J. F.; Sun, B.; Lynn, D. M., Structure/property Relationships in Erodible Multilayered Films: Influence of Polycation Structure on Erosion Profiles and The Release of Anionic Polyelectrolytes. *Langmuir* **2006,** *22* (1), 239-245.
65. Lynn, D. M.; Langer, R., Degradable Poly(beta-amino esters): Synthesis, Characterization, and Self-assembly with Plasmid DNA. *J Am Chem Soc.* **2000,** *122* (44), 10761-10768.
66. Smith, R. C.; Leung, A.; Kim, B.-S.; Hammond, P. T., Hydrophobic Effects in the Critical Destabilization and Release Dynamics of Degradable Multilayer Films. *Chem Mater.* **2008,** *21* (6), 1108-1115.
67. Zacharia, N. S.; DeLongchamp, D. M.; Modestino, M.; Hammond, P. T., Controlling Diffusion and Exchange in Layer-by-layer Assemblies. *Macromolecules* **2007,** *40* (5), 1598-1603.
68. Krogman, K. C.; Zacharia, N. S.; Schroeder, S.; Hammond, P. T., Automated Process For Improved Uniformity and Versatility of Layer-by-layer Deposition. *Langmuir* **2007,** *23* (6), 3137-3141.
69. Cho, J.; Char, K.; Hong, J. D.; Lee, K. B., Fabrication of Highly Ordered Multilayer Films Using A Spin Self-assembly Method. *Adv Mater* **2001,** *13* (14), 1076-+.
70. Lewis, K.; Klibanov, A. M., Surpassing Nature: Rational Design of Sterile-surface Materials. *Trends Biotechnol* **2005,** *23* (7), 343-348.
71. Haldar, J.; An, D.; Alvarez de Cienfuegos, L.; Chen, J.; Klibanov, A. M., Polymeric Coatings that Inactivate Both Influenza Virus and Pathogenic Bacteria. *Proc Natl Acad Sci U S A* **2006,** *103* (47), 17667-17671.
72. Park, D.; Wang, J.; Klibanov, A. M., One-step, Painting-like Coating Procedures to Make Surfaces Highly and Permanently Bactericidal. *Biotechnol Prog* **2006,** *22* (2), 584-589.
73. Milovic, N. M.; Wang, J.; Lewis, K.; Klibanov, A. M., Immobilized N-alkylated Polyethylenimine Avidly Kills Bacteria by Rupturing Cell Membranes with No Resistance Developed. *Biotechnol Bioeng* **2005,** *90* (6), 715-722.
74. Hsu, B. B.; Ouyang, J.; Wong, S. Y.; Hammond, P. T.; Klibanov, A. M., On Structural Damage Incurred by Bacteria Upon Exposure to Hydrophobic Polycationic Coatings. *Biotechnol Lett* **2011,** *33* (2), 411-416.
75. Mukherjee, K.; Rivera, J. J.; Klibanov, A. M., Practical Aspects of Hydrophobic Polycationic Bactericidal "Paints". *Appl Biochem Biotechnol* **2008,** *151* (1), 61-70.
76. Lin, J.; Murthy, S. K.; Olsen, B. D.; Gleason, K. K.; Klibanov, A. M., Making Thin Polymeric Materials, Including Fabrics, Microbicidal and Also Water-repellent. *Biotechnol Lett* **2003,** *25* (19), 1661-1665.
77. Lichter, J. A.; Rubner, M. F., Polyelectrolyte Multilayers with Intrinsic Antimicrobial Functionality: The Importance of Mobile Polycations. *Langmuir* **2009,** *25* (13), 7686-7694.
78. Tiller, J. C.; Liao, C. J.; Lewis, K.; Klibanov, A. M., Designing Surfaces that Kill Bacteria on Contact. *Proc Natl Acad Sci U S A* **2001,** *98* (11), 5981-5985.
79. Lee, S. B.; Koepsel, R. R.; Morley, S. W.; Matyjaszewski, K.; Sun, Y. J.; Russell, A. J., Permanent, Nonleaching Antibacterial Surfaces. 1. Synthesis by Atom Transfer Radical Polymerization. *Biomacromolecules* **2004,** *5* (3), 877-882.
80. Thome, J.; Hollander, A.; Jaeger, W.; Trick, I.; Oehr, C., Ultrathin Antibacterial Polyammonium Coatings on Polymer Surfaces. *Surface & Coatings Technology* **2003,** *174*, 584-587.

81. Lenoir, S.; Pagnoulle, C.; Detrembleur, C.; Galleni, M.; Jerome, R., New Antibacterial Cationic Surfactants Prepared by Atom Transfer Radical Polymerization. *J Polym Sci Pol Chem* **2006,** *44* (3), 1214-1224.
82. Cheng, Z. P.; Zhu, X. L.; Shi, Z. L.; Neoh, K. G.; Kang, E. T., Polymer Microspheres with Permanent Antibacterial Surface from Surface-initiated Atom Transfer Radical Polymerization. *Ind Eng Chem Res* **2005,** *44* (18), 7098-7104.
83. Cen, L.; Neoh, K. G.; Kang, E. T., Surface Functionalization Technique for Conferring Antibacterial Properties to Polymeric and Cellulosic Surfaces. *Langmuir* **2003,** *19* (24), 10295-10303.
84. Edge, M.; Allen, N. S.; Turner, D.; Robinson, J.; Seal, K., The Enhanced Performance of Biocidal Additives in Paints and Coatings. *Prog Org Coat* **2001,** *43* (1-3), 10-17.
85. Lin, J.; Qiu, S. Y.; Lewis, K.; Klibanov, A. M., Bactericidal Properties of Flat Surfaces and Nanoparticles Derivatized with Alkylated Polyethylenimines. *Biotechnol Prog* **2002,** *18* (5), 1082-1086.
86. Klibanov, A. M., Permanently Microbicidal Materials Coatings. *J Mater Chem* **2007,** *17* (24), 2479-2482.
87. Haldar, J.; Chen, J.; Tumpey, T. M.; Gubareva, L. V.; Klibanov, A. M., Hydrophobic Polycationic Coatings Inactivate Wild-type and Zanamivir- and/or Oseltamivir-resistant Human and Avian Influenza Viruses. *Biotechnol Lett* **2008,** *30* (3), 475-9.
88. Gottenbos, B.; van der Mei, H. C.; Klatter, F.; Nieuwenhuis, P.; Busscher, H. J., In Vitro and In Vivo Antimicrobial Activity of Covalently Coupled Quaternary Ammonium Silane Coatings on Silicone Rubber. *Biomaterials* **2002,** *23* (6), 1417-1423.
89. Isquith, A. J.; Abbott, E. A.; Walters, P. A., Surface-Bonded Antimicrobial Activity of An Organosilicon Quaternary Ammonium Chloride. *Applied Microbiology* **1972,** *24* (6), 859-863.
90. Mukherjee, K.; Rivera, J. J.; Klibanov, A. M., Practical aspects of hydrophobic polycationic bactericidal "paints". *Applied Biochemistry and Biotechnology* **2008,** *151* (1), 61-70.
91. Decher, G.; Hong, J. D., Buildup of Ultrathin Multilayer Films by a Self-Assembly Process .2. Consecutive Adsorption of Anionic and Cationic Bipolar Amphiphiles and Polyelectrolytes on Charged Surfaces. *Berichte Der Bunsen-Gesellschaft-Physical Chemistry Chemical Physics* **1991,** *95* (11), 1430-1434.
92. Kim, B. S.; Lee, H.; Min, Y. H.; Poon, Z.; Hammond, P. T., Hydrogen-bonded Multilayer of pH-responsive Polymeric Micelles with Tannic Acid for Surface Drug Delivery. *Chem Commun (Camb).* **2009,** (28), 4194-4196.
93. Kim, B. S.; Smith, R. C.; Poon, Z.; Hammond, P. T., MAD (Multiagent Delivery) Nanolayer: Delivering Multiple Therapeutics from Hierarchically Assembled Surface Coatings. *Langmuir* **2009,** *25* (24), 14086-14092.
94. Farhat, T. R.; Hammond, P. T., Designing A New Generation of Proton-exchange Membranes Using Layer-by-Layer Deposition of Polyelectrolytes. *Adv Funct Mater.* **2005,** *15* (6), 945-954.
95. Schmidt, D. J.; Pridgen, E. M.; Hammond, P. T.; Love, J. C., Layer-by-Layer Assembly of a pH-Responsive and Electrochromic Thin Film. *J Chem Educ* **2010,** *87* (2), 208-211.
96. Dai, J. H.; Bruening, M. L., Catalytic Nanoparticles Formed by Reduction of Metal Ions in Multilayered Polyelectrolyte Films. *Nano Lett* **2002,** *2* (5), 497-501.
97. Chua, P. H.; Neoh, K. G.; Kang, E. T.; Wang, W., Surface Functionalization of Titanium with Hyaluronic Acid/chitosan Polyelectrolyte Multilayers and RGD for Promoting Osteoblast Functions and Inhibiting Bacterial Adhesion. *Biomaterials* **2008,** *29* (10), 1412-1421.
98. Shukla, A.; Fleming, K. E.; Chuang, H. F.; Chau, T. M.; Loose, C. R.; Stephanopoulos, G. N.; Hammond, P. T., Controlling The Release of Peptide Antimicrobial Agents from Surfaces. *Biomaterials* **2010,** *31* (8), 2348-2357.
99. Thomas, M.; Lu, J. J.; Ge, Q.; Zhang, C. C.; Chen, J. Z.; Klibanov, A. M., Full Deacylation of Polyethylenimine Dramatically Boosts Its Gene Delivery Efficiency and Specificity to Mouse Lung. *Proc Natl Acad Sci U S A.* **2005,** *102* (16), 5679-5684.
100. Haldar, J.; Weight, A. K.; Klibanov, A. M., Preparation, Application and Testing of Permanent Antibacterial and Antiviral Coatings. *Nat Protoc* **2007,** *2* (10), 2412-2147.

101. Fujita, S.; Shiratori, S., The Initial Growth of Ultra-thin Films Fabricated by A Weak Polyelectrolyte Layer-by-layer Adsorption Process. *Nanotechnology* **2005,** *16* (9), 1821-1827.
102. Choi, J.; Rubner, M. F., Influence of the Degree of Ionization on Weak Polyelectrolyte Multilayer Assembly. *Macromolecules* **2005,** *38* (1), 116-124.
103. Dobrynin, A. V.; Rubinstein, M., Theory of Polyelectrolytes In Solutions and At Surfaces. *Prog Polym Sci* **2005,** *30* (11), 1049-1118.
104. Murata, H.; Koepsel, R. R.; Matyjaszewski, K.; Russell, A. J., Permanent, Non-leaching Antibacterial Surfaces - 2: How High Density Cationic Surfaces Kill Bacterial Cells. *Biomaterials* **2007,** *28* (32), 4870-4879.
105. Nurdin, N.; Helary, G.; Sauvet, G., Biocidal Polymers Active by Contact .3. Aging of Biocidal Polyurethane Coatings in Water. *J Appl Polym Sci* **1993,** *50* (4), 671-678.
106. Ryser, H. J. P., A Membrane Effect of Basic Polymers Dependent on Molecular Size. *Nature* **1967,** *215* (5104), 934-&.
107. Fischer, D.; Li, Y. X.; Ahlemeyer, B.; Krieglstein, J.; Kissel, T., In Vitro Cytotoxicity Testing of Polycations: Influence of Polymer Structure on Cell Viability and Hemolysis. *Biomaterials* **2003,** *24* (7), 1121-1131.
108. Murguia, M. C.; Vaillard, V. A.; Sanchez, V. G.; Conza, J. D.; Grau, R. J., Synthesis, Surface-active Properties, and Antimicrobial Activities of New Double-chain Gemini Surfactants. *J Oleo Sci* **2008,** *57* (5), 301-8.
109. Madigan, M. T.; Martinko, J. M.; Dunlap, P. V.; Clark, D. P., *Brock Biology of Microorganisms*. 12th ed.; Benjamin Cummings: Boston, 2008.
110. Denyer, S. P.; Maillard, J. Y., Cellular Impermeability and Uptake of Biocides and Antibiotics in Gram-negative Bacteria. *J Appl Microbiol* **2002,** *92*, 35s-45s.
111. Guerin-Mechin, L.; Dubois-Brissonnet, F.; Heyd, B.; Leveau, J. Y., Quaternary Ammonium Compound Stresses Induce Specific Variations in Fatty Acid Composition of Pseudomonas aeruginosa. *Int J Food Microbiol* **2000,** *55* (1-3), 157-9.
112. Choppin, P. W.; Compans, R. W., The structure of influenza virus. *The Influenza Viruses and Influenza* **1975**.
113. Hsu, B. B.; Wong, S. Y.; Hammond, P. T.; Chen, J. Z.; Klibanov, A. M., Mechanism of Inactivation of Influenza Viruses by Immobilized Hydrophobic Polycations. *Proc Natl Acad Sci U S A* **2011,** *108* (1), 61-66.
114. **!!! INVALID CITATION !!!**
115. Koschwanez, H. E.; Reichert, W. M., In Vitro, In Vivo and Post Explantation Testing of Glucose-detecting Biosensors: Current Methods and Recommendations. *Biomaterials* **2007,** *28* (25), 3687-3703.
116. Polikov, V. S.; Tresco, P. A.; Reichert, W. M., Response of Brain Tissue to Chronically Implanted Neural Electrodes. *J Neurosci Methods* **2005,** *148* (1), 1-18.
117. Anderson, J. M., Biological Responses to Materials. *Annu. Rev. Mater. Res.* **2001,** *31*, 81-110.
118. Morais, J. M.; Papadimitrakopoulos, F.; Burgess, D. J., Biomaterials/Tissue Interactions: Possible Solutions to Overcome Foreign Body Response. *Aaps Journal* **2010,** *12* (2), 188-196.
119. Darouiche, R. O., Current Concepts - Treatment of Infections Associated with Surgical Implants. *N Engl J Med.* **2004,** *350* (14), 1422-1429.
120. Johnson, J. R.; Kuskowski, M. A.; Wilt, T. J., Systematic Review: Antimicrobial Urinary Catheters to Prevent Catheter-associated Urinary Tract Infection in Hospitalized Patients. *Ann Intern Med.* **2006,** *144* (2), 116-126.
121. Hall-Stoodley, L.; Costerton, J. W.; Stoodley, P., Bacterial Biofilms: From The Natural Environment to Infectious Diseases. *Nat Rev Microbiol.* **2004,** *2* (2), 95-108.
122. Nelson, J. L.; Roeder, B. L.; Carmen, J. C.; Roloff, F.; Pitt, W. G., Ultrasonically Activated Chemotherapeutic Drug Delivery In A Rat Model. *Cancer Res.* **2002,** *62* (24), 7280-7283.
123. Costerton, J. W.; Ellis, B.; Lam, K.; Johnson, F.; Khoury, A. E., Mechanism of Electrical Enhancement of Efficacy of Antibiotics in Killing Biofilm Bacteria. *Antimicrob Agents Chemother.* **1994,** *38* (12), 2803-2809.

124. Wong, S. Y.; Li, Q.; Veselinovic, J.; Kim, B. S.; Klibanov, A. M.; Hammond, P. T., Bactericidal and Virucidal Ultrathin Films Assembled Layer by Layer from Polycationic N-alkylated Polyethylenimines and Polyanions. *Biomaterials* **2010,** *31* (14), 4079-4087.
125. Ho, C. H.; Tobis, J.; Sprich, C.; Thomann, R.; Tiller, J. C., Nanoseparated Polymeric Networks with Multiple Antimicrobial Properties. *Adv Mater.* **2004,** *16* (12), 957-+.
126. Sauerbrey, G. Z., *Phys.* **1959,** *155*, 206-22.
127. Shukla, A.; Fleming, K. E.; Chuang, H. F.; Chau, T. M.; Loose, C. R.; Stephanopoulos, G. N.; Hammond, P. T., Controlling the Release of Peptide Antimicrobial Agents from Surfaces. *Biomaterials* *31* (8), 2348-57.
128. Warner, T. D.; Giuliano, F.; Vojnovic, I.; Bukasa, A.; Mitchell, J. A.; Vane, J. R., Nonsteroid Drug Selectivities for Cyclo-oxygenase-1 Rather than Cyclo-oxygenase-2 Are Associated with Human Gastrointestinal Toxicity: A Full In Vitro Analysis. *Proc Natl Acad Sci U S A* **1999,** *96* (13), 7563-8.
129. Giuliano, F.; Ferraz, J. G.; Pereira, R.; de Nucci, G.; Warner, T. D., Cyclooxygenase Selectivity of Non-steroid Anti-inflammatory Drugs in Humans: Ex Vivo Evaluation. *Eur J Pharmacol* **2001,** *426* (1-2), 95-103.
130. Tang, L.; Lucas, A. H.; Eaton, J. W., Inflammatory Responses to Implanted Polymeric Biomaterials: Role of Surface-adsorbed Immunoglobulin G. *J Lab Clin Med* **1993,** *122* (3), 292-300.
131. Baxamusa, S. H.; Gleason, K. K., Random Copolymer Films with Molecular-Scale Compositional Heterogeneities that Interfere with Protein Adsorption. *Adv Funct Mater.* **2009,** *19* (21), 3489-3496.
132. Jackson, A. M.; Myerson, J. W.; Stellacci, F., Spontaneous Assembly of Subnanometre-ordered Domains In The Ligand Shell of Monolayer-protected Nanoparticles. *Nat Mater* **2004,** *3* (5), 330-336.
133. Donlan, R. M., Biofilm Formation: A Clinically Relevant Microbiological Process. *Clin Infect Dis* **2001,** *33* (8), 1387-1392.
134. Pavithra, D.; Doble, M., Biofilm Formation, Bacterial Adhesion and Host Response on Polymeric Implants - Issues and Prevention. *Biomed Mater* **2008,** *3* (3), 034003-034015.
135. Wisniewski, N.; Reichert, M., Methods For Reducing Biosensor Membrane Biofouling. *Colloids Surf B Biointerfaces* **2000,** *18* (3-4), 197-219.
136. Hucknall, A.; Rangarajan, S.; Chilkoti, A., In Pursuit of Zero: Polymer Brushes that Resist the Adsorption of Proteins. *Adv Mater* **2009,** *21* (23), 2441-2446.
137. Lynch, A. S.; Robertson, G. T., Bacterial and Fungal Biofilm Infections. *Annu Rev Med* **2008,** *59*, 415-28.
138. Grundmann, H.; Aires-de-Sousa, M.; Boyce, J.; Tiemersma, E., Emergence and Resurgence of Meticillin-resistant Staphylococcus aureus As A Public-health Threat. *Lancet* **2006,** *368* (9538), 874-85.
139. Prime, K.; Whitesides, G., Self-assembled Organic Monolayers: Model Systems for Studying Adsorption of Proteins at Surfaces. *Science* **1991,** *252* (5009), 1164-1167.
140. Prime, K. L.; Whitesides, G. M., Adsorption of Proteins onto Surfaces Containing End-Attached Oligo(Ethylene Oxide) - a Model System Using Self-Assembled Monolayers. *J Am Chem Soc* **1993,** *115* (23), 10714-10721.
141. Ostuni, E.; Chapman, R. G.; Holmlin, R. E.; Takayama, S.; Whitesides, G. M., A Survey of Structure-property Relationships of Surfaces that Resist the Adsorption of Protein. *Langmuir* **2001,** *17* (18), 5605-5620.
142. Jiang, S. Y.; Cao, Z. Q., Ultralow-Fouling, Functionalizable, and Hydrolyzable Zwitterionic Materials and Their Derivatives for Biological Applications. *Adv Mater* **2010,** *22* (9), 920-932.
143. McArthur, S. L.; McLean, K. M.; Kingshott, P.; St John, H. A. W.; Chatelier, R. C.; Griesser, H. J., Effect of Polysaccharide Structure on Protein Adsorption. *Colloids Surf B Biointerfaces* **2000,** *17* (1), 37-48.
144. Luk, Y. Y.; Kato, M.; Mrksich, M., Self-assembled Monolayers of Alkanethiolates Presenting Mannitol Groups are Inert to Protein Adsorption and Cell Attachment. *Langmuir* **2000,** *16* (24), 9604-9608.

145. Jeon, S. I.; Lee, J. H.; Andrade, J. D.; Degennes, P. G., Protein Surface Interactions in the Presence of Polyethylene Oxide .1. Simplified Theory. *J Colloid Interface Sci* **1991,** *142* (1), 149-158.
146. McPherson, T.; Kidane, A.; Szleifer, I.; Park, K., Prevention of Protein Adsorption by Tethered Poly(ethylene oxide) Layers: Experiments and Single-chain Mean-field Analysis. *Langmuir* **1998,** *14* (1), 176-186.
147. Harder, P.; Grunze, M.; Dahint, R.; Whitesides, G. M.; Laibinis, P. E., Molecular Conformation in Oligo(ethylene glycol)-terminated Self-assembled Monolayers on Gold and Silver Surfaces Determines Their Ability to Resist Protein Adsorption. *J Phys Chem B* **1998,** *102* (2), 426-436.
148. Zheng, J.; Li, L. Y.; Chen, S. F.; Jiang, S. Y., Molecular Simulation Study of Water Interactions with Oligo (ethylene glycol)-terminated Alkanethiol Self-assembled Monolayers. *Langmuir* **2004,** *20* (20), 8931-8938.
149. Li, L. Y.; Chen, S. F.; Zheng, J.; Ratner, B. D.; Jiang, S. Y., Protein Adsorption on Oligo(ethylene glycol)-terminated Alkanethiolate Self-assembled Monolayers: The Molecular Basis for Nonfouling Behavior. *J Phys Chem B* **2005,** *109* (7), 2934-2941.
150. Chen, S. F.; Zheng, J.; Li, L. Y.; Jiang, S. Y., Strong Resistance of Phosphorylcholine Self-assembled Monolayers to Protein adsorption: Insights Into Nonfouling Properties of Zwitterionic Materials. *J Am Chem Soc* **2005,** *127* (41), 14473-14478.
151. He, Y.; Hower, J.; Chen, S. F.; Bernards, M. T.; Chang, Y.; Jiang, S. Y., Molecular Simulation Studies of Protein Interactions with Zwitterionic Phosphorylcholine Self-assembled Monolayers In The Presence of Water. *Langmuir* **2008,** *24* (18), 10358-10364.
152. Hung, A.; Mwenifumbo, S.; Mager, M.; Kuna, J. J.; Stellacci, F.; Yarovsky, I.; Stevens, M. M., Ordering Surfaces On the Nanoscale: Implications for Protein Adsorption. *J Am Chem Soc* **2011,** *133* (5), 1438-1450.
153. Gudipati, C. S.; Finlay, J. A.; Callow, J. A.; Callow, M. E.; Wooley, K. L., The antifouling and fouling-release performance of hyperbranched fluoropolymer (HBFP)-poly(ethylene glycol) (PEG) composite coatings evaluated by adsorption of biomacromolecules and the green fouling alga Ulva. *Langmuir* **2005,** *21* (7), 3044-53.
154. Macritchie, F., Proteins at Interfaces. *Adv Protein Chem* **1978,** *32*, 283-326.
155. Centrone, A.; Penzo, E.; Sharma, M.; Myerson, J. W.; Jackson, A. M.; Marzari, N.; Stellacci, F., The Role of Nanostructure In The Wetting Behavior of Mixed-monolayer-protected Metal Nanoparticles. *Proc Natl Acad Sci U S A* **2008,** *105* (29), 9886-9891.
156. Hobara, D.; Imabayashi, S.; Kakiuchi, T., Preferential Adsorption of Horse Heart Cytochrome C on Nanometer-scale Domains of A Phase-separated Binary Self-assembled Monolayer of 3-mercaptopropionic Acid and 1-hexadecanethiol on Au(111). *Nano Lett* **2002,** *2* (9), 1021-1025.
157. Hederos, M.; Konradsson, P.; Liedberg, B., Synthesis and Self-assembly of Galactose-terminated Alkanethiols and Their Ability to Resist Proteins. *Langmuir* **2005,** *21* (7), 2971-2980.
158. Wong, S. Y.; Moskowitz, J. S.; Veselinovic, J.; Rosario, R. A.; Timachova, K.; Blaisse, M. R.; Fuller, R. C.; Klibanov, A. M.; Hammond, P. T., Dual Functional Polyelectrolyte Multilayer Coatings for Implants: Permanent Microbicidal Base with Controlled Release of Therapeutic Agents. *J Am Chem Soc* **2010,** *132* (50), 17840-17848.
159. Yoo, D.; Shiratori, S. S.; Rubner, M. F., Controlling Bilayer Composition and Surface Wettability of Sequentially Adsorbed Multilayers of Weak Polyelectrolytes. *Macromolecules* **1998,** *31* (13), 4309-4318.
160. Cini, N.; Tulun, T.; Decher, G.; Ball, V., Step-by-Step Assembly of Self-Patterning Polyelectrolyte Films Violating (Almost) All Rules of Layer-by-Layer Deposition. *J Am Chem Soc* **2010,** *132* (24), 8264-8265.
161. Kotov, N. A., Layer-by-layer Self-assembly: The Contribution of Hydrophobic Interactions. *Nanostruct Mater* **1999,** *12* (5-8), 789-796.
162. Picart, C.; Lavalle, P.; Hubert, P.; Cuisinier, F. J. G.; Decher, G.; Schaaf, P.; Voegel, J. C., Buildup Mechanism for Poly(L-lysine)/hyaluronic Acid Films onto A Solid Surface. *Langmuir* **2001,** *17* (23), 7414-7424.

163. Fischer, P.; Laschewsky, A., Layer-by-layer Adsorption of Identically Charged Polyelectrolytes. *Macromolecules* **2000,** *33* (3), 1100-1102.
164. Johnston, A. P. R.; Read, E. S.; Caruso, F., DNA Multilayer Films on Planar and Colloidal Supports: Sequential Assembly of Like-charged Polyelectrolytes. *Nano Lett* **2005,** *5* (5), 953-956.
165. Sigal, G. B.; Mrksich, M.; Whitesides, G. M., Effect of Surface Wettability on The Adsorption of Proteins and Detergents. *J Am Chem Soc* **1998,** *120* (14), 3464-3473.
166. Rixman, M. A.; Dean, D.; Macias, C. E.; Ortiz, C., Nanoscale Intermolecular Interactions Between Human Serum Albumin and Alkanethiol Self-assembled Monolayers. *Langmuir* **2003,** *19* (15), 6202-6218.
167. Belaaouaj, A.; Kim, K. S.; Shapiro, S. D., Degradation of Outer Membrane Protein A in Escherichia coli Killing by Neutrophil Elastase. *Science* **2000,** *289* (5482), 1185-8.
168. Porter, M. D.; Bright, T. B.; Allara, D. L.; Chidsey, C. E. D., Spontaneously Organized Molecular Assemblies .4. Structural Characterization of Normal-Alkyl Thiol Monolayers on Gold by Optical Ellipsometry, Infrared-Spectroscopy, and Electrochemistry. *Journal of the American Chemical Society* **1987,** *109* (12), 3559-3568.
169. Malamy, M. H.; Horecker, B. L., Release of Alkaline Phosphatase from Cells of Escherichia Coli Upon Lysozyme Spheroplast Formation. *Biochemistry-Us* **1964,** *3* (12), 1889-&.